



POLITECNICO
MILANO 1863

SCUOLA DI INGEGNERIA INDUSTRIALE
E DELL'INFORMAZIONE

Functionalized carbon nanotubes as adsorbents for wastewater remediation

TESI DI LAUREA MAGISTRALE IN
ENVIRONMENTAL AND LAND PLANNING ENGINEERING-
INGEGNERIA PER L'AMBIENTE E IL TERRITORIO

Author: **Anna Reale**

Student ID: 103436

Advisor: Prof. Cristian Gambarotti

Co-advisor: Dott.ssa Ada Truscello

Academic Year: 2022-2023

Alla mia famiglia

Abstract

The scarcity of clean water for domestic, industrial, and energy purposes is an increasingly relevant issue, especially in the context of climate change. Therefore, wastewater treatment for reuse becomes of paramount importance.

Adsorption is a particularly important treatment for the removal of organic and inorganic pollutants; such pollutants can be, in some cases, toxic, ecotoxic, carcinogenic, mutagenic, and bioaccumulative.

The first part of the thesis regards the preparation of the adsorbents and the study of their efficiency in the removal of the organic dyes Rhodamine B and Methyl Orange, and the inorganic Cu(II) cation, chosen as reference pollutants. In this context, carbon nanotubes appropriately functionalized to enhance their efficiency and hybrid materials, composed of nanotubes and clay, are prepared. In particular, regarding carbon nanotubes, the modifications involve functionalization with alkyl chain bearing carboxylic groups and choline moiety. For comparison, experiments with non-functionalized carbon nanotubes and clay, a common adsorbent, are also carried out.

In the second part of the thesis the results of the tests, and a comparison of the adsorption efficiencies achieved by the various types of adsorbents are discussed. A possible explanation of the results is reported.

Key-words: adsorption, clay, CNTs, functionalization, metal ions, Rhodamine B, Methyl Orange

Abstract in italiano

La scarsità di acqua pulita per scopi domestici, industriali ed energetici è un problema sempre più rilevante, soprattutto nel contesto dei cambiamenti climatici. Pertanto, il trattamento delle acque reflue per il loro riutilizzo diventa di primaria importanza.

L'adsorbimento è un trattamento particolarmente importante per la rimozione di inquinanti organici e inorganici; tali inquinanti possono essere, in alcuni casi, tossici, ecotossici, cancerogeni, mutageni e bioaccumulabili.

La prima parte di questa tesi si concentra sulla preparazione di alcuni adsorbenti e sull'attuazione di test per valutare la loro efficienza nell'adsorbimento di sostanze quali ioni Cu(II), Rodamina B e Metilarancio, utilizzati come inquinanti di riferimento. I materiali usati sono adsorbenti comuni come l'argilla e adsorbenti emergenti come i nanotubi di carbonio opportunamente funzionalizzati per aumentarne l'efficienza.

In particolare, per i nanotubi, le principali modifiche prevedono la funzionalizzazione con catene lunghe (spacers) contenenti gruppi carbossilici e la funzionalizzazione con unità colina. L'adsorbente ibrido utilizzato è composto da argilla e nanotubi funzionalizzati con unità colina.

La seconda parte della tesi presenta i risultati dei test condotti e un confronto delle efficienze di adsorbimento ottenute dai vari tipi di adsorbenti.

Inoltre, si propone un'interpretazione iniziale dei risultati basata sulle osservazioni ottenute e dati di letteratura esistenti, con uno sguardo rivolto verso i promettenti sviluppi teorici e pratici che un proseguimento a cui questo studio può portare.

Parole chiave: adsorbimento, argilla, CNTs, funzionalizzazione, ioni metallici, Rodamina B, Metilarancio

Contents

Abstract	i
Abstract in italiano	iii
Contents	v
1 Introduction	1
1.1. Water scarcity and Wastewater as Resource.....	1
1.2. Water remediation and its importance	5
1.2.1. Pretreatments	7
1.2.2. Primary treatments.....	9
1.2.3. Secondary treatments.....	10
1.2.4. Tertiary treatments	16
1.3. Carbonaceous materials	19
1.3.1. Carbon nanotubes.....	22
1.4. Nanotechnologies in wastewater management.....	24
1.4.1. Adsorption as the most widely used process in nanotechnologies ..	27
1.4.2. A focus on CNTs in wastewater management.....	30
2 Experimental part	36
2.1. Materials and Methods.....	36
2.2. CNTs functionalization	37
2.2.1. Synthesis of Glutaryl Peroxide	37
2.2.2. CNTs functionalization with Glutaryl Peroxide	39
2.2.3. Functionalization of CNT-X-COL	40
2.3. Preparation of CNTs/clay hybrid material.....	41
2.4. Calibration curves	41
2.4.1. Calibration curve for Cu(II) sulfate pentahydrate $\text{CuSO}_4 \cdot 5\text{H}_2\text{O}$	42
2.4.2. Calibration curve for Cu(II) nitrate trihydrate $\text{Cu}(\text{NO}_3)_2 \cdot 3\text{H}_2\text{O}$	45
2.4.3. Calibration curve for Rhodamine B	46
2.4.4. Calibration curve for Methyl Orange	48
2.5. Adsorption tests	49
2.5.1. Adsorption tests for Cu(II) sulfate pentahydrate $\text{CuSO}_4 \cdot 5\text{H}_2\text{O}$	51
2.5.2. Adsorption tests for Rhodamine B.....	52

2.5.3.	Adsorption tests for Methyl Orange.....	53
2.5.4.	Adsorption tests for Cu(II) nitrate trihydrate $\text{Cu}(\text{NO}_3)_2 \cdot 3\text{H}_2\text{O}$	55
3	Results and Discussion	56
3.1.	MWCNTs functionalization	56
3.1.1.	MWCNTs functionalization with Glutaryl Peroxide	56
3.1.2.	Preparation of CNT-X-COL	58
3.1.3.	Preparation of CNTs/clay hybrid material	59
3.2.	Adsorption tests	59
3.2.1.	Calibration curves	61
3.3.	Adsorption of Rhodamine B by CNTs	62
3.3.1.	Comparison between the adsorbents used.....	62
3.3.2.	Adsorption isotherm studies	66
3.4.	Adsorption of Methyl Orange by CNTs	70
3.4.1.	Comparison between the adsorbents used.....	70
3.4.2.	Variation of efficiency as a function of contact time	72
3.4.3.	Adsorption isotherm studies	74
3.4.4.	Efficiency in different conditions	77
3.5.	Discussion of the data for dyes	78
3.6.	Adsorption of Cu(II) sulfate pentahydrate by CNT/clay hybrid materials 80	
3.6.1.	Comparison between the adsorbents used.....	81
3.6.2.	Variation of efficiency as a function of contact time	83
3.7.	Adsorption of Cu(II) nitrate trihydrate by clay and its problem	84
4	Conclusion and future developments.....	85
	Bibliography.....	89
	List of Figures.....	101
	List of Tables	104
	List of Schemes.....	105
	Acknowledgments.....	106

1 Introduction

1.1. Water scarcity and Wastewater as Resource

Wastewater, also known as sewage or effluent, refers to any water that has been contaminated by human activities and requires treatment before it can be safely released back into the environment or reused.

Wastewater is primarily composed of water, accounting for up to 99% of its content. The remaining fraction consists of various components, including solids, dissolved and particulate matter, microorganisms, nutrients, heavy metals, and micropollutants. However, it's important to note that the specific composition of wastewater varies depending on its source and the activities it comes into contact with (1).

Initially, the focus has been primarily on civil and industrial wastewater as a significant source of pollution and contamination in water treatment. Despite this, the significance of agricultural runoff is now gaining increased attention. This is due to the substantial amounts of pesticides and fertilizers being utilized in agricultural practices, which ultimately contribute to the phenomenon of surface water eutrophication (2).

Nowadays, water scarcity is a pressing global issue, with water demand outpacing population growth in recent years (Figure 1.1). As a result, many regions are facing challenges in delivering sustainable water services (3).

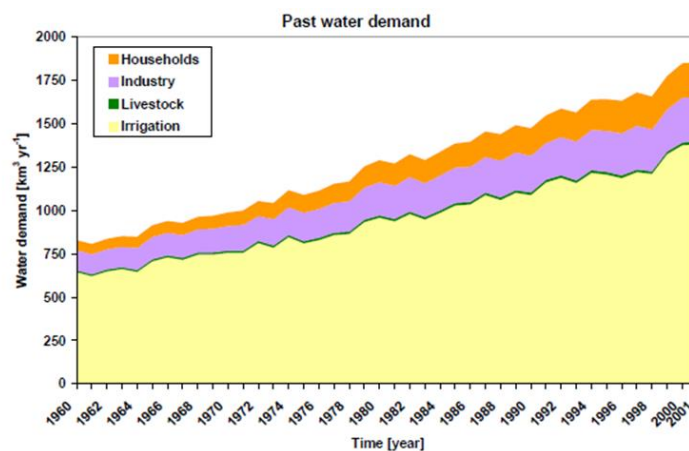


Figure 1.1: Estimated net sectoral and total water demand from 1960 to 2001 in $\text{km}^3 \text{ yr}^{-1}$, (4).

This problem is exacerbated by demographic growth, economic development, and the finite nature of water resources, especially in arid regions.

It is expected that by 2025, approximately 1.8 billion people will be living in countries or regions experiencing "absolute" water scarcity, with access to less than 500 cubic meters of water per year per capita. Additionally, two-thirds of the world's population could be living under "stress" conditions, with water availability ranging between 500 and 1000 m³ per year per capita (5).

Rapid urbanization further intensifies the strain on water resources, placing heavy demands on neighboring water sources.

Moreover, the time has come to recognize that environmental services and ecosystem functions cannot be treated as mere byproducts of water usage. The complex interplay between global development, water demand, and the impacts of climate change and energy demands further complicate the relationship.

The climate change, precisely, is another crucial point: it is one of the most important causes of the continuous increase in drought (6).

Rising temperatures due to climate change directly affect the hydrological cycle and contribute to increased evaporation rates; climate change also alters precipitation patterns, causing shifts in the timing, intensity, and distribution of rainfall. Some regions may experience decreased precipitation, resulting in prolonged dry periods and more frequent or severe drought events (7).

Drought, recognized as one of the most significant natural hazards in certain regions of the world, poses a considerable threat to society with far-reaching negative consequences encompassing environmental and socio-economic aspects.

In Europe, a comparison between the periods of 1976-1990 and 1991-2006 reveals a doubling in both the affected area and population due to this natural phenomenon. The cumulative cost associated with these episodes over the course of three decades reached a staggering 100 billion euros.

For instance, during the severe drought of 2003, which stands out as one of the most intense, more than a third of the European Union's territory and over 100 million people were affected, resulting in an economic impact of 13 billion euros (8).

It is important to address global changes and their impacts on water scarcity and drought through sustainable water management practices and adaptation strategies. This includes improving water conservation, promoting water-efficient agriculture, implementing effective land use planning. By addressing the root causes of global changes and adopting resilient approaches, we can reduce the vulnerability to drought and ensure the long-term sustainability of water resources (9).

As a result of strong population growth, global population is projected to exceed nine billion by 2050 while the water resources will not change (Figure 1.2). However, the

existing wastewater infrastructure, which is already inadequate and outdated, is struggling to meet the demands (10).

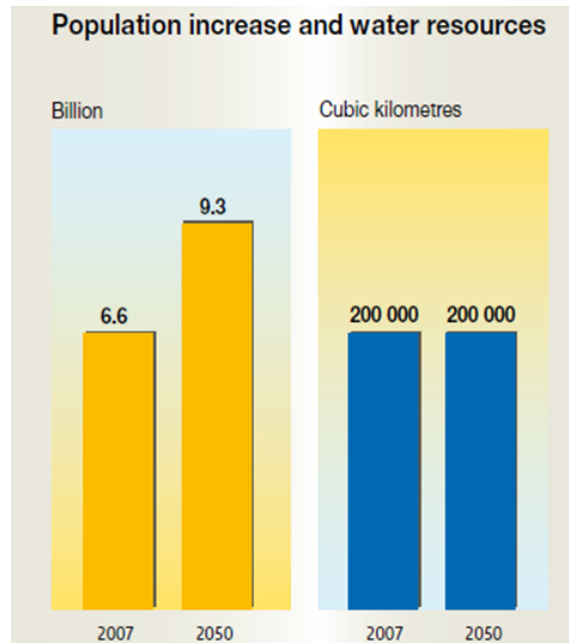


Figure 1.2: (10).

With the population growth and the effects of climate change, the situation is poised to worsen.

Despite this challenge, it persists a prevailing perception that wastewater is merely a source of pollution that necessitates treatment and disposal. Consequently, it is commonly regarded as a growing problem rather than a valuable and sustainable resource.

Fortunately, a paradigm shift is currently underway, particularly in developed countries, where enhanced wastewater management practices are being embraced (11).

The objective is to move beyond solely addressing pollution and to recognize the potential value inherent in wastewater (Figure 1.3).

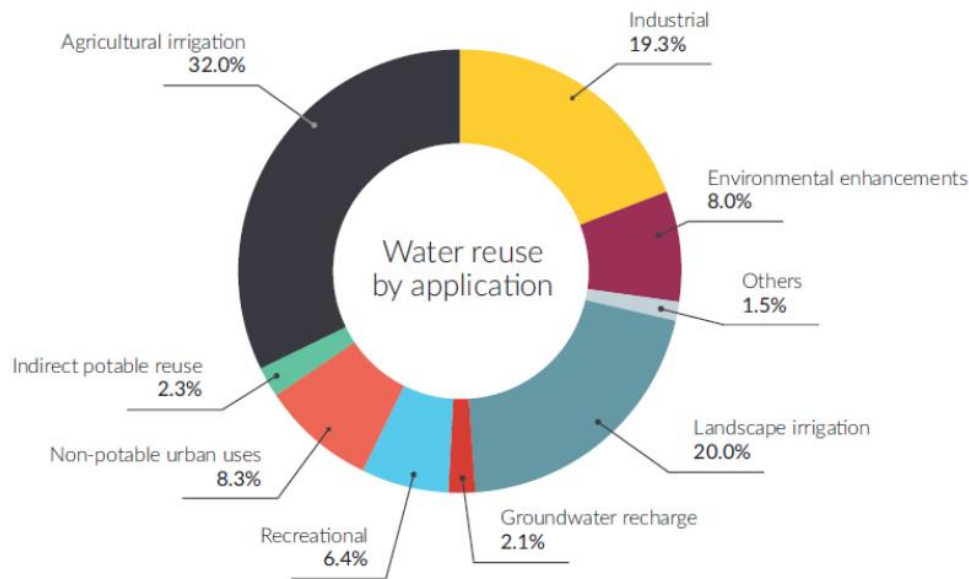


Figure 1.3: Global water reuse after tertiary treatment: market share by application, (12).

Consequently, the wastewater sector in developed nations is transitioning from traditional wastewater treatment plants towards a new perspective that considers them as facilities for water resource recovery. These advanced facilities have the capability to produce clean water, recover valuable nutrients (Figure 1.4), and reduce reliance on fossil fuels by utilizing renewable energy source (13).

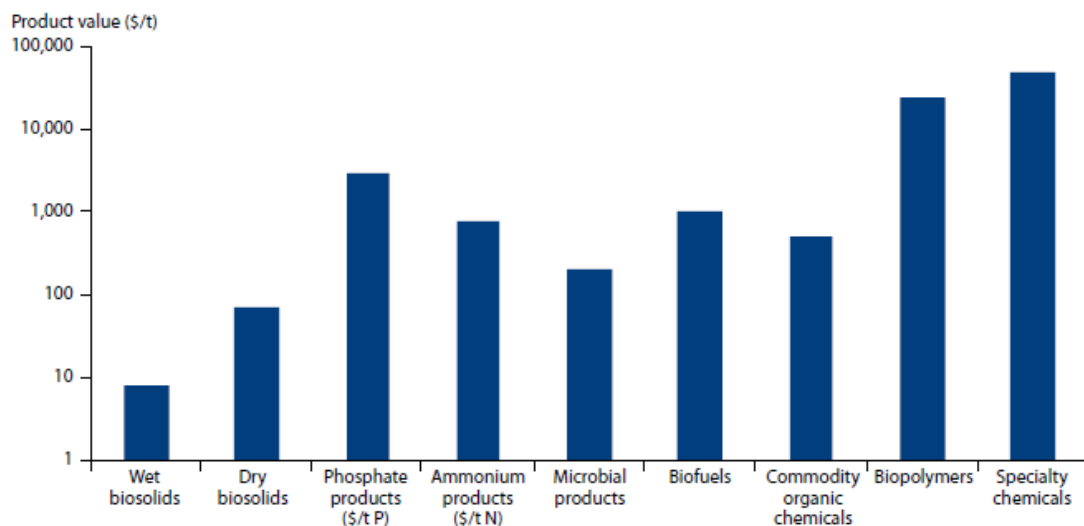


Figure 1.4: Value in dollars per ton of substance, material, or product recovered from wastewater treatment, (14).

This shift towards a more comprehensive and sustainable approach to wastewater management not only addresses environmental concerns but also opens opportunities for resource optimization.

The relationship between wastewater and climate change can be summarized from three perspectives. Firstly, changing climatic conditions impact the quantity and quality of available water, which in turn affects water usage practices. This necessitates adjustments in how wastewater is managed and treated to adapt to the evolving climate. Secondly, climate change requires the implementation of adaptation measures in wastewater management, including strategies for energy and resources recovery. Then, wastewater treatment processes contribute to the emission of greenhouse gases, such as carbon dioxide (CO₂) and methane (CH₄), so it is crucial to address these emissions to minimize the impact of wastewater treatment on climate change.

Regarding this last factor, methane production resulting from wastewater treatment can contribute to the major energy crisis we are facing.

Indeed, the sludge resulting from the treatment is highly polluting; however, if properly utilized through specific processes such as anaerobic digestion, they can produce biogas containing methane. The potential for energy recovery from the sludge depends on their composition (15).

In conclusion, recognizing the value of wastewater and adopting innovative approaches in its management can pave the way for a more sustainable and resilient future. By going beyond traditional treatment methods, we can transform wastewater into a valuable resource and contribute to the efficient utilization of water, energy, and nutrients in a world facing growing challenges (16).

1.2. Water remediation and its importance

Every anthropogenic source, whether it is industrial, domestic, commercial, or related to agricultural processes, generates significant amounts of toxic and damaging effluent.

Domestic wastewater consists of substances introduced by a community during or after usage. As a result, it contains human bodily waste and residues, as well as compounds containing nitrogen and phosphorus.

It is increasingly common to detect the presence of synthetic compounds such as surfactants, typically found in detergents used for household cleaning.

Moreover, domestic wastewater poses potential health risks due to its content of pathogenic microorganisms (17).

Wastewater from industrial sources presents a diverse form of pollution, as it depends on the production and processing processes of the respective industrial facility.

Industrial activities give rise to sewage that often contains toxic and hazardous pollutants resulting from the products used and production methods employed. This

industrial wastewater may contain insoluble and suspended solids, organic compounds, nutrient salts (containing ions such as NH_4^+ , SO_4^{2-} , and PO_4^{3-}), corrosive substances (such as alkalis and solvents), cleaning agents, lubricants, disinfectants, and other hazardous substances including hydrocarbons, chlorinated molecules, organic halogenated compounds and heavy metals (18).

The most important elements in wastewater originating from agricultural activities are typically related to the excessive use of fertilizers and these elements include nutrients; in fact, agricultural runoff often contains high concentrations nitrogen, with particular reference to organic and ammoniacal nitrogen, and phosphorus containing salts.

Excessive nutrient loading can lead to eutrophication, an overgrowth of algae and aquatic plants. This excessive growth depletes oxygen levels in the water, resulting in temporary oxygen deficiencies.

The chemical substances like pesticides pose environmental risks and can have adverse effects on aquatic organisms and ecosystems if not properly managed (19).

Water remediation is of utmost importance for several reasons. Firstly, it is crucial for environmental protection as it helps restore and maintain the health of ecosystems by reducing contaminants and pollutants in water bodies. This is vital for preserving biodiversity and ensuring the overall ecological well-being.

Secondly, water remediation is essential for safeguarding human health. By treating water sources and removing harmful substances, pathogens, and pollutants, it reduces the risk of waterborne diseases and ensures access to clean and safe water for drinking, sanitation, and hygiene.

Finally, as previously discussed, water remediation plays a significant role in ensuring the sustainable use of water resources.

The significance of wastewater treatment has grown significantly in recent years due to several factors. One of the primary reasons is the diminishing availability of water resources.

As mentioned before, as freshwater sources become scarcer, there is a greater need to effectively treat and reuse wastewater to meet the increasing water demands (20). This point permits a better rational use of the water resources with low quality being used, for example, for irrigation and good quality freshwater is being used for potable water and other special purpose (21).

Furthermore, environmental regulations have imposed lower limits on permissible contaminant levels in wastewater, requiring industries to adopt more advanced treatment technologies to ensure compliance.

As mentioned before, wastewater can also present an opportunity for energy recovery. In fact, the sludge produced from the wastewater treatment process is becoming increasingly important for biogas production. Wastewater treatment processes

consume energy for both mechanical and biological operations (22). The produced sludge is generally rich in organic carbon, usually present in a reduced form, capable of releasing a significant amount of energy. The methane content in the biogas varies depending on the type of organic matter digested and the process conditions, ranging from a minimum of 50% to approximately 80% (23).

Wastewater treatment involves a series of processes aimed at removing contaminants and pollutants from wastewater to make it safe for discharge or reuse. The main treatments used in wastewater treatment plants include physical, chemical, and biological processes.

Conventional wastewater treatment includes pretreatments, primary and secondary and tertiary treatments (Figure 1.5).

Tertiary treatments are generally used to improve effluent quality (24).

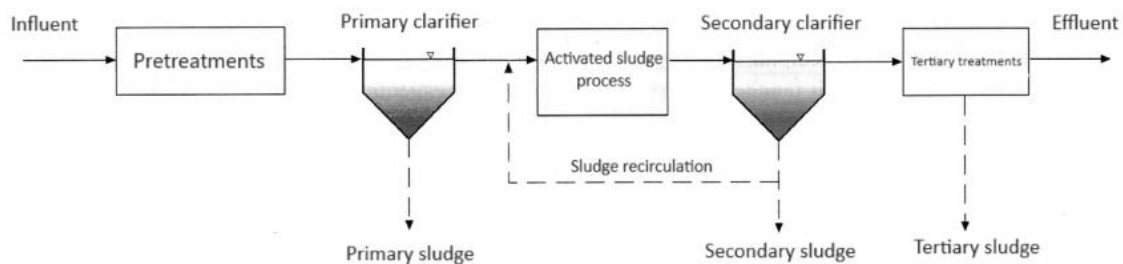


Figure 1.5: *General scheme for treatment of wastewater, (25).*

1.2.1. Pretreatments

In the initial phase of wastewater treatment, screens are employed to eliminate larger debris and foreign materials that could potentially harm equipment downstream.

This pre-treatment occurs through a screening process.

Screening allows for the removal of these larger solid debris, floating solids, and other foreign objects to protect and preserve the integrity and functioning of subsequent wastewater treatment plants.

It is a mechanical process with the main component being a grid system, typically made of stainless steel or specific corrosion-resistant plastic materials. The grids can be fixed or movable. Water, passing through the grid, is purified from objects such as stones, coarse waste, and woods (Figure 1.6).

The effectiveness of the process depends on the spacing of the grid openings, their shape, and the velocity of water flow through them.

The flow velocity in the inlet channel and through the grid is indeed the parameter that affects the suspension of the material, the pressure drops across the grid, and the risk of carried-away material that has been trapped.

The cleaning system is automated and is regulated based on the upstream-downstream pressure drop across the grid, on the order of a few centimeters, or on a time basis, although the latter option is generally less effective.

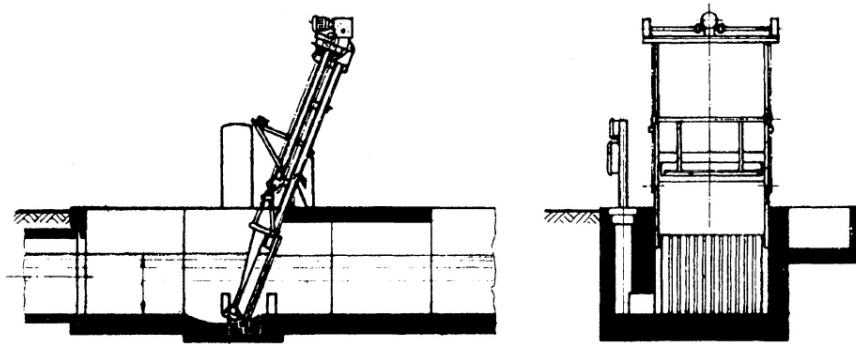


Figure 1.6: *Cross-section and frontal section of a grid (Source: Politecnico di Milano, Trattamento delle acque reflue).*

Following this, the treatment process involves the separation and extraction of grit, silt and oil. Grit removal plays a vital role in safeguarding mechanical equipment and pumps by minimizing wear and tear caused by abrasion and reducing the risk of blockages. The separation of these different components occurs in the same basin through settling and surfacing (Figure 1.7).

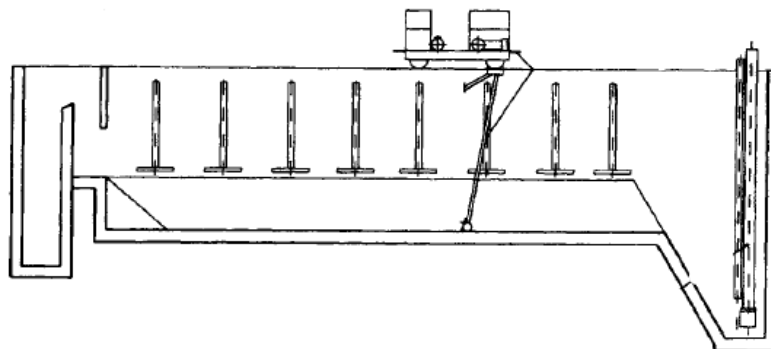


Figure 1.7: *Aerated sand trap and oil separator (Source: Politecnico di Milano, Trattamento delle acque reflue).*

The process is typically carried out by an aerated grit chamber, which is a basin where the water velocity is significantly reduced to facilitate the settling of sands, while an aeration system allows the flotation of oils.

1.2.2. Primary treatments

Primary treatments focus on the sedimentation process, which involves the use of clarifiers to settle solids.

The primary sedimentation phase aims to remove most of small-sized solid particles from the liquid flow by gravity.

These solids, if left in suspension, would compromise the efficiency of subsequent treatment stages, particularly aerobic processes.

Sedimentation occurs through various physical processes, each typical of a different phase of the treatment plant.

In fact, while grit removal is a discrete process, based on the independent settling of particles moving at terminal velocity according to Stokes' law, in primary sedimentation flocculent settling prevails.

This means that solid particles coalesce and flocculate, forming variable-sized flocs with different sedimentation velocities: Stokes' law remains valid, but only punctually and instantaneously, thus it cannot be used to describe the phenomenon as a whole.

Sedimentation tanks, or lamellar settlers, consist of a rectangular or circular basin in which multiple inclined plates are placed. These plates are arranged parallel to each other and inclined at an angle between 45 and 60 degrees relative to the water surface (Figure 1.8). This configuration facilitates the sedimentation of flocs and the sliding of captured material, thereby preventing clogging and malfunctions of the operating unit.

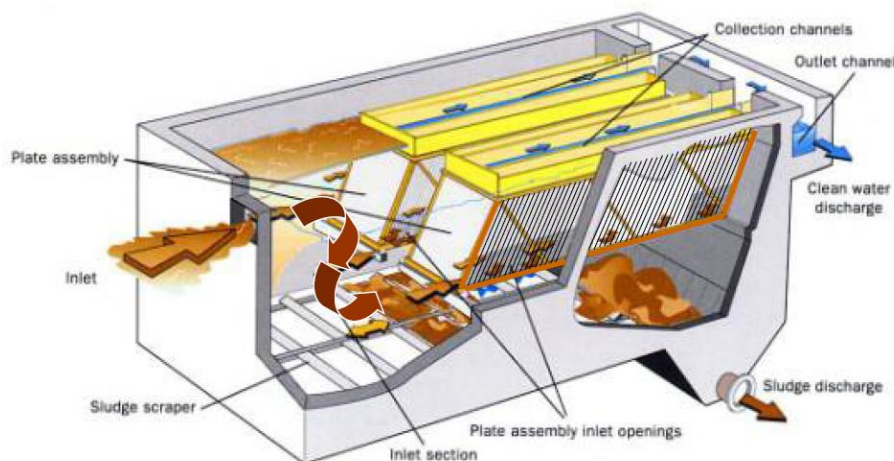


Figure 1.8: *Lamellar settler* (Source: Politecnico di Milano, *Trattamento delle acque reflue*).

Additionally, other methods may be utilized to further remove suspended particles and improve the overall quality of the treated wastewater, for example gravity settling, chemical coagulation, or filtration.

By implementing these steps, the settled solids can be effectively removed (26).

Additionally, any floating materials present in the wastewater that have not been previously removed, such as fats, oil, and grease, are typically skimmed off the surface of the tank. This is done using mechanisms such as skimmers or siphons, which remove the floating materials and prevent them from mixing back into the treated wastewater.

1.2.3. Secondary treatments

The secondary treatment stage typically involves the activated sludge process, which derives its name from the production of an activated mass of microorganisms capable of aerobically stabilizing the organic content of the wastewater, typically measured as COD (Chemical Oxygen Demand).

In this process, the wastewater is introduced into an aerated tank where the activated sludge, consisting of microorganisms, is mixed with the wastewater (27).

The basic infrastructure of an activated sludge process consists of a continuous-flow bioreactor in which suspended heterotrophic microorganisms consume colloidal and dissolved organic matter. The reactor is aerated to provide dissolved oxygen (DO) for aerobic biodegradation. Bacteria consume a portion of colloidal and dissolved carbonaceous compounds to meet their energy needs (catabolism) and synthesize another portion, along with a small percentage of ammonium and phosphorus, into new cellular tissues (anabolism).

A settling tank (referred to as secondary settler or clarifier) where activated sludge (flocculated biomass) is gravitationally separated from the treated wastewater (28).

Typically, there is a recirculation of sludge collected in the hopper at the head of the bioreactor: this allows decoupling the hydraulic retention time (HRT) from the sludge retention time (SRT). A sludge recirculation line enables the return of the majority of the settled sludge to the bioreactor, thus maintaining a high bacterial concentration in the reactor to enhance the removal of biological nutrients.

The specific biomass growth for this process is influenced by various factors such as pH, temperature, substrate availability, oxygen availability, presence of macronutrients such as phosphorus and nitrogen and the presence of inhibitors.

Specifically, regarding temperature, these are mesophilic microorganisms, operating within a range of 20 to 40 °C.

Bacterial growth is well described by Monod kinetics, which is the most commonly used kinetic model for modeling biomass growth (29), where bacterial synthesis is proportional to the consumption of biomass itself (Equation 1.1); μ indicates the bacterial growth rate, $\mu_{\max 20^{\circ}\text{C}}$ is the maximum growth rate that would be achieved at

substrate concentrations sufficiently high not to be limiting at 20 °C. This parameter is a characteristic of each bacterial species and each substrate.

At last $\mu_{T,pH}$ represents the bacterial growth rate under specific conditions of pH, temperature, substrate presence, oxygen, and nutrients; in general, 'K' represents the half-saturation constant of the specified element or substrate.

$$\frac{dx}{dt} = \mu \cdot x$$

$$\mu_{T,pH} = \mu_{max20^{\circ}C} \cdot \frac{S}{S + K_S} \cdot \frac{N}{N + K_N} \cdot \frac{P}{P + K_P} \cdot \frac{O_2}{O_2 + K_{O_2}} \cdot \theta^{(T-20^{\circ}C)} \cdot f(pH)$$

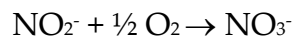
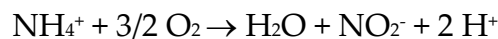
Equation 1.1: *Monod kinetic.*

As mentioned earlier, the presence of nitrogen compounds in the flow can pose significant risks to human health and ecosystems. For this reason, the 'Testo Unico in materia ambientale' (Legislative Decree 3 April 2006, no. 152) sets increasingly stringent limits regarding the discharge of ammonia, nitrites and nitrates.

Therefore, coupled with the activated sludge process, we have the nitrification and denitrification processes.

Nitrogen is eliminated through a two-step process: firstly, ammonium is oxidized to nitrate in oxygen-rich conditions (nitrification step); subsequently, the resulting nitrate is converted into nitrogen gas under oxygen-depleted conditions (denitrification step) (30).

Nitrification is carried out by aerobic autotrophic bacteria, particularly the Ammonia Oxidising Bacteria (AOB) (Equation 1.2) and the Nitrite Oxidising Bacteria (NOB) (Equation 1.3). The AOB are responsible for the oxidation of ammonia to nitrite, a process that occurs naturally in sewers, while the NOB convert nitrite to nitrate (31).



Equation 1.2: *Ammonia Oxidising Bacteria.*

Nitrification primarily occurs under mesothermic conditions, between 20 and 35 °C, and at a neutral pH (7,2-8).

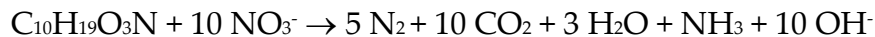
Generally, the growth kinetics of NOB (Nitrite Oxidising Bacteria) are higher than that of AOB (Ammonia Oxidising Bacteria), hence there are no accumulations of nitrite.

Often, the aerobic process for COD (Chemical Oxygen Demand) removal and the nitrification process are combined in the same reactor.

Denitrification is an anoxic heterotrophic process. The bacteria involved in this process transform biodegradable COD using nitrous oxides as electron acceptors (32).

The nitrate formed from nitrification in municipal wastewater or already present in some industrial effluents is reduced to molecular nitrogen N_2 , a sparingly soluble gas in water that is released into the atmosphere.

Assuming a generic formula for biodegradable COD $C_{10}H_{19}O_3N$, the denitrification reaction is:



Equation 1.3: *Nitrite Oxidising Bacteria.*

The kinetics of nitrate removal are proportional to the bacterial growth kinetics; hence, the rate depends on how rapidly biodegradable the organic substrate is.

Unfortunately, the value of the substrate present in the anoxic denitrification reactor is not directly calculable because it depends on the growth rate and nitrate removal rate, as well as the extent of recirculation. Therefore, experimental and empirical expressions are employed to calculate the denitrification rate.

The most used plant layout is the one involving pre-denitrification, ensuring that biodegradable COD is not entirely consumed in the aerobic activated sludge reactor (Figure 1.9).

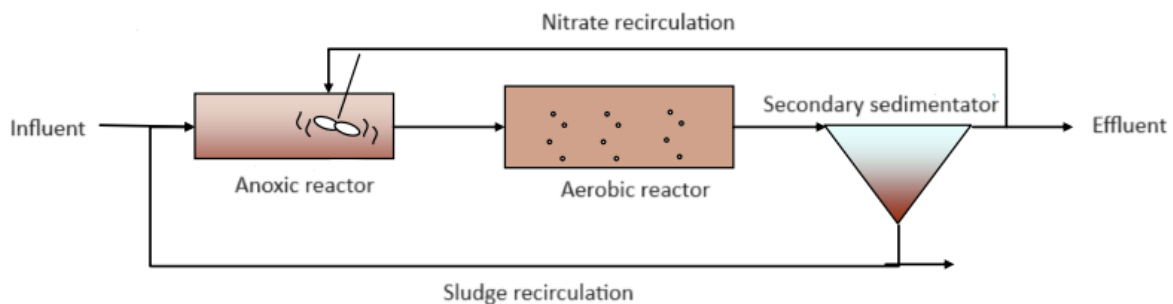


Figure 1.9: *Pre-denitrification, (33).*

On the other hand, in the case of post-denitrification, it would be necessary to dose rapidly biodegradable organic substances, such as methanol or acetic acid, to support denitrification, thereby increasing operating costs.

The combination of autotrophic and heterotrophic processes for converting organic nitrogen into N_2 is efficient in meeting regulatory standards. However, the growth rate of autotrophic organisms is slow, and heterotrophic denitrifying organisms work

efficiently only under anaerobic conditions. This is why two separate reactors are used, impacting both plant costs and footprint (34).

To address these challenges, several new processes, such as anammox (anaerobic ammonium oxidation), comammox (complete ammonia oxidation), short-cut nitrification denitrification have been proposed.

Alternatively, there are various secondary treatment options available, which can be classified into four main categories: fixed film systems, suspended growth systems (MBBR), membrane bioreactors (MBR), and sequencing batch reactors (SBR).

Fixed film systems utilize a solid medium, such as rocks or plastic media, to provide surfaces on which microorganisms can grow and treat the wastewater.

The supports can be non-submerged with natural aeration, where the flow percolates from the top, referred to as trickling filters. Alternatively, the support can be submerged directly in the flow itself, with forced aeration.

Suspended growth systems (MBBR) (Figure 1.10) involve the continuous mixing of wastewater with microorganisms in an aerated tank. The supports are small movable elements known as biocarriers with a density similar to that of water to ensure their suspension in the fluid. These elements have an extremely high specific surface area (from 400 up to 1200 m²/m³) to promote biomass growth (35).

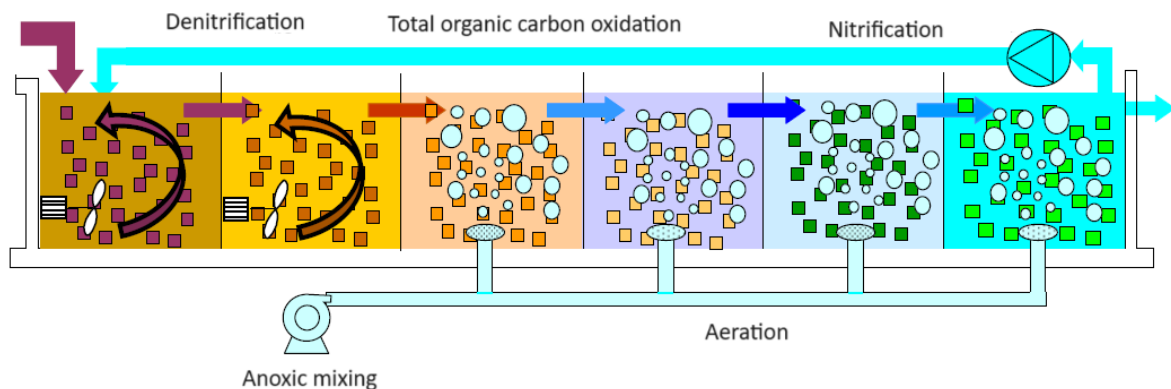


Figure 1.10: MBBR schematic process (Source: Politecnico di Milano)

At the reactor outlet, there is a suitable sieve system that prevents the biocarriers from escaping with the flow; aeration is forced.

Both configurations allow for a reduction in the reactor's footprint as the biomass is more concentrated. Additionally, there is no need for sludge recirculation, making these configurations relatively simple. On the other hand, they require higher investment costs, more advanced pretreatments to avoid the risk of clogging, and longer startup times.

Membrane bioreactors (MBR) use a combination of biological treatment and membrane filtration to achieve high-quality effluent.

The MBR is a suspended growth activated sludge system that utilizes microporous membranes for solid/liquid separation instead of using secondary clarifiers (36).

The membrane acts as a filtering support that retains suspended or dissolved substances based on the size of its pores. Flow through the membrane is achieved by applying a trans-membrane pressure (TMP), and this depends on factors such as solution viscosity, temperature, membrane thickness, cutoff, and the level of fouling.

The use of membranes represents a significant technological advancement in the field of wastewater, as it overcomes the drawbacks of conventional activated sludge systems. These drawbacks include the large space required for secondary clarifiers, issues related to liquid-solid separation, and excess sludge production. This system indeed provides high-quality effluents, shorter SRT and HRT, and the potential for simultaneous nitrification and denitrification in the case of long SRT (37).

One of the disadvantages of this system, with higher energy consumption, is membrane fouling as it significantly reduces performance and increases pressure drop.

The fouling of the membrane in MBRs is attributed to suspended particulates, colloids, solutes, and floc particles. These materials deposit on the membrane surface and within the membrane pores, clogging the pores and leading to a decrease in membrane permeability (Figure 1.11).

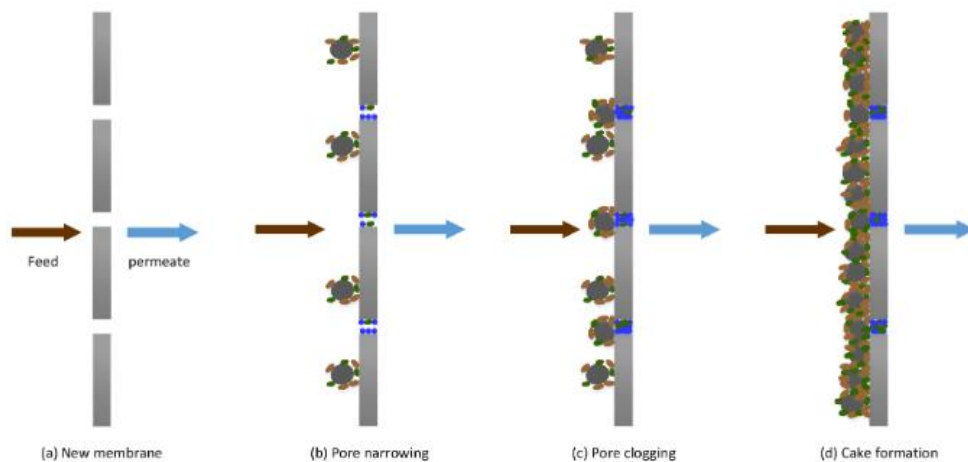


Figure 1.11: *Membrane fouling*, (39) .

The wide variety of components, both organic and inorganic, that make up fouling, makes controlling this issue highly complex (38).

The typical configurations can be either external membrane, where the membrane is placed in a compartment outside the main biological reactor, or immersed membrane, where the membrane is submerged (Figure 1.12).

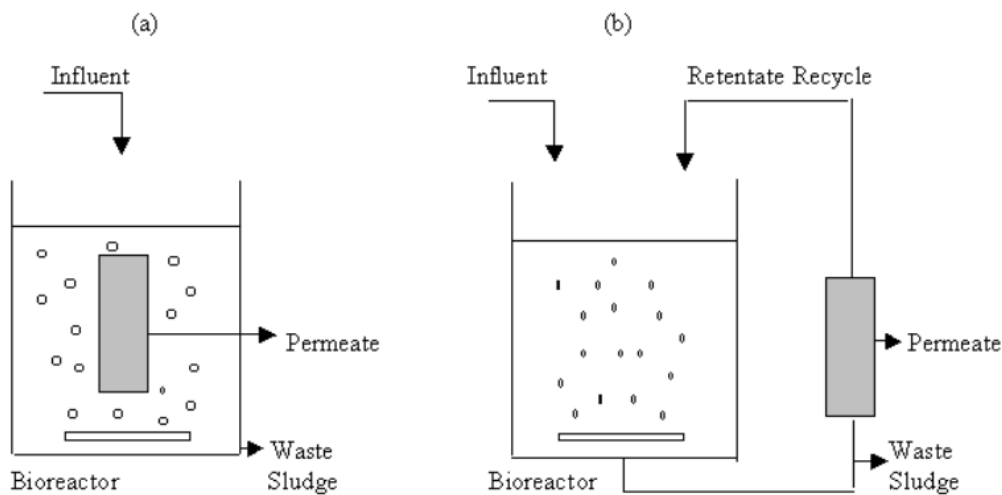


Figure 1.12: (a) Submerged MBR configuration (b) External MBR configuration, (40).

The material of which the membrane is composed affects its fouling propensity. Membranes can be classified into ceramic membranes, polymeric membranes, and composite membranes. Ceramic membranes have the advantage of being inert and exhibiting high chemical resistance; they are also easy to clean.

Polymeric membranes are more common because they are less expensive than ceramic ones. The materials they are made of vary widely, including polyethersulfone (PES), polyethylene (PE), and polypropylene (PP), among many others. They tend to foul more easily compared to ceramic ones.

Composite membranes are made from two or more materials to combine the strengths of the constituent materials in the final product.

Sequencing batch reactors (SBR) operate in a batch mode, where the wastewater is treated in discrete cycles.

The plant of the SBR type involves, within a single reaction basin, all the phases of the activated sludge water treatment process occurring sequentially in time (41).

This configuration (Figure 1.13) is a 'fill and draw' activated sludge system is used for both municipal and industrial wastewater treatment. In this system, aeration, sedimentation, and clarification can be achieved using a single batch reactor. It operates without a clarifier (42).

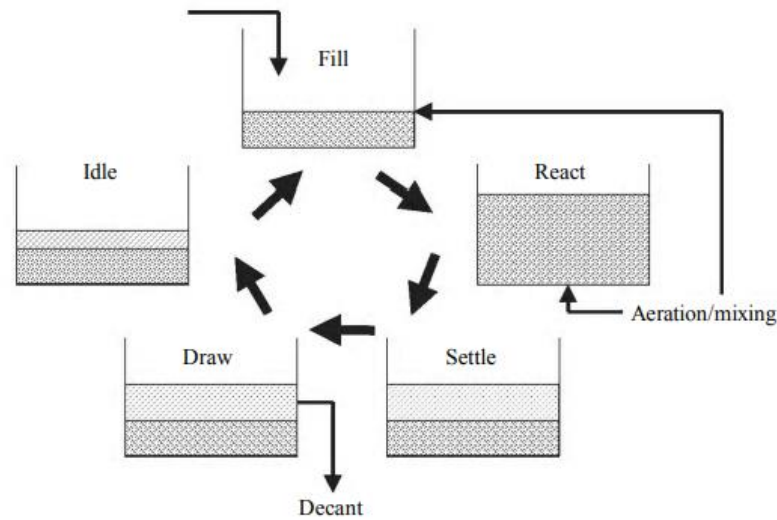


Figure 1.13: SBR configuration, (43).

These systems have the advantage of being very compact and flexible, allowing for adaptation of reaction methods and feeding times. However, they require more sophisticated controls and management systems as well as frequent maintenance.

1.2.4. Tertiary treatments

Tertiary treatments in the field of wastewater remediation refer to additional treatment stages that follow primary and secondary treatments. These treatments are designed to further enhance the quality of the treated water, making it suitable for specific purposes such as industrial reuse, irrigation, or discharge into sensitive environments.

Some of the key tertiary treatments include advanced filtration (microfiltration, ultrafiltration), disinfection that can be achieved using methods such as chlorine addition, ozone, ultraviolet (UV) radiation, or advanced oxidation processes, nitrogen and phosphorous containing nutrients removal.

Disinfection is a crucial step in wastewater treatment. Wastewater can contain a wide variety of microorganisms, some of which are pathogens. These microorganisms fall into four categories: Bacteria, Viruses, Protozoa, and Helminths (including Nematodes). This is why all treatment plants must be equipped with a disinfection system.

Bacteriological limits are specified in the authorization issued by the competent authority, depending on the intended use of the water body. Therefore, different limits apply to water intended for bathing, irrigation, domestic use, or industrial use.

The disinfecting agents used include sodium hypochlorite, chlorine dioxide, peracetic acid (PAA), ozone, and UV rays.

Disinfection by chlorination is one of the most commonly used disinfection methods in wastewater treatment due to its low cost, ease of management, and high efficiency in destroying microorganisms. However, its toxicity is well known; chlorine can also generate dangerous disinfection by-products by reacting with the organic matter present in wastewater, for example trichloromethane (44).

Peracetic acid is a valid alternative to the use of chlorine, being a broad-spectrum disinfectant with good efficacy, reduced ecotoxicity, and negligible production of by-products. The weakness of this disinfectant is its low persistence, as it tends to naturally decay in water (45).

Ozone is a disinfectant that has been widely used in this field, especially as a substitute for chlorinated compounds. Ozone is unstable in water and, decomposing rapidly, leads to the formation of hydroxyl radicals, another powerful oxidant that can contribute to disinfection (46).

UV disinfection offers the advantage of avoiding the use of chemical substances, thus preventing the formation of by-products. UV consists of electromagnetic radiation between X-rays and visible light in the wavelength range from 100 to 400 nm, and the germicidal effect of UV rays is between 220 and 320 nm. UV lamps that emit radiation at 254 nm (UV-C) are the ones with the highest germicidal effect (47) (Figure 1.14).

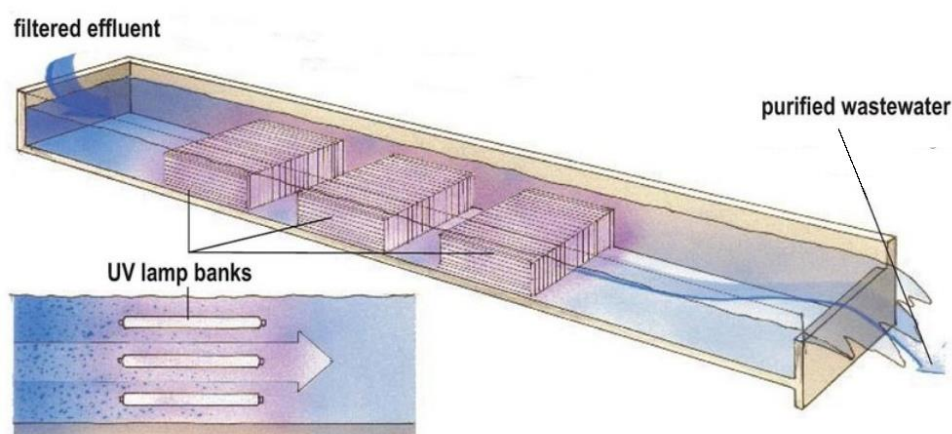


Figure 1.14: : UV configuration consisting of a channel through which the polluted fluid flows, passing through UV lamps, (49).

Short-wavelength ultraviolet light destroys the DNA/RNA of microorganisms and disrupts their cellular activities and reproduction, a phenomenon known as photolysis (48).

Finally, there is adsorption: this process can be employed to remove specific contaminants from the treated water.

Among these products to be removed, there are toxic pollutants such as dyes, heavy metals, surfactants, personal care products, pesticides, and pharmaceuticals, as well as emerging pollutants (e.g., PFAS) (50).

Adsorption involves the use of porous materials to capture and retain pollutants. In fact, adsorption technology can remove organic materials from wastewater that resist removal by biological treatment and inorganic pollutants that have escaped the previous capture processes.

The materials typically used are traditional adsorbents such as zeolites, clays, and activated carbons (AC), while the most used nanostructured materials are CNTs, fullerenes, and graphene.

Zeolites are crystalline microporous aluminosilicate minerals, whose elementary units consist of SiO_4 and AlO_4 tetrahedra, widely used as adsorbents and ion exchangers. They belong to the group of tectosilicate minerals, and some of them can be found in nature (about fifty varieties of natural zeolites are known). Their well-defined pore size and the ability to easily regenerate while maintaining their initial properties make zeolites a highly desirable material for various applications.

Zeolites are a complex adsorption system, consisting of micropores, which are the first to fill with pollutants, mesopores, and macropores. In the past, zeolites were primarily used for the removal of pollutants from gas streams. Nowadays, they are also applied in the field of wastewater treatment, particularly notable for the removal of aromatic hydrocarbons (51).

Clays, both natural and synthetic, are also highly important in this field. They have been used for many decades as adsorbents, for instance, for the removal of metals. Clay minerals are primarily phyllosilicate minerals and typically have particle sizes smaller than $2\ \mu\text{m}$ (52).

Due to their complex porous structure with a high surface area, both the internal and external surfaces of clays can readily interact with dissolved species effectively. Clays are thus an appealing product, also due to their low cost, making them highly attractive in this regard.

Typically, carbon adsorption is a process that involves passing the wastewater effluent through a bed or canister filled with activated carbon granules or powder. This method is highly effective in removing more than 98% of trace organic substances present in the water. The trace organic substances in the water are adsorbed to the surface of the carbon, allowing them to be effectively removed from the water (53).

The adsorbent material, depending on the configuration adopted in the plant, for example, if it is placed inside a dedicated fixed-bed reactor, can be regenerated. The

regeneration of the material involves stripping the adsorbed pollutant, so that the active sites of the adsorbent are clean again.

Regeneration is generally a rather costly process, as it is not always possible to carry it out in situ, but often it needs to be done ex situ.

It can be done through the application of hot steam, and this is one of the more economical alternatives.

Alternatively, there is thermal desorption, carried out inside furnaces (rotary, fixed-bed, or fluidized bed). However, this technique causes the emission of large amounts of CO₂ and the pollutants adsorbed in the flue gas.

In the chemical regeneration of the adsorbent, specific chemical reagents are used to desorb or decompose the adsorbates.

There are also other regeneration mechanisms based on the application of microwaves, electrochemical regeneration, and bioregeneration (54).

1.3. Carbonaceous materials

Nanomaterials are an interesting class of materials that encompass a wide variety of samples, with at least one dimension falling between 1 and 100 nm (55).

They represent an excellent example of emerging technology, and this field of science enables the creation of highly technological and high-performance engineered products.

It is difficult to find a single internationally accepted definition of nanomaterials, which is why a precise definition of nanomaterials is still a topic of discussion within the scientific community (56).

Nanomaterials serve as foundational elements in the domains of nanoscience and nanotechnology: these scientific fields encompass the research, development, manufacturing, and processing of such materials in science, energy, medicine, engineering, technology, sensors, and industries (Figure 1.15).

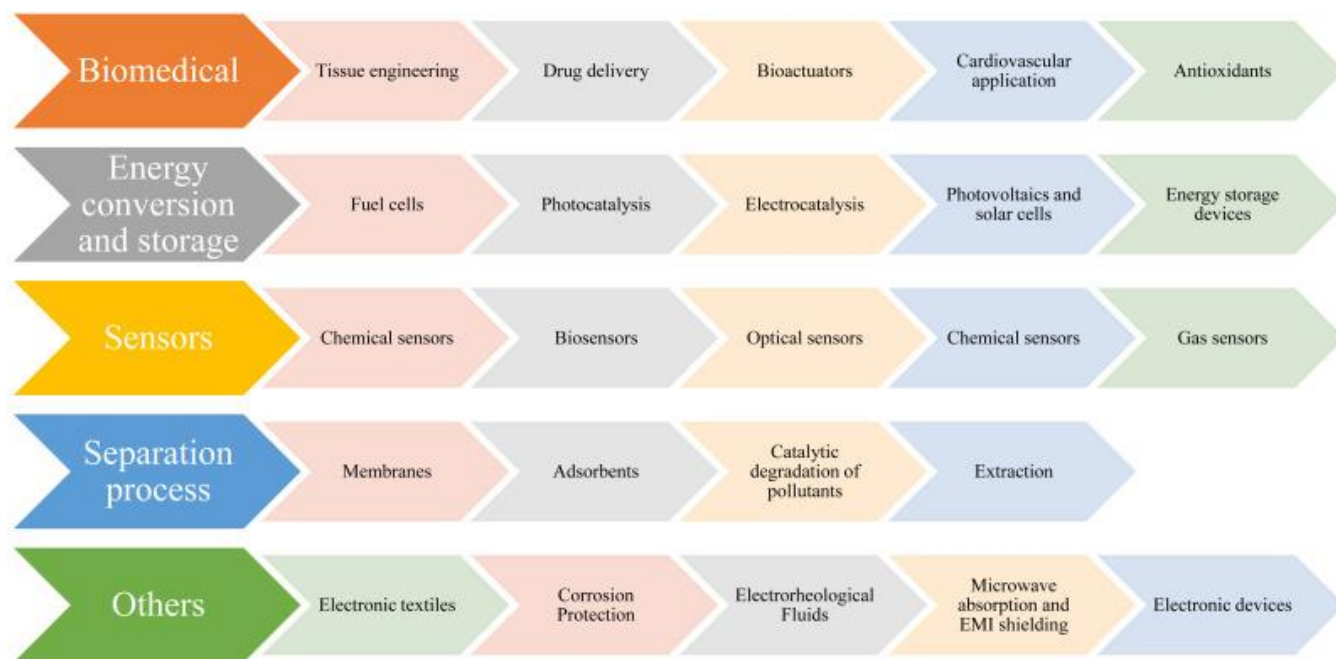


Figure 1.15: *Application of nanomaterials, (57).*

The precise control of nanomaterials' size, shape, and composition poses a significant challenge, yet it profoundly influences their performance (58).

Indeed, it is possible to produce nanomaterials with excellent mechanical, magnetic, electrical, physical, and catalytic properties by precisely controlling the size, shape, synthesis conditions, and appropriate functionalization.

There are several methods for the synthesis of these materials.

The synthesis mechanism of nanomaterials itself, along with the parameters that characterize it, strongly influences the properties of the final product. This is why scientists and engineers are making significant progress in improving the synthesis methods of these materials (59).

In general, we can classify two main approaches: the first one is the "bottom-down" method, which is based on reducing the dimensions of larger structures through mechanical force. The second is the "bottom-up" approach, which involves assembling nanostructures from molecules and atoms (60).

In this context, carbon nanostructures (CNS) play a prominent role, as they are composed of an element that forms the basis of life on planet Earth and is widely available through various natural sources.

Among the typical graphitic nanostructures, there are carbon nanotubes (CNTs), carbon nanofibers (CNFs), graphene, graphene oxides, fullerenes, carbon nanohorns, onion-like carbon (OLC), nano diamonds and graphene dots (Figure 1.16) (61).

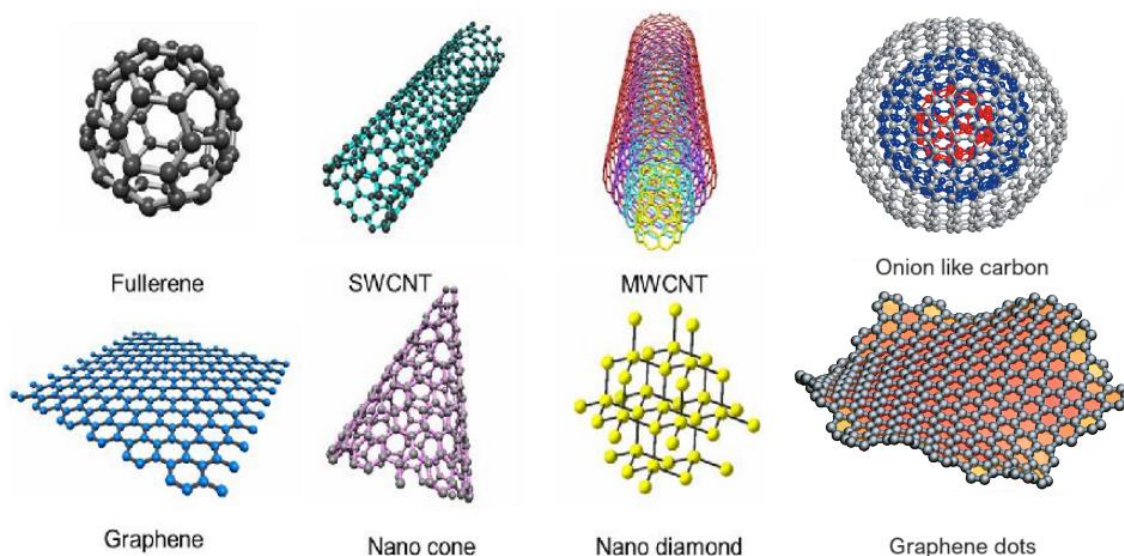


Figure 1.16: *Graphitic nanostructures, (62).*

The specific hybridization properties of carbon, combined with the sensitivity of the carbon structure to perturbations in synthesis conditions, allow for highly tailored manipulation. Therefore, the physical, chemical, and electronic properties of carbon nanomaterials are strongly linked to the structural conformation of carbon and, thus, its hybridization state (63).

The aforementioned materials are nanomaterials consisting of networks of sp^2 -hybridized carbon atoms, primarily held together by conjugated carbon-carbon double bonds that create a system of π electrons extended throughout the nanostructure. This is, in fact, the origin of their excellent electrical conductivity, which is accompanied by other properties such as thermal conductivity, mechanical strength, and high specific surface (64).

Due to their exceptionally high surface energy, large specific surface area, and quantum confinement effects, materials produced at the nanoscale exhibit many unique features, including optical, magnetic, electrical properties, among others. In particular, carbon materials have proven to be exceptional options as adsorbents, catalysts, or catalyst supports, outperforming traditional materials in various scenarios (65).

The research community is extremely interested in investigating innovative areas of carbon nanotechnology due to the quick advancements in science and technology. Their versatility and tailored properties make them indispensable in diverse fields, but their economic feasibility will be a key aspect to expand their use. Indeed, while carbon nanomaterials are economically feasible for research purposes, their utilization in

regular industrial practice is still limited. Moreover, modifications make the product more expensive (66).

1.3.1. Carbon nanotubes

The thesis now focuses on carbon nanotubes, discovered by Sumio Iijima in 1991.

Carbon nanotubes (CNTs) are carbon allotropes with a tubular nano-architecture, composed of cylindrical graphene sheets arranged in a hexagonal sp^2 beehive pattern. The carbon atoms in each plane are separated by a distance of 0.142 nm, while the thickness of the plane is 0.335 nm (67).

Depending on the number of layers, CNTs are classified as single-wall carbon nanotubes (SWCNTs) or multiwall carbon nanotubes (MWCNTs) (Figure 1.17). SWCNTs consist of a single layer of graphene tightly wrapped into a hexagonal cylindrical structure, with lengths ranging from 20 to 1000 nm and diameters between 0.3 and 3 nm. MWCNTs, on the other hand, have a coaxial cylinder with a hollow core surrounded by a graphene sheet. MWCNTs typically have diameters between 1 and 100 nm, internal diameters of 1 to 3 nm, and lengths ranging from 1 to several μm (68).



Figure 1.17: *Single-wall and multiwall carbon nanotubes, (69).*

The range of variability in these measurements is due to the synthesis method used for their production.

Due to their nanometric diameter, CNTs have a very large specific surface area.

The strength of the sp^2 carbon-carbon bonds gives carbon nanotubes exceptional mechanical properties (70), contributing to their strength.

The Young's modulus of CNTs, a measure of material stiffness, exceeds that of all carbon fibers, with values greater than 1 TPa, approximately 5 times higher than steel (71).

In addition, thanks to theoretical and experimental studies, they have also shown high tensile strength, making them suitable for enhancing the mechanical properties of other compounds (72).

Besides to their outstanding mechanical properties, carbon nanotubes exhibit extraordinary electronic properties. They possess high electrical conductivity comparable to copper (73).

Indeed, the electrical conductivities of SWCNTs and MWCNTs are about 10^2 – 10^6 S cm^{-1} and 10^3 – 10^5 S cm^{-1} , respectively. SWCNTs and MWCNTs also display excellent thermal conductivities of ~ 6000 W m^{-1} K^{-1} and ~ 2000 W m^{-1} K^{-1} , respectively, remaining stable at temperatures exceeding 600 °C (74).

Notably, carbon nanotubes can exist in metallic or semiconducting forms. Because of this, it has been one of the key elements in the construction of electronic devices such as diodes, transistors, and interconnectors (75).

There are numerous challenges to enhance the utilization of carbon nanotubes (CNTs), such as issues with agglomeration and interfacial bonding dispersion in aqueous media due to their hydrophobic nature. Indeed, CNT clusters form due to van der Waals attraction and hydrophobicity: these clusters, because of their strong interactions, hinder solubility or dispersion in water and organic solvents. This makes them less suitable for certain applications such as biomedical devices, drug delivery, and cellular biology (76).

To overcome these challenges, surface modification becomes essential, and this can be achieved through functionalization of multiwall carbon nanotubes (77).

Researchers have envisioned surface modification of CNTs to enhance their chemical properties.

CNT surface functionalization can be carried out through covalent and non-covalent methods, depending on the desired linkage between CNTs and functional molecules (78) (Figure 1.18).

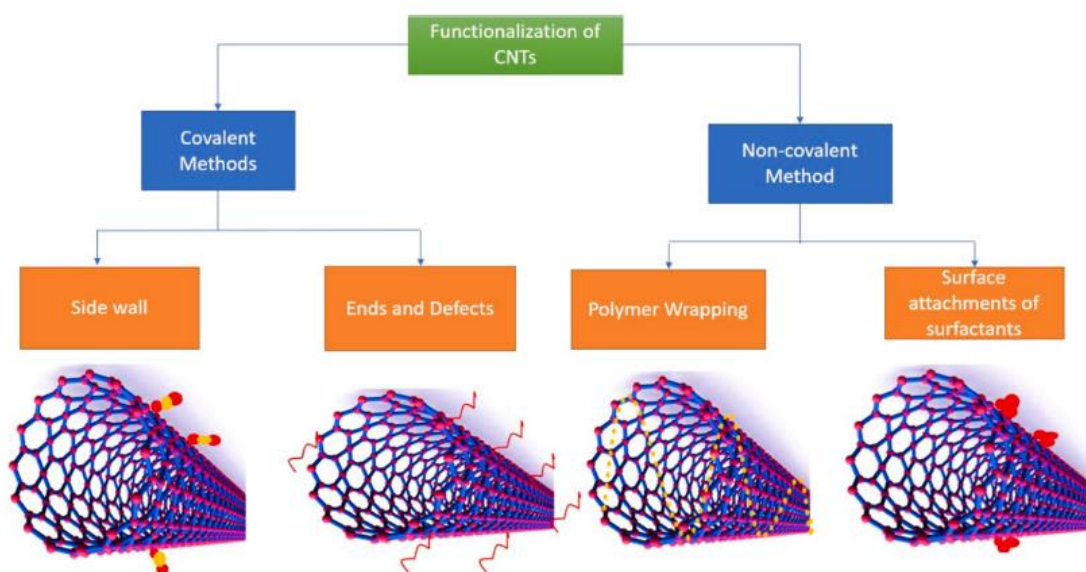


Figure 1.18: Surface functionalization, (80).

Covalent functionalization, in which the functional group is covalently attached to the sidewalls of the carbon nanotubes, involves attaching functional groups like OH, COOH, and NH₂ onto the CNT surface through sharing of electrons. This type of functionalization modifies the surface of the product, thus altering its initial properties.

On the other hand, non-covalent functionalization relies on van der Waals forces, electrostatic interactions, π - π interactions, CH- π interactions promoting the dispersion of CNTs in a wide variety of solvents and polymers, thus expanding their range of applications (79).

Indeed, surface modification plays a crucial role in improving the surface properties of CNTs. Functionalized CNTs can be better tailored for specific applications, opening up new possibilities for their utilization.

Actually, carbon nanotubes have found extensive use in a wide range of applications owing to their numerous properties. They have been employed in energy storage and conversion devices, sensors, hydrogen storage media, nanosized semiconductor devices, probes, drug delivery systems, artificial implants, and high-strength composites (81).

Beyond these applications, CNTs have also proven valuable in wastewater treatment and drinking water purification. This is attributed to their enhanced adsorption, catalytic, and electrochemical properties, as well as their high mechanical strength, specific surface area, superior water transport capability, and excellent chemical inertness. In the field of water treatment, CNTs have been successfully utilized for oil-water separation, water desalination, and the removal of emerging pollutants, including persistent organic and inorganic pollutants (82).

1.4. Nanotechnologies in wastewater management

Nanotechnologies have been widely embraced in various sectors, such as medicine, pharmacy, energy, chemistry, electricity, food production, military, physics, materials science, biotechnology, and other commercial fields, thanks to their unique properties because their structures are determined on the nanometer scale.

As the global population continues to grow, leading to increased demands for environmental resources, nanotechnologies have emerged as a critically important area in the environmental sector, offering numerous advantages (83).

In the environmental field, technology can be applied in four areas: remediation, protection, mitigation, and enhancement. Currently, the most rapidly advancing field is remediation.

Especially, nanotechnology has demonstrated remarkable achievements in wastewater treatment.

Indeed, in recent decades, a large quantity of highly hazardous organic compounds has been synthesized and released into ecosystems, including pesticides, heavy metals, fuels, polychlorinated biphenyls (PCBs) (Figure 1.19), polycyclic aromatic hydrocarbons (PAHs) (Figure 1.20), perfluorinated alkylated substances (PFAS) (Figure 1.21) (84).

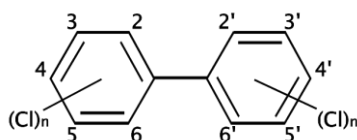


Figure 1.19: PCBs.

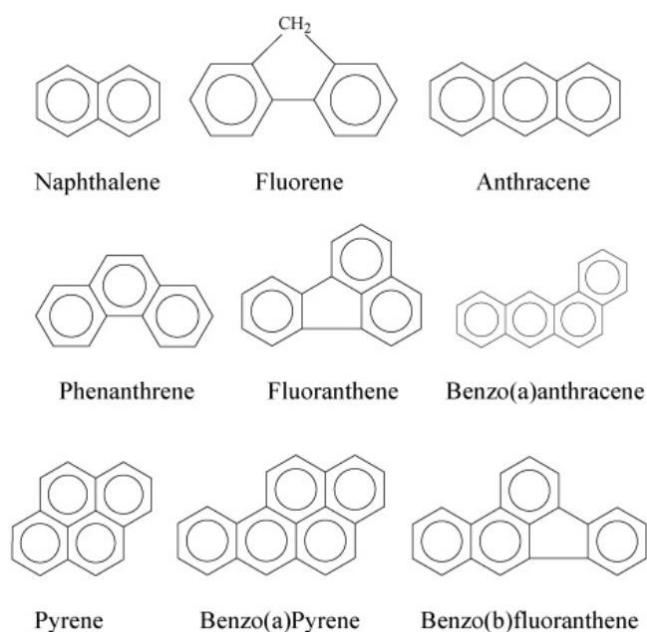


Figure 1.20: PAHs, (85).

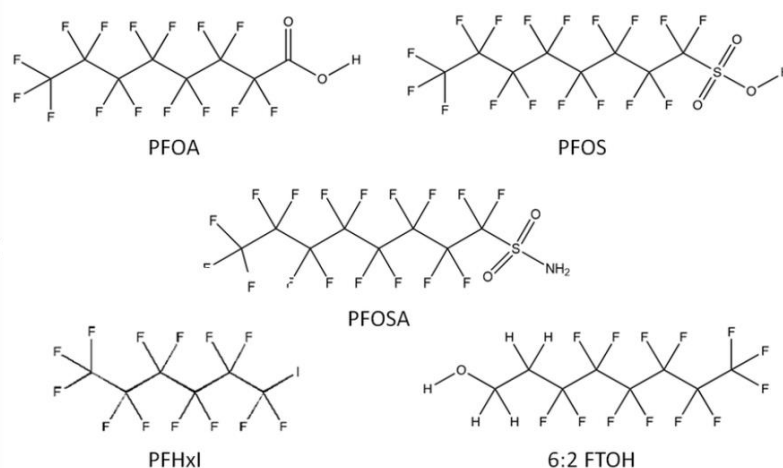


Figure 1.21: Chemical structure of some PFAS, (86).

These substances pose a significant challenge for the contemporary world. Unfortunately, many traditional solutions for cleaning up these substances are very costly and often not very efficient.

But carbonaceous nanomaterials present unprecedented opportunities to create more effective adsorbent and redox-active media for wastewater purification.

Nanomaterials have proven to be highly effective in removing various pollutants from wastewater, such as heavy metals, organic and inorganic solvents, dyes, as well as biological toxins and disease-causing pathogens like cholera and typhoid (87).

Currently, there is a pressing need for the development of novel wastewater treatment methodologies to efficiently remove contaminants from wastewater. In this way, nanotechnology stands out as a potential solution in this regard, offering nanomaterial-based wastewater treatment options.

Nanomaterials, as previously discussed, possess unique properties, including high surface-to-volume ratios, extremely small in size, high sensitivity and reactivity, high adsorption capacity, and ease of functionalization, that is the easy incorporation of desired structures and functional groups on the adsorption surface. These properties grant them the potential to overcome the limitations associated with traditional methods (88).

In municipal and industrial wastewater treatment, advanced application of nanotechnologies is, meanwhile, established via adsorption processes, photocatalytic degradation, and partly by membrane filtration processes (89).

1.4.1. Adsorption as the most widely used process in nanotechnologies

Overall, adsorption is the most common, cheapest, fastest, and the oldest method employed in water purification.

In fact, adsorption is a widely used technique in water and wastewater treatment for the removal of organic and inorganic contaminants, often serving as a polishing step.

The term "adsorption" was introduced in 1881 by the chemist Kayser, although many phenomena related to adsorption have been known since ancient times. The first qualitative observations were made in the second half of the 1700s by the chemist Scheele through experiments with charcoals and clays. Subsequently, Lowitz conducted studies on adsorption in the field of decolorization, which were then furthered mathematically in 1814 by Saussure who discovered the exothermic nature of the process. Many other scientists engaged in the study of this phenomenon from a practical standpoint, paving the way for the "pioneering" theoretical age of the field, namely the modeling of adsorption isotherm equations (90).

Adsorption is an exothermic surface phenomenon that entails the transfer of a phase, such as a molecule or ion present in either liquid or gaseous bulk, referred to as the adsorbate, onto a solid (or rarely liquid) surface known as the adsorbent. This transfer occurs through physicochemical or chemical interactions, under specific conditions (91).

Adsorption can be categorized into three types based on the interactions between the adsorbent and adsorbate: chemisorption, physical adsorption and ion exchange (Figure 1.22).

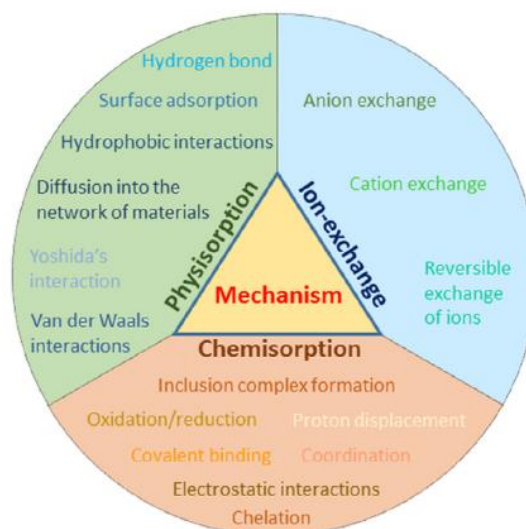


Figure 1.22: *The adsorption mechanisms, (93).*

Chemisorption is an irreversible process driven by strong chemical interactions; it often requires high temperatures, and this is associated with the activation energy.

Instead, physisorption is a reversible process where weak intermolecular physical forces, such as π - π interactions, dipole-dipole interactions, van der Waals forces, hydrogen bonding, and so on, play a role in the interaction between the adsorbate and the adsorbent surface (92). It is not a site-specific process like chemisorption since the adsorbate is free to cover the entire surface.

Ion exchange adsorption is a physicochemical process that occurs in a wide range of colloidal systems such as clays and engineered nano-colloidal particles. For instance, in the case of clays, they have surfaces with electric charge that allows them to adsorb ions present in the surrounding solution.

Therefore, adsorption involves the transfer of a portion of the pollutant concentration in the solution to the surface of the adsorbent. As the process continues, an equilibrium state is reached where the same amount of pollutant is both adsorbed and desorbed simultaneously.

The position of this equilibrium depends on the temperature, the solute, the pH, the solvent, ionic strength, and many other variables related to the entire adsorption system (94).

The function that represents the amount of adsorbate per unit of adsorbent as a function of equilibrium concentration in the solution at a given temperature is called the adsorption isotherm.

These adsorption models are crucial for calculating the adsorption capacity and provide a lot of information on how the adsorbent and the pollutant interact with each other (95).

There are many expressions of isotherm models that have developed over the years. They have been formulated based on kinetics, thermodynamics, and empirical approaches (96).

Based on the number of parameters, adsorption models are classified as one-parameter, two-parameter, and three-parameter models.

Some curves describe monolayer adsorption, while others describe multilayer adsorption.

Among the well-known isotherms, the following are notable: Langmuir, Temkin, Freundlich, Brunauer-Emmett-Teller (BET), Henry, Dubinin-Radushkevich (DR), Redlich-Peterson, Toth, Koble-Corrigan, Sips, Hill, Flory-Huggins.

In general, isotherms can be classified based on the shape of the curve; in particular, the IUPAC organization has categorized isotherms into six classes (97) (Figure 1.23).

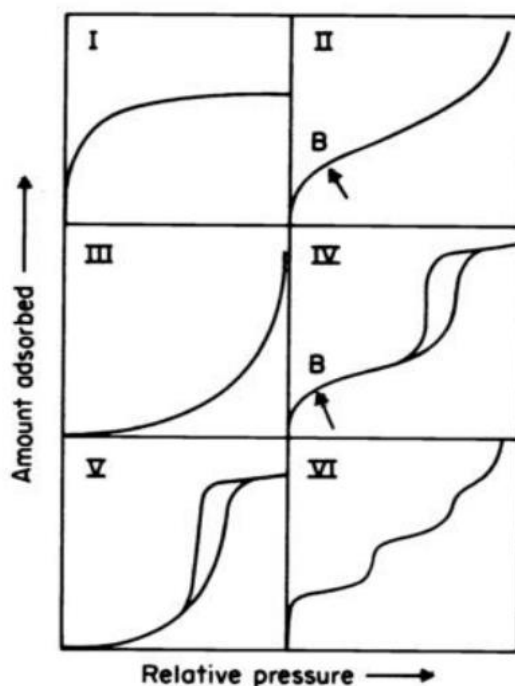


Figure 1.23: IUPAC classification, (98).

Conventional adsorbents, bentonites, zeolites, biochar, clays, and activated carbons have certain limitations, such as restricted active sites, lack of selectivity, and slow adsorption kinetics (99).

Nano-adsorbents, on the other hand, bring about considerable advancements by offering exceptionally high specific surface areas and associated sorption sites. They also feature short intraparticle diffusion distances and the ability to tune pore size and surface chemistry (100).

By employing nano-adsorbents, the efficiency of adsorption processes can be significantly enhanced, leading to more effective contaminant removal and improved water purification outcomes.

However, it is important to acknowledge that nanotechnology also comes with certain risks. Due to their extremely small size, nanomaterials can potentially enter the human body or the bodies of aquatic animals, leading to possible toxicity. The level of toxicity may vary depending on the surrounding conditions, such as pH, concentration, and contact time (101).

The theme of exposure to nanomaterials currently holds a significant role within the scientific community. In particular, non-governmental organizations engaged in safety and environmental concerns have called for transparency regarding the potential negative effects of nanotechnologies. Indeed, by proactively studying the potential risks of an emerging technology, we can avoid reacting to problems caused by risks that are identified belatedly. The increasingly widespread use of

nanomaterials in numerous fields undoubtedly leads to their dispersion, even accidentally, in the environment (102).

The most extensively conducted studies focus on toxicological assessments regarding human health, aiming to evaluate the risks that these particles may pose. Given the nanometric nature of the particles, the three main pathways of exposure to the human body are inhalation, ingestion, and dermal penetration.

A precise description of the effects that these technologies can have on health is still elusive, although effects on blood vessel linings, blood clot formation, vascular effects, and depositions in nasal and alveolar airways have been observed (103).

In conclusion, while scientists have made significant progress in exploring nanotechnology, there is still much to be done to fully understand and address potential risks associated with this new technology.

1.4.2. A focus on CNTs in wastewater management

CNTs have the potential to pave the way for a new generation of carbonaceous adsorbents, thanks to their layered and hollow architecture and versatile surface chemistry. They stand out as the most anisotropic materials currently available.

CNTs have gained popularity as adsorbent materials due to their unique properties, which include high sorption potential. Their malleable surface charge allows for targeted collection of specific water pollutants. Additionally, their fibrous material with an enormous pore size provides greater surface exposure, enhancing their adsorption capabilities (104).

Pollutant adsorption on CNTs is primarily driven by four fundamental forces: π - π interactions, hydrophobic interactions, electrostatic interactions, and charge transfer. These interactions enable effective binding of pollutants to CNTs (105).

CNTs provide four distinct active adsorption sites: the internal sites within the hollow tube structure, the interstitial channels between the walls, the grooves located between the peripheral nanobundles, and the exposed external surface area (Figure 1.24). These active sites contribute to the high adsorption capacity and efficiency of CNTs in removing pollutants from water and wastewater, making them a valuable candidate for advanced water treatment applications (106).

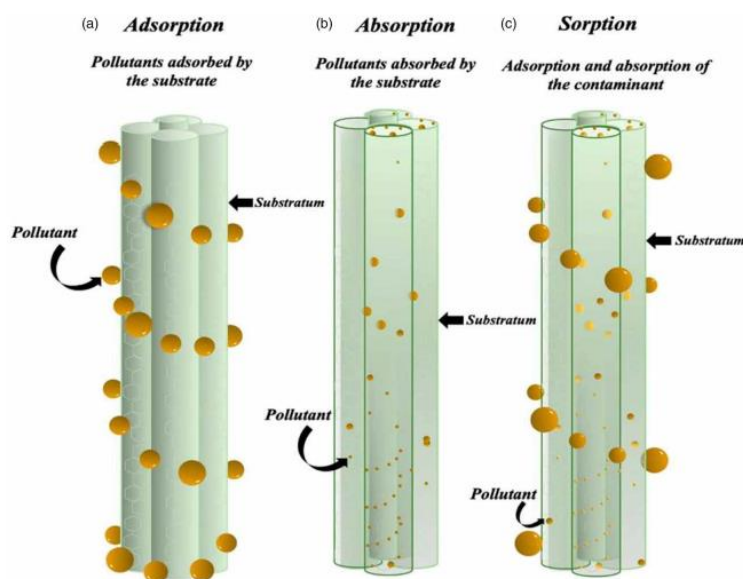


Figure 1.24: Schematic illustration of the adsorption process for CNTs, (107).

CNTs are shown to have high adsorption capacities for heavy metals.

Raw CNTs are a stable material. They are relatively poor adsorbents for metals in themselves, but adding a new functional group to their surface can greatly increase their selectivity and sensitivity towards heavy metals (108).

Oxidized CNTs have a high adsorption capacity for metal ions with fast kinetics. The surface functional groups of CNTs, such as carboxyl, hydroxyl, carbonyl and phenol, serve as the major adsorption sites for metal ions, primarily through electrostatic attraction and chemical bonding (109).

Mercury, lead, chromium, and cadmium are regarded as four of the most concerning heavy metals due to their non-biodegradable, bioaccumulative, and extremely hazardous nature. These heavy metals pose serious threats to plant, animal, and human health, even at trace levels of concentration (110).

In addition to the six heavy metals of concern mentioned above, other heavy metals have also been studied due to their wide industrial use and the threats they pose to humans and ecosystems. Other heavy metals that have been studied for removal by functionalized carbon-based nanomaterials include Cr(IV), Cu(II), Zn(II), Ni(II), Co(II), and radioactive U(VI) (111).

As mentioned earlier, the mechanisms by which metallic ions are absorbed by CNTs are complex and have been attributed to electrostatic attraction, absorption-precipitation, and chemical interaction between metallic ions and the functional groups on the surface of CNTs.

In any case, ion exchange appears to be the predominant mechanism in the removal process (112).

It has also been observed that the adsorption efficiency is influenced by parameters such as temperature and pH (113).

Several studies have demonstrated that the percentage of metallic ions on the surface of CNTs increases with rising temperature. This is attributed to the fact that at higher temperatures, the activation energy of adsorption is lower (114).

Furthermore, there are also many studies confirming that an increase in pH enhances adsorption. In fact, at low and neutral pH (2-7), the adsorption rate is low, while at higher pH levels (8-11), it increases (115,116)

In the aqueous phase, CNTs tend to form loose bundles or aggregates due to the hydrophobic nature of their graphitic surface. This bundling reduces the effective surface area available for adsorption. However, CNT aggregates also contain interstitial spaces and grooves, which serve as high adsorption energy sites also for organic molecules (117).

This is very important because, as mentioned earlier, organic contaminants have become one of the most serious environmental problems. The removal of organic contaminants as dyes, pesticides, and pharmaceuticals/drugs, SOCs (synthetic organic compounds) in general and common industrial organic waste (for example phenols, aromatic amines) from aqueous solutions is of particular interest because they are refractory and persistent in the environment.

Therefore, CNTs exhibit much higher adsorption capacity for certain bulky organic molecules compared to activated carbon. Although activated carbon possesses a comparable measured specific surface area to CNT bundles, it contains a significant number of micropores that are inaccessible to bulky organic molecules (118).

Moreover, if the CNTs is functionalized with groups such as $-\text{COOH}$, $-\text{OH}$, these functional groups as hydrogen-bonding donors can also form a hydrogen bond with organic molecules. Sometimes the competitive sorption between CNTs and organic molecules can occur because of stronger hydrogen bonding interaction between functional groups of CNTs and water than adsorbate molecules.

Consequently, this can result in the insignificant effects of hydrogen-bonding interactions on the adsorption of solutes that lack hydrogen-bonding donor ability (119).

In particular, CNTs could be one of the most promising adsorbents for this purpose due to their high adsorption capacity for organic dyes. In fact, it has been demonstrated that MWCNTs outperform activated carbon (AC) in the removal of dyes from aqueous solutions. Unfortunately, this is based on a still limited number of studies on this matter (120).

Moreover, specifically functionalized nanotubes have been shown to exhibit better performance.

The same considerations can be made for pharmaceuticals. Thanks to their highly specific surface area and ample volume of micropores, CNTs are considered superior adsorbents for the removal of pharmaceutical products.

The use of CNTs for pesticide removal appears promising. Considering the widespread use of pesticides, greater efforts should be directed towards investigating the removal of pesticide residues from drinking water and wastewater (121).

Regarding hazardous organic compounds such as phenols, amines, and other toxic pollutants to both humans and the environment, CNTs are already being considered for a wide range of wastewater treatment applications.

In particular, phenols and amines, which are part of the list of priority substances, are widely found in effluents from pesticides, petrochemicals, pharmaceuticals, and other industries. They can exist as undissociated or dissociated species in the aqueous phase, and due to their relatively high solubility, they can spread rapidly. Based on several experimental studies, CNTs appear to be an excellent alternative to activated carbons, showing promising results in terms of superior efficiency, especially when the adsorbent is functionalized (122).

Also, many chlorinated compounds have been included in the list of priority substances by the United States Environmental Protection Agency (USEPA) due to their extremely high toxicity.

Among these, trichloroethylene (TCE) and tetrachloroethylene (PCE) are mentioned (Figure 1.25). These are solvents used in the chemical and pharmaceutical industries, dry cleaning, and metal degreasing.

They can cause damage to the nervous system, and studies on carcinogenicity have shown an increase in tumors in rats exposed to these substances (123).

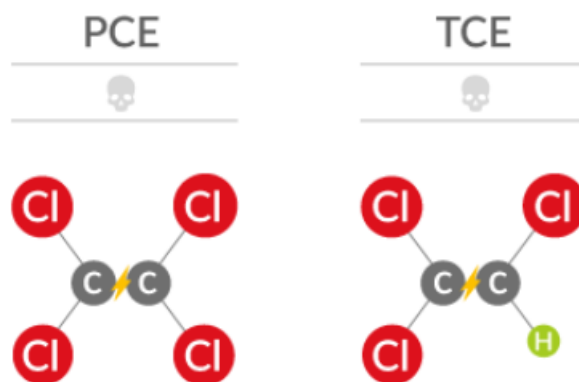


Figure 1.25: PCE and TCE structures.

Multi-wall nanotubes have shown good adsorption results for these substances at a pH range of 3 to 9. Additionally, adsorption is favored at lower temperatures and has shorter contact times to reach equilibrium at high pollutant concentrations. This is due to the diffusion mechanisms that control the adsorption of the pollutant on the nanotubes. In fact, mass diffusivity on the adsorbent increases with the concentration of the pollutant (124).

The contamination by PCBs is a highly significant issue; polychlorinated biphenyls are classic persistent organic pollutants, highly toxic and resistant to degradation.

Because of their persistence and low degradability, the use of a highly efficient adsorbent is of fundamental importance.

It has been demonstrated that appropriately functionalized CNTs exhibit excellent removal efficiencies over a fairly wide pH range, specifically between 2 and 10 (125).

Additionally, further interesting considerations can be made regarding the use of CNTs for the removal of PAHs. What has been observed is that as the number of benzene rings and functional groups increases, adsorption strongly increases. This is likely due to the greater number of contact points between the pollutant and the surface of the nanotube.

Not only that, but the adsorption capacity also increases with increasing hydrophobicity and chlorination level (126).

A recent area of concern is related to PFAS. They constitute a large family of compounds (more than 4700 substances) widely used in numerous industrial sectors, with their use in textiles being particularly well-known (Figure 21). The C-F bond makes them extremely stable substances, which renders them highly persistent once released into the environment (127).

It has been demonstrated that they are responsible for numerous adverse effects, in addition to having a tendency to accumulate in living organisms. At a medical level, effects on the endocrine system have been recognized, interfering with growth hormones, behavior, and fertility. Even more serious is the correlation between long-term exposure to these substances and the onset of kidney and testicular tumors, thyroid and neonatal diseases (128).

The treatment of water contaminated with these compounds typically involves physical methods, including reverse osmosis, ion exchange, and adsorption on granular activated carbon, as well as some biological processes. Unfortunately, the aforementioned persistence of these pollutants means that the sludge produced from these treatments is rich in PFAS (129).

Even thermal methods are challenging as they lead to the formation of undesirable byproducts (130).

Nanotechnologies can provide an excellent alternative for PFAS removal through adsorption. In fact, although PFAS adsorption depends on many factors, it is a highly effective method on carbonaceous materials (131).

Indeed, unmodified carbon nanotubes already demonstrate a higher adsorption capacity for organic compounds compared to other materials, and this capacity further increases in the presence of metallic catalysts (132).

The fundamental concepts that emerge are that both the specific surface area and the volume of the adsorbent are influential but not exclusive characteristics on the adsorption capacity. The predominant driving force that repels the organic pollutants from water on the surface of CNTs is hydrophobic forces.

As emphasized earlier, functionalization of CNTs is a very important strategy that can significantly increase the adsorption capacity for various analyzed pollutants, both organic and inorganic (133).

2 Experimental part

2.1. Materials and Methods

The MWCNTs used in this thesis work were prepared at Politecnico di Milano using the well-known protocol in the literature called "Chemical Vapor Deposition" (CVD). The purity of the obtained nanotubes, in terms of graphitic carbon, exceeds 95% by weight, and the impurities consist solely of the catalysts, iron and aluminum, that remains trapped inside the nanotube aggregates.

The estimated dimensions of the MWCNTs are as follows: outer diameter 14-20 nm, inner diameter 2-5 nm, average number of walls 12-15, length 1-10 μm .

TEM observations were performed with a Philips CM200 field emission transmission electron microscope; the sample of nanotubes, dispersed in 4% aqueous SDS, were deposited on holey carbon films on 200 mesh copper grids and then observed under accelerated voltage of 200 kV.

In the following, two TEM images of MWCNTs are shown (Figure 2.1).

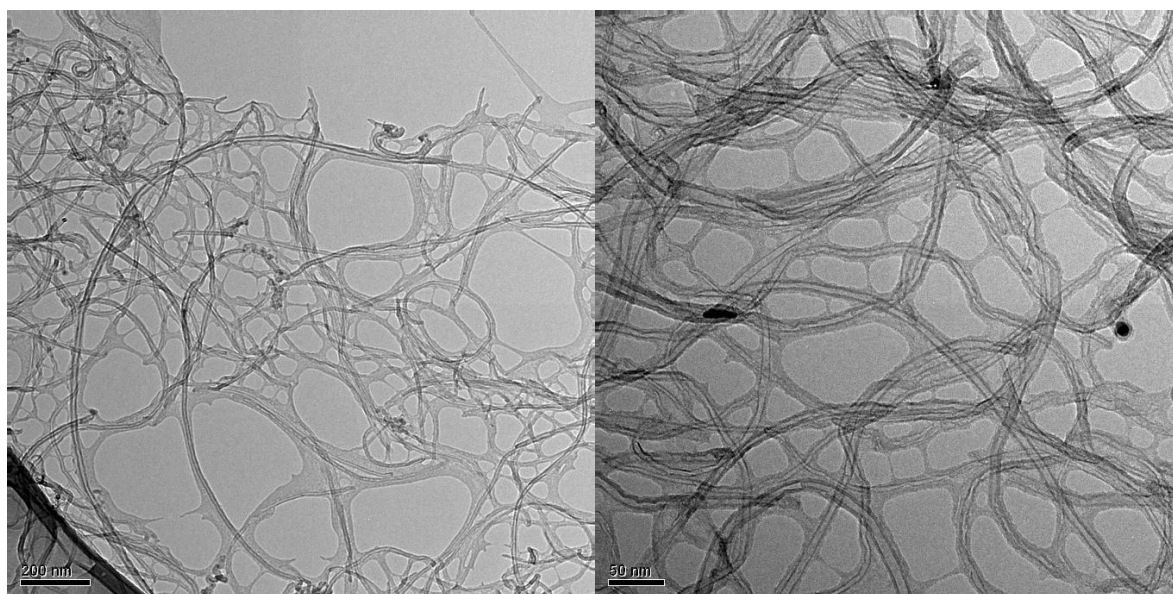


Figure 2.1: TEM images of MWCNTs.

The clay used is a Montmorillonite-Nanofil 116, which is an inorganic nano-dispersible layered silicate based on refined natural bentonite. It is a natural clay with a cation exchange capacity (CEC) of 116 mEq/100 g. It appears as a beige-colored powder and has a density ranging from 600 to 1100 kg/m^3 ; the average particle size is < 25 nm.

TGA curves were recorded using a Perkin Elmer STA 6000. The analyses were performed in air from 35 °C to 900 °C with a continuous heating rate of 10 °C/min.

A Bruker AV 400 MHz instrument equipped with a 5 mm multinuclear probe with reverse detection was used to record ^1H NMR spectra (400 MHz). 16 scans were acquired with an acquiring time of 2 seconds for ^1H . ^1H chemical shifts (δ) are given in ppm relative to the residual proton of the solvent.

The sonication of the nanotubes was performed using an ultrasonic bath, Ultrasonic Cleaner 3200 EP S3, manufactured by Soltec.

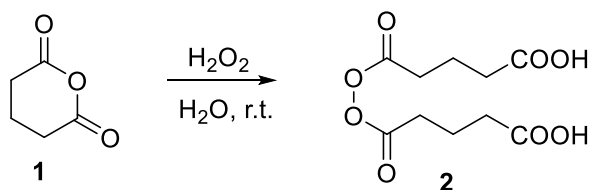
To carry out UV readings, the HP 8452A Diode-Array Spectrophotometer was used. It is a microprocessor-controlled single-beam spectrophotometer that analyzes the UV/Visible spectrum in a range from 190 to 820 nm with a resolution of 2 nm. The HP 8452A Diode-Array Spectrophotometer is controlled by a computer equipped with HP UV-Vis software.

The samples for analysis were centrifuged using a Centrifuge 4206 600 rpm - ALC.

The surfaces of the analyzed adsorbent materials were investigated by scanning electron microscopy images (SEM, Gemini 152 field emission SEM Supra 25, Carl Zeiss, Oberkochen, Germany). The images were obtained in the Inlens mode at 5 kV.

2.2. CNTs functionalization

2.2.1. Synthesis of Glutaryl Peroxide



Glutaric anhydride (12.54 g) is mixed with water (20 mL) in a 50 ml round flask. Subsequently, it is stirred on a magnetic stirrer (400 rpm).

While the aqueous dispersion of glutaric anhydride is stirred, 30% volume H_2O_2 (16 mL) is dropwise added. (134)

Initially, upon observing the contents of the round bottom flask, flakes are observed to form. Subsequently, after 15 minutes, the solution becomes clear. Then, the mixture

is cooled at 0-5°C (ice bath), kept at this temperature for 1h at 0-5°C obtaining glutaryl peroxide as a white precipitate.

The solid is recovered by filtration under vacuum using an enhanced Büchner funnel with the filter paper inside. It is filtered twice, then dried under vacuum at room temperature obtaining 8.45 g of a solid.

From the ^1H NMR analysis (Figure 2.2), it was deduced that the purity of the solid is about 85% and the remaining 15% is glutaric acid (**3**) (Figure 2.3). The latter product is not problematic and therefore no further purification was performed.

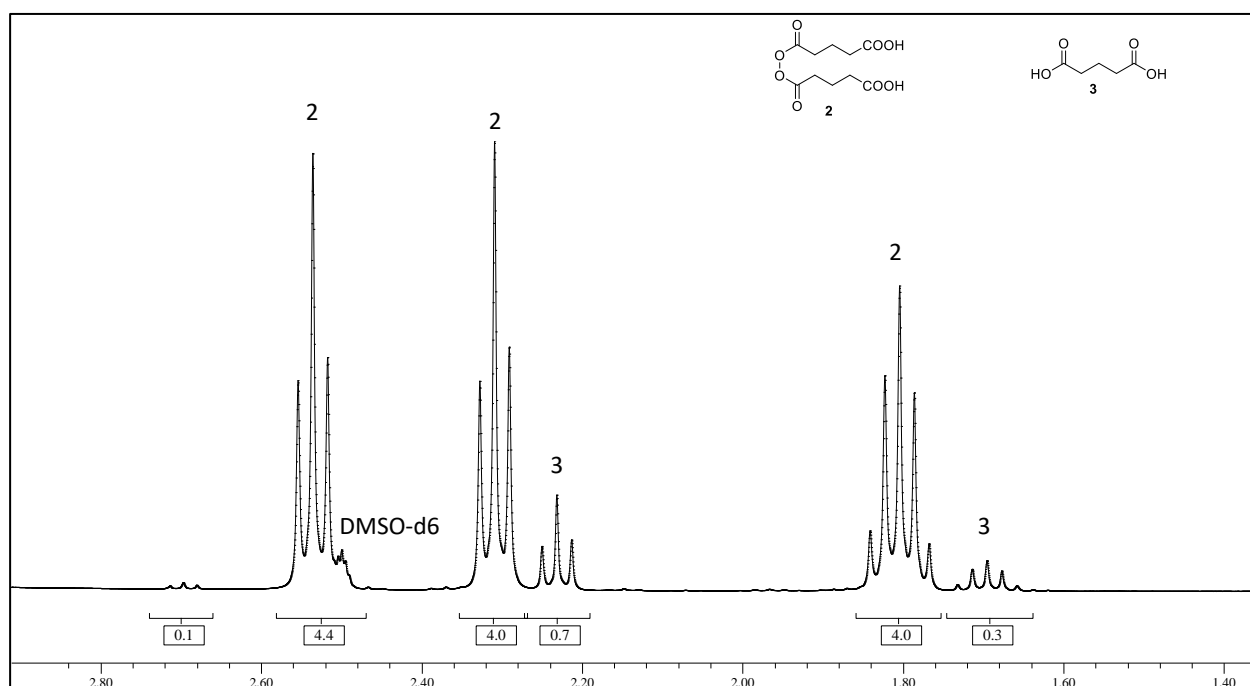


Figure 3.2: ^1H NMR analysis of glutaryl peroxide in DMSO-d_6 .

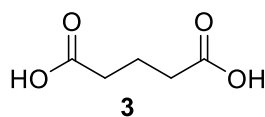
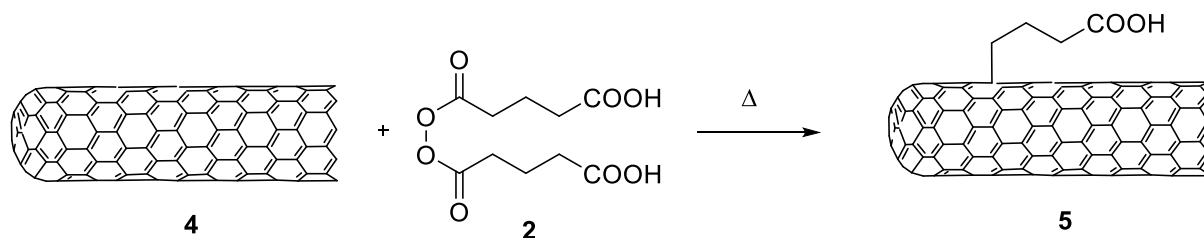


Figure 2.3: glutaric acid.

In the ^1H spectrum above, the shifts of the signals related to the methylene ($-\text{CH}_2-$) hydrogen atoms in the molecule are assigned as follows: at 1.84 ppm there is a quintet related to the two central methylenes of the alkyl chains, at 2.32 ppm the triplet related to the two methylenes in α to the carboxylic group, and at 2.54 ppm the triplet related to the two methylenes in α to the peroxide group.

2.2.2. CNTs functionalization with Glutaryl Peroxide



Glutaryl peroxide (7.2 mg) (2), CNTs (1.0 g) (4), and distilled water (100 mL) are placed in a 250 mL round bottom flask equipped with a condenser (135). The mixture is stirred at a temperature of 90 °C (oil bath) for 6 hours. Then, the modified nanotubes (5) are filtered on a sintered glass filter under vacuum and washed with hot water six times (each time with 100 mL of H₂O), then washed with acetone (3 × 50 mL) and dried in an oven overnight obtaining 5.

The obtained product is a functionalized nanotube, CNT-(CH₂)₃COOH (5), which will be referred to as CNT-X-COOH throughout the discussion.

Thermogravimetric analysis (TGA) of the CNT-X-COOH product (5) was performed (Figure 2.4).

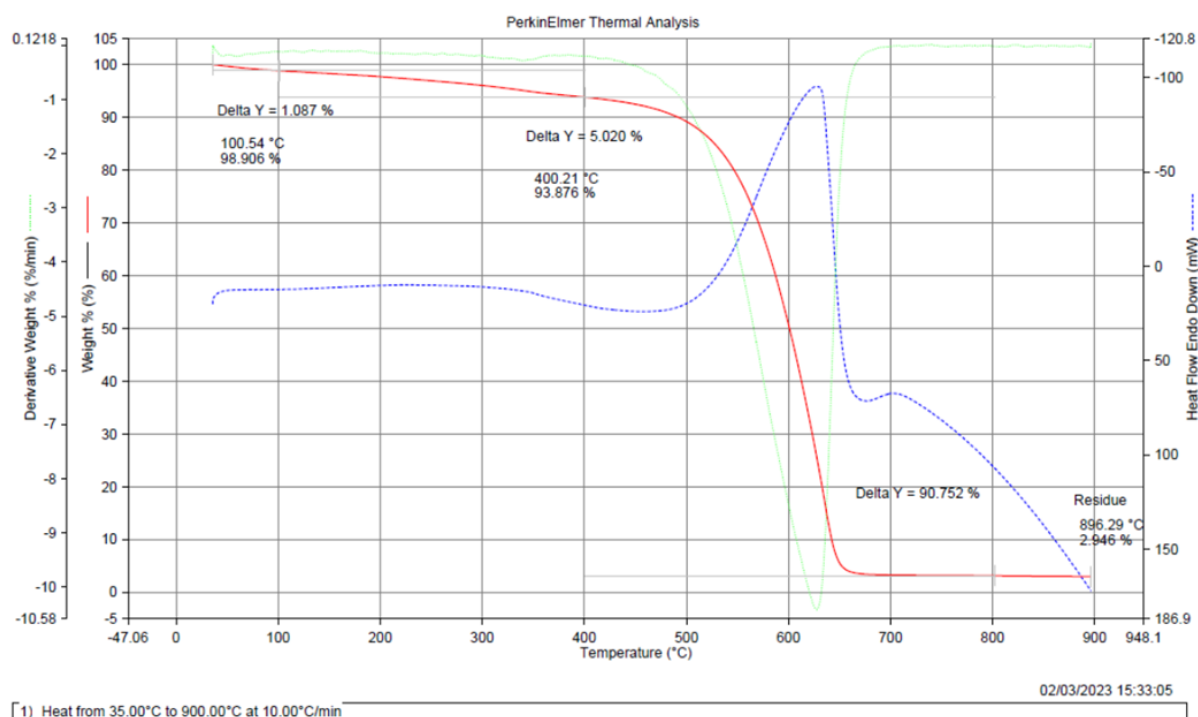
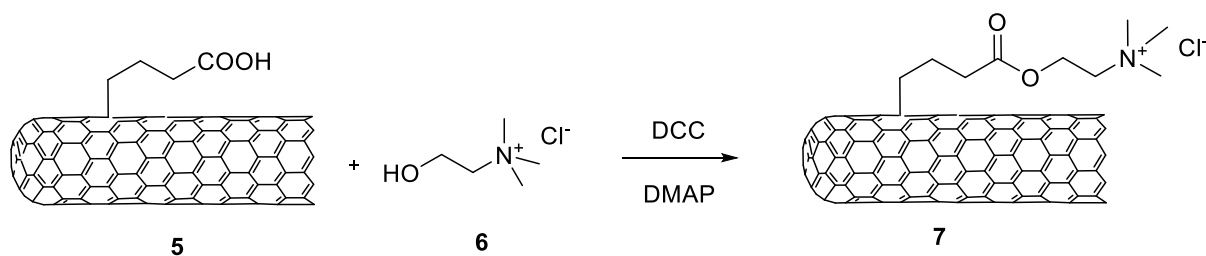


Figure 2.4: TGA of CNT-X-COOH.

2.2.3. Functionalization of CNT-X-COL



Inside a round bottom flask under nitrogen atmosphere, 0.5 g of CNT-X-COOH (**5**), 250 mg (1.8 mmol) of choline (**6**), 70 mL of dry *N,N*-dimethylformamide (DMF), 44 mg (0.36 mmol) of 4-dimethylaminopyridine (DMAP), (Figure 2.5), and 250 mg (1.8 mmol) of *N,N'*-dicyclohexylcarbodiimide DCC, (Figure 2.6), are placed. (135)

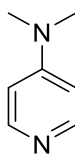


Figure 2.5: DMAP structure.

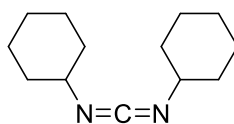


Figure 2.6: DCC structure.

The mixture is stirred (500 rpm) at room temperature for six days. After this time, the viscous black suspension is filtered under vacuum on a sintered glass filter, and the black solid is washed: four times with DMF (50 mL each time), and 7 times with acetone (50 mL each time). It has to be noted that the filtration with DMF requires a relative long time. The product is then placed in an oven to dry obtaining CNT-(CH₂)₃COO(CH₂)₂N(CH₃)₃⁺Cl⁻ which will be referred to as CNT-X-COL (**7**) throughout the discussion.

The TGA analysis of (**7**) was performed (Figure 2.7):

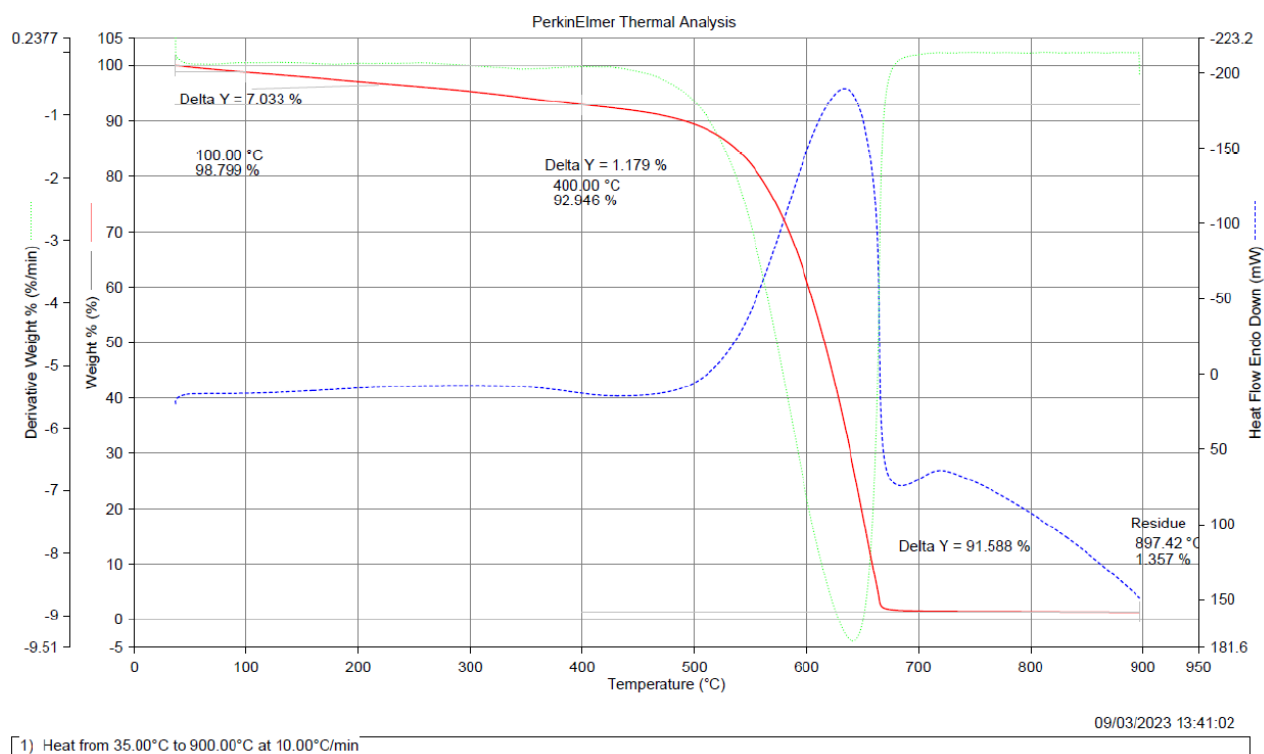


Figure 2.7: TGA of CNT-X-COL (7).

The same procedure was subsequently repeated with other CNT-X-COOH to prepare other crops of 7.

2.3. Preparation of CNTs/clay hybrid material

Two hybrid materials using different CNTs/clay ratio are prepared in a 25 mL round bottom flask by suspending clay (Montmorillonite-Nanofil 116) and nanotubes in 10 ml of acetone. The suspensions are sonicated in an ultrasound bath for 10 minutes. Then, vacuum filtration is performed to remove moisture and acetone. The mixture is placed in an oven at 100 °C for one hour.

The first material was prepared by mixing 100 mg of CNTs and 100 mg of clay (ratio 1:1).

The second material was prepared by mixing 100 mg of CNTs and 20 mg of clay (ratio 1:0.2).

2.4. Calibration curves

The calibration curves are calculated for four aqueous solutions dissolving respectively: Cu(II) sulfate pentahydrate and ammonia, Cu(II) nitrate trihydrate,

Rhodamine B, and Methyl Orange, selected as reference pollutant respectively for metal cations and dyes.

These are obtained for each one through the readings of their respective absorbances using the UV-Vis spectrophotometer. Quartz cuvettes are used. This is a critical point, as previous measurements revealed interference when using plastic cuvettes.

On a Cartesian plane, the molar concentration (mmol/mL) of the solutions for each one is placed on the x-axis, while the absorbance values of these solutions at a selected wavelength are placed on the y-axis. Points are then identified and interpolated by a straight line using the MS Excel function.

2.4.1. Calibration curve for Cu(II) sulfate pentahydrate $\text{CuSO}_4 \cdot 5\text{H}_2\text{O}$

The five standard solutions used to calculate the calibration curve are prepared by weighing each time Cu(II) sulfate pentahydrate (Figure 2.8) and dissolving it in distilled water. Then, aqueous ammonia to each solution is added (pH 11.4-11.7).

The copper-ammonia complex solutions are referred to as copper(II) sulfate pentahydrate or generally CuSO_4 throughout the thesis to avoid confusion with aqueous solution of copper(II) nitrate trihydrate that, as follows, will be used for the tests at neutral pH.

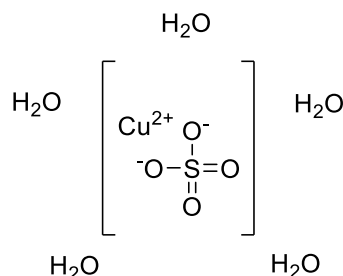


Figure 2.8: *Copper(II) sulfate pentahydrate.*

All five solutions of CuSO_4 pentahydrate ($M = 249.69 \text{ g/mol}$) are prepared in 250 mL volumetric flasks with the intent to obtain solution 1 at a concentration about 0.005 M, and the other solutions respectively with concentration 75%, 50%, 25% and 10% with respect to solution 1. In Table 2.1, the measured weighs and concentrations are reported.

Table 2.1: *Weight, concentration, and pH for CuSO₄ solutions.*

	Weight (mg)	Concentration (mmol/mL)	pH
Solution 1	325.0	0.005210	11.4
Solution 2	237.8	0.003810	/
Solution 3	156.1	0.002501	/
Solution 4	78.0	0.001320	/
Solution 5	34.7	0.000556	11.7

The absorbances are measured with the spectrophotometer reported above. The absorbance curve shows a maximum at 600 nm, so the values has been recorded at this wavelength.

For each of the five solutions, five absorbance values at 600 nm are measured (Table 2.2). The mean value is then calculated from these five values (A1, A2, A3, A4, A5). The data used to calculate the calibration curve are summarized in Table 2.3.

Table 2.2: *Absorbances for various CuSO₄ solutions.*

	Solution 1	Solution 2	Solution 3	Solution 4	Solution 5
A1	0.24405	0.18564	0.11768	0.06683	0.02740
A2	0.24429	0.18559	0.11873	0.06819	0.02751
A3	0.24413	0.18552	0.11856	0.06693	0.02745
A4	0.24408	0.18538	0.11826	0.06683	0.02805
A5	0.24400	0.18532	0.11696	0.06690	0.02747
Mean	0.24411	0.18549	0.11804	0.06713	0.02758

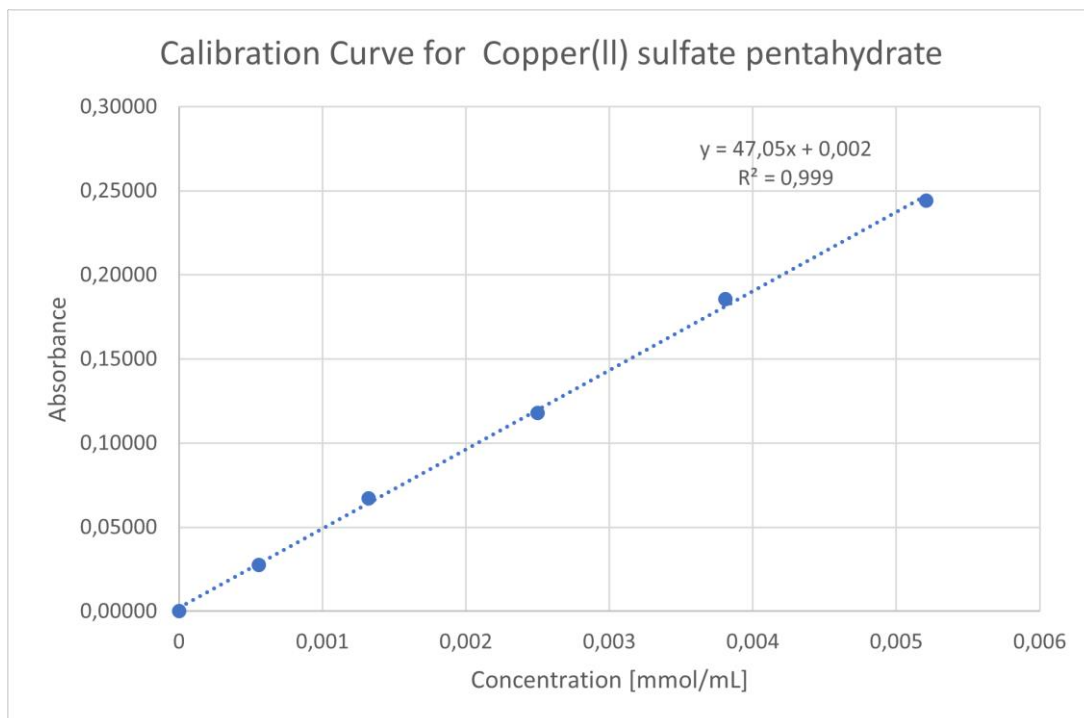
Table 2.3: Absorbance values for CuSO_4 solutions.

	Concentration (mmol/mL)	Absorbance (600 nm)
Solution 1	0.005210	0.24411
Solution 2	0.003810	0.18549
Solution 3	0.002501	0.11804
Solution 4	0.00132	0.06713
Solution 5	0.000556	0.02758
Point 0	0	0

The 'Point 0' was added to ensure that the line passes through the origin of the axes as it is expected for pure water (blank sample).

The R-squared (R^2) value of the linear interpolation is very high, close to 1: the higher the R-squared value, the higher the predictive reliability of the model.

The result is shown in Figure 2.9:

Figure 2.9: Calibration curve for CuSO_4 .

2.4.2. Calibration curve for Cu(II) nitrate trihydrate $\text{Cu}(\text{NO}_3)_2 \cdot 3\text{H}_2\text{O}$

In this case, there is no need to add ammonia, allowing us to work at a neutral pH.

The five solutions of CuNO_3 trihydrate ($M = 249.69 \text{ g/mol}$) (Figure 2.10) are prepared in 250 mL volumetric flasks (Table 2.4). with the intent to obtain solution 1 at a concentration about 0.005 M, and the other solutions respectively with concentration 75%, 50%, 25% and 10% with respect to solution 1.

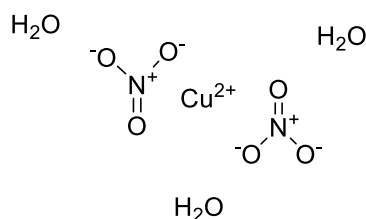


Figure 2.10: *Copper(II) nitrate trihydrate structure.*

In Table 2.4, the measured weighs and concentrations are reported. As before, the UV absorbance readings are then performed with the spectrophotometer. The absorbance curve shows a maximum at 300 nm, so the readings will be taken at this wavelength using quartz cuvettes. For each of the five solutions, five absorbance values at 300 nm are measured. The mean value is then calculated from these five values.

Table 2.4: *Weight, concentration and absorbance for $\text{Cu}(\text{NO}_3)_2$.*

	Weight (mg)	Concentration (mmol/mL)	Absorbance
Solution 1	963.0	0.060618	0.2396
Solution 2	723.0	0.045510	0.1690
Solution 3	490.0	0.030844	0.1128
Solution 4	249.0	0.015674	0.0566
Solution 5	100.0	0.006295	0.0216

The obtained interpolation was good, and the resulting calibration curve is shown in Figure 2.11.

Notice that before the measurements, the solutions were allowed to stabilize for 7 days as the values recorded just after the preparation of the solutions were not reliable.

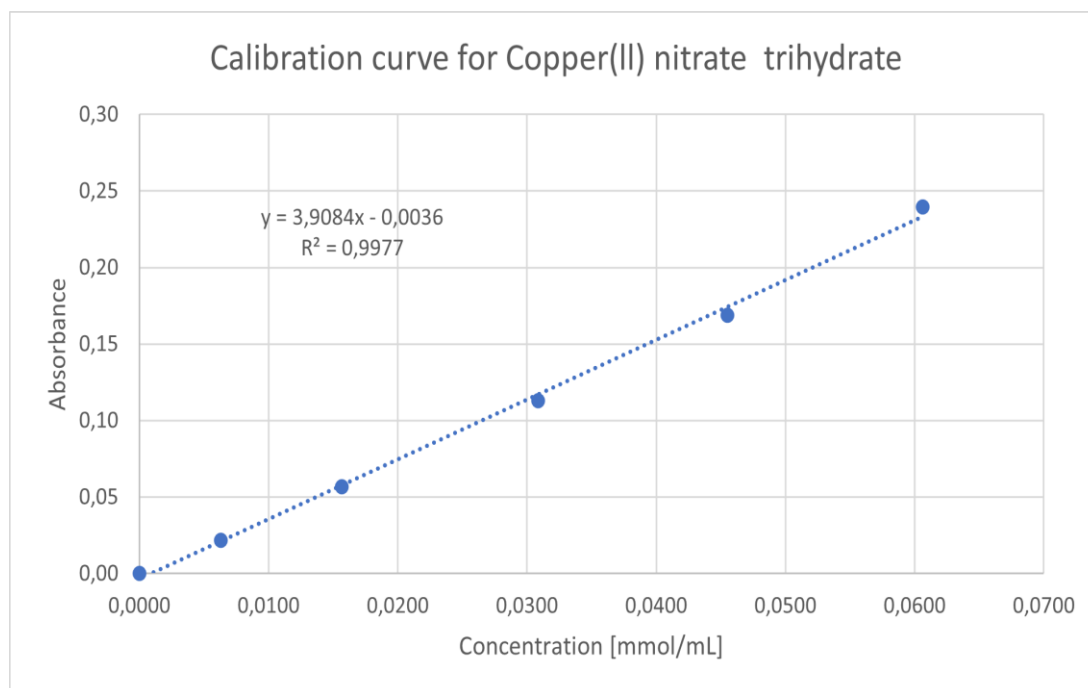


Figure 2.11: Calibration curve for Copper(II) nitrate trihydrate.

2.4.3. Calibration curve for Rhodamine B

The calibration curve for Rhodamine B (Figure 2.12) was obtained by preparing a stock solution ('Solution 0'). This stock solution, with a series of subsequent dilutions, gave rise to four solutions used for the curve.

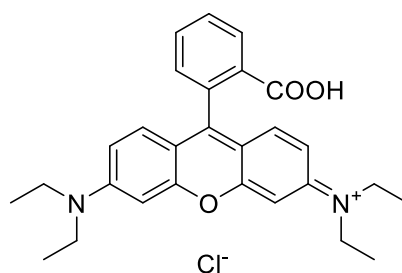


Figure 2.12: Rhodamine B structure.

Five solutions of rhodamine B ($M = 479.01 \text{ g/mol}$) are prepared in 250 mL volumetric flasks. Solutions 1-4 are obtained by dilution of a standard solution (about $1 \times 10^{-4} \text{ M}$) using glass graduated pipettes, previously tested, are used (Table 2.5).

Five values of absorbance for each solution (solutions 1-4), are recorded at a wavelength of 553 nm. The resulting calibration curve is shown in Figure 2.13:

Table 2.5: Weight, concentration and absorbance for Rhodamine B.

	Weight (mg)	Concentration (mmol/mL)	Absorbance
Standard Solution	13.14 mg/250 mL	9.982×10^{-6}	/
Solution 1	Dilution 1:10	4.40×10^{-6}	0.45231
Solution 2	Dilution 1:25	2.20×10^{-6}	0.21682
Solution 3	Dilution 1:125	9.00×10^{-7}	0.089237
Solution 4	Dilution 1:250	4.40×10^{-7}	0.056235

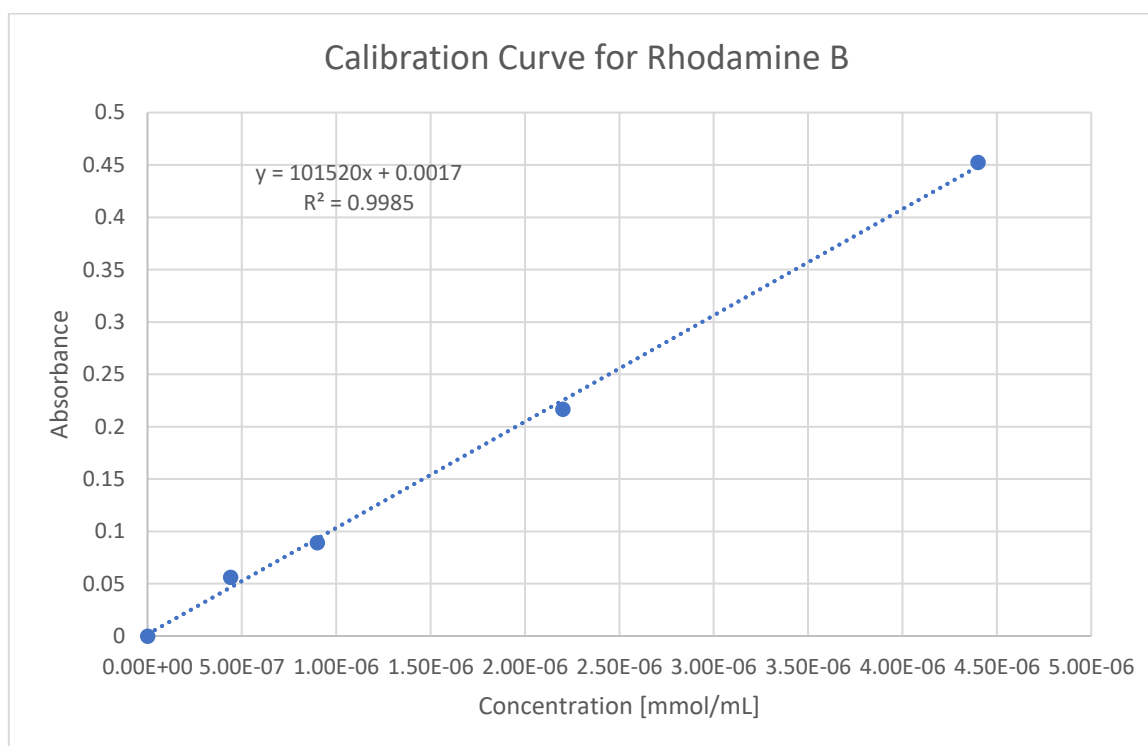


Figure 2.13: Calibration curve for Rhodamine B.

The R-squared (R^2) value of the linear interpolation is very high, close to 1: this indicates that the higher predictive power of the model.

2.4.4. Calibration curve for Methyl Orange

As for rhodamine, also for methyl orange ($M=327.33$ g/mol) (Figure 2.14) the calibration curve was calculated by preparing a standard solution. This solution, with a series of subsequent dilutions, gave rise to four solutions used to calculate the calibration curve (Table 2.6).

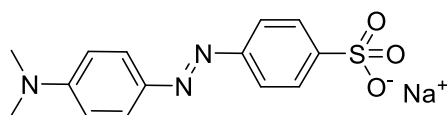


Figure 2.14: *Methyl Orange structure.*

The UV absorbance readings are then performed with the spectrophotometer. The absorbance curve shows a peak at 465 nm, so the readings are taken at this wavelength, using quartz cuvettes.

Table 2.6: *Weight, concentration and absorbance for Methyl Orange.*

	Weight (mg)	Concentration (mmol/mL)	Absorbance (553 nm)
Standard Solution	8.20 mg/250 mL	1.04×10^{-4}	/
Solution 1	Dilution 1:10	1.04×10^{-5}	0.256000
Solution 2	Dilution 1:25	4.16×10^{-6}	0.109923
Solution 3	Dilution 1:125	2.08×10^{-6}	0.044233
Solution 4	Dilution 1:250	8.30×10^{-7}	0.025300

The result is shown in Figure 2.15.

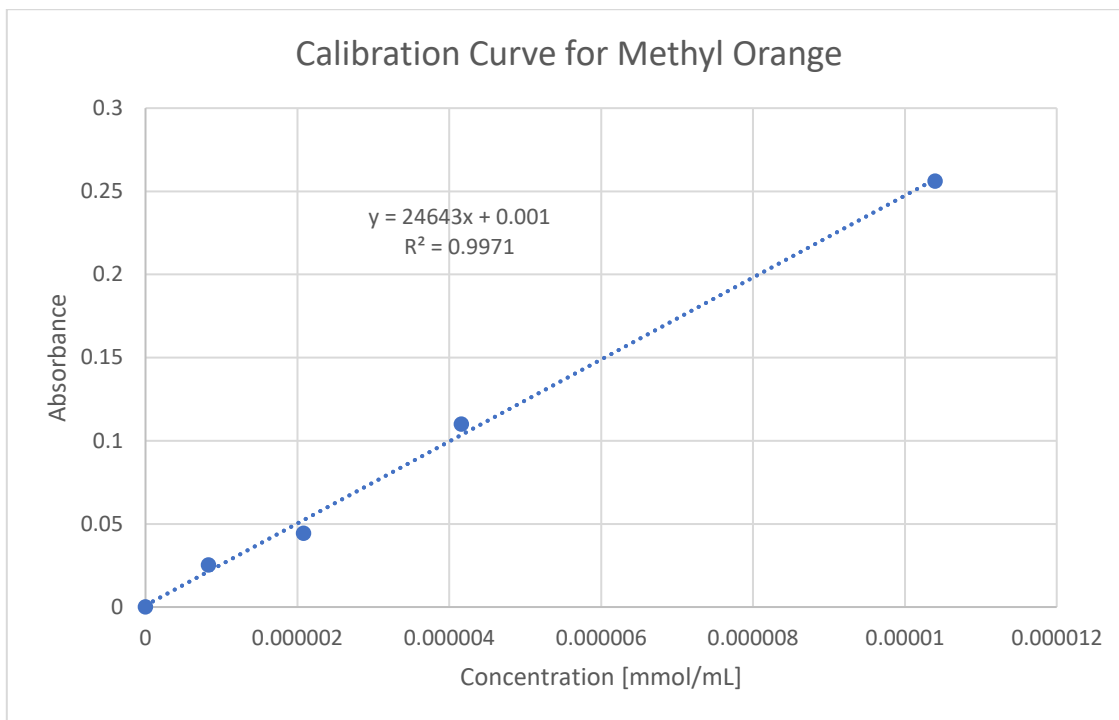


Figure 2.15: Calibration curve for Methyl Orange.

Again, the (R-squared) R^2 has a good value, close to 1.

2.5. Adsorption tests

The adsorption tests were carried out for Cu(II) sulfate pentahydrate, Cu(II) nitrate trihydrate, Rhodamine B, and Methyl Orange. The tests involved the use of various types of adsorbents: pure clay (Montmorillonite-Nanofil 116), non-functionalized nanotubes (CNT-BASE), nanotubes functionalized with carboxylic groups on the surface (CNT-COOH), nanotubes bearing a butyric acid function (CNT-X-COOH) and this latter further modified with choline (CNT-X-COL). In addition, CNT-X-COOH were converted into the corresponding salt with aqueous NaOH obtaining CNT-X-COO⁻Na⁺ (indicated as CNT-X-COO⁻ throughout the thesis) (Figure 2.16).

The hybrid materials obtained from nanotubes and clay in ratios of 1:1 (CNT-X-COL/clay 1:1) and 1:0.2 (CNT-X-COL/clay 1:0.2) were also tested.

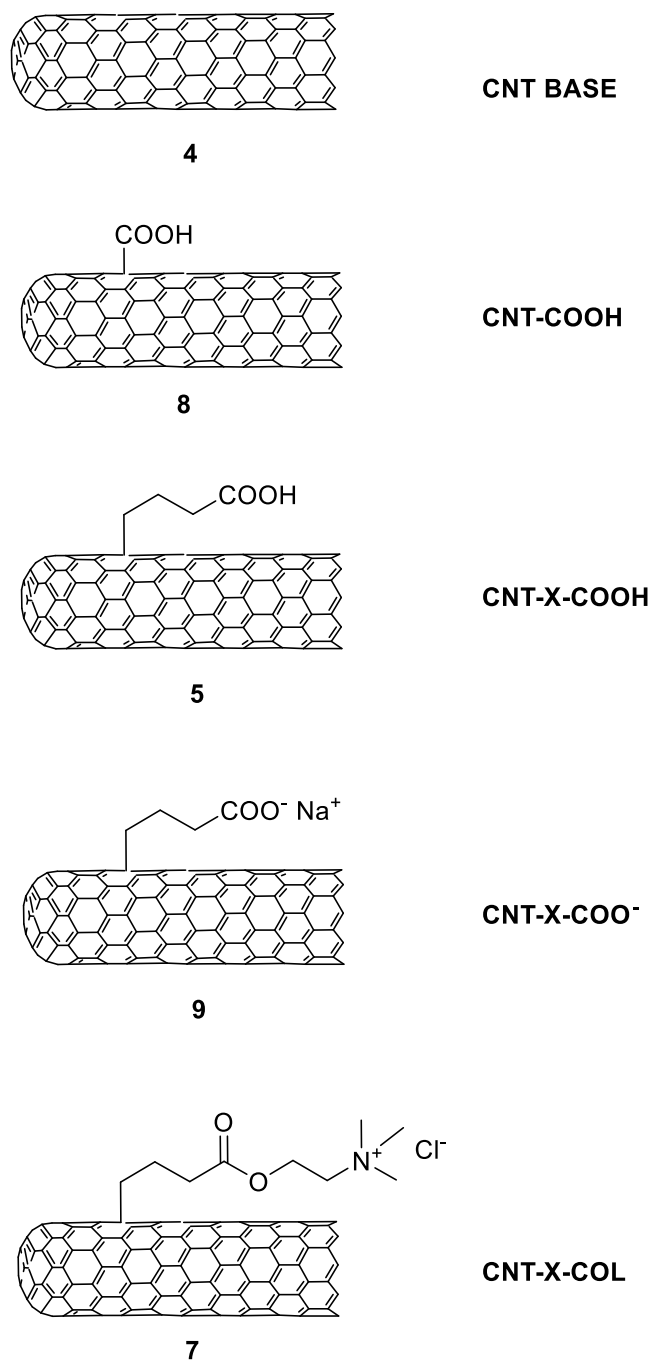


Figure 2.16: CNTs tested in the thesis.

For the two copper salts and the two dyes, *ad hoc* tests were carried out in different conditions by varying: solution volumes, amounts of adsorbents, and contact times. This study aimed to determine which adsorbent or combination of multiple adsorbents yielded the best capture efficiency.

2.5.1. Adsorption tests for Cu(II) sulfate pentahydrate $\text{CuSO}_4 \cdot 5\text{H}_2\text{O}$

All tests were performed using a 5 mL solution volume at room temperature (23-25 °C). The solution chosen for the tests was the most concentrated, namely 'Solution 1' (0.005210 mmol/mL).

'Solution 1' is placed in a 50 mL round bottom flask. Inside the flask, a specific adsorbent or hybrid adsorbents are also added in the quantity as reported in Table 2.7.

The flasks are first placed in an ultrasonic bath for three minutes (140 W, 2L). Then, they are mixed using a magnetic stirrer at 500 rpm for the time reported in Table 2.7. Subsequently, the sample is centrifuged for two minutes at 5000 rpm. The clear solution is withdrawn from the centrifuge tube using a Pasteur pipette, filtered through cotton and transferred in a quartz cuvette.

The blank for the UV readings consists of distilled water and is analyzed in a quartz cuvette as well.

The UV absorbances are recorded at 600 nm.

Table 2.7: Tests for CuSO_4 .

Sample	Solution volume	Adsorbent	Contact time
AR05a	5 mL	25.00 mg of clay	30 min
AR05b	5 mL	25.00 mg of clay	60 min
AR06a	5 mL	5.25 mg of clay	30 min
AR06b	5 mL	5.12 mg of clay	60 min
AR06c	5 mL	4.97 mg of clay	120 min
AR07	5 mL	25.00 mg of clay + 25.00 mg of CNT-X-COL	60 min
AR08	5 mL	25.00 mg of CNT-X-COL/clay 1:1	60 min
AR09	5 mL	50.00 mg of CNT-X-COL/clay 1:1	60 min
AR11	5 mL	25.00 mg of CNT-X-COL	60 min
AR12	5 mL	30.00 mg of CNT-X-COL/clay 1:0.2	60 min

2.5.2. Adsorption tests for Rhodamine B

All tests were performed using a 5 mL or 25 mL solution volume at room temperature (23-25 °C). The solution chosen for the tests was the most concentrated, namely 'Solution 1' (4.40×10^{-6} mmol/mL).

'Solution 1' is poured in a 50 mL round bottom flask and a specific adsorbent or hybrid adsorbents are also added in the quantity reported in Table 2.8.

In the preliminary tests, the samples were sonicated. Then, it was decided to proceed without sonication because, when using carbon nanotubes as the adsorbent, regardless of functionalization, a part of them dissolved in the solution. This creates a kind of gray clear ink that makes UV measures not reliable despite filtration through cotton.

The samples were mixed using a magnetic stirrer at 500 rpm for the time reported in Table 2.8. Subsequently, the sample is centrifuged for two minutes at 5000 rpm. The clear solution was withdrawn from the centrifuge tube using a Pasteur pipette and it was filtered through cotton and transferred in a quartz cuvette.

The blank for the UV readings consists of distilled water and was analyzed in a quartz cuvette as well. The UV absorbances are recorded at 553 nm.

Table 2.8: Tests for Rhodamine B.

Sample	Solution volume	Adsorbent	Contact time
AR13	5 mL	5.2 mg of CNT-X-COL	60 min
AR14	5 mL	5.1 mg of clay	60 min
AR15	5 mL	5.3 mg of CNT-X-COL/clay 1:0,2	60 min
AR16	5 mL	5.2 mg CNT-X-COOH	60 min
AR17	25 mL	5.2 mg of CNT-X-COL/clay 1:0,2	60 min
AR18	25 mL	5.2 mg CNT-X-COOH	60 min
AR19	25 mL	5.3 mg of CNT-X-COL	60 min
AR20	5 mL	5.6 mg of CNT-X-COL	60 min
AR21	5 mL	10.2 mg of CNT-X-COL/clay 1:0,2	60 min

AR22	25 mL	5.4 mg of CNT-X-COL	60 min
AR23	25 mL	5.3 mg CNT-X-COOH	60 min
AR25	25 mL	2.2 mg of CNT-X-COL	60 min
AR26	25 mL	2.1 mg of CNT-X-COOH	60 min
AR27	25 mL	2.2 mg of CNT BASE	60 min
AR28	25 mL	2.2 mg of CNT BASE	60 min
AR29	25 mL	2.2 mg of CNT-COO-	60 min
AR30	25 mL	2.2 mg of CNT-COO-	60 min
AR40	25 mL	2.2 mg of CNT-COOH	60 min
AR41	25 mL	2.2 mg of CNT-X-COOH	30 min
AR42	25 mL	2.3 mg of CNT-COOH	30 min
AR45	25 mL	2.2 mg of CNT BASE	24 h
AR46	25 mL	2.2 mg of CNT-X-COOH	24 h
AR48	25 mL	2.2 mg of CNT BASE	30 min

2.5.3. Adsorption tests for Methyl Orange

All tests were performed using a 25 mL or 50 mL solution volume at room temperature (23-25 °C). and the solutions chosen for the tests were the 'Solution 1' (1.04×10^{-5} mmol/mL) and the standard solution (1.04×10^{-4} mmol/mL).

It was decided, in this case, to use a larger volume of solution in order to avoid 100% of absorbance, a useless value.

The solutions were poured in a 50 mL flask when using 25 mL of the solution, and in a 100 mL flask when using 50 mL, and the adsorbents were added in the quantity reported in Tables 2.9a and 2.9b. The samples were mixed using a magnetic stirrer at 500 rpm for the time reported in Tables 2.9a and 2.9b.

Subsequently, the samples were centrifuged for two minutes at 5000 rpm.

The clear solutions were withdrawn from the centrifuge tube using a Pasteur pipette, filtered through cotton and transferred in a quartz cuvette.

The blank for the UV readings consists of distilled water.

The UV absorbances are recorded at 465 nm.

Table 2.9a: *Experimental parameters for "Solution 1".*

Sample	Solution volume	Adsorbent	Contact time
AR33	25 mL	2.2 mg of CNT-X-COL	60 min
AR34	25 mL	2.2 mg of CNT-X-COOH	60 min
AR35	25 mL	2.2 mg of CNT BASE	60 min
AR36	25 mL	2.2 mg of CNT BASE	24 h
AR37	25 mL	2.4 mg of clay	60 min
AR38	25 mL	2.2 mg of CNT-COOH	60 min
AR43	25 mL	2.3 mg of CNT-X-COOH	30 min
AR44	25 mL	2.2 mg of CNT-COOH	30 min
AR47	25 mL	2.2 mg of CNT-X-COOH	24 h
AR49	25 mL	2.2 mg of CNT BASE	30 min

Table 2.9b: *Experimental parameters for standard solution.*

Sample	Solution volume	Adsorbent	Contact time
AR50	25 mL	20.1 mg of CNT-X-COOH	60 min
AR51	25 mL	20.1 mg of CNT BASE	60 min
AR52	50 mL	20.0 mg of CNT-X-COOH	60 min
AR53	50 mL	20.0 mg of CNT BASE	60 min

2.5.4. Adsorption tests for Cu(II) nitrate trihydrate $\text{Cu}(\text{NO}_3)_2 \cdot 3\text{H}_2\text{O}$

The adsorption tests were all performed on 5 mL of the most concentrated solution, namely 'Solution 1' (0.060618 mmol/mL).

'Solution 1' was poured in a 25 mL round bottom flask. Inside the flask, a specific adsorbent or hybrid adsorbents were added in the quantity reported in Table 2.10.

The suspensions were mixed using a magnetic stirrer at 500 rpm for the time reported in Table 10. Then, the sample is centrifuged for five minutes at 5000 rpm.

In this case a longer centrifugation time is used as it was found that the clay was not completely deposited at the bottom of the tube and the solution was not perfectly clear. This problem occurred both when using clay as an adsorbent and when using carbon nanotubes exchanged with clay.

In this regard, even filtration through cotton is useless as some nanoparticles are still present after filtration.

Although longer centrifugation, in all the tests, it was not possible to obtain clear solutions.

Table 2.10: Tests for $\text{Cu}(\text{NO}_3)_2$.

Sample	Solution volume	Adsorbent	Contact time
AR24	5 mL	25.0 mg of clay	60 min
AR31	5 mL	5.3 mg of clay	60 min
AR55	5 mL	5.0 mg of clay	60 min
AR56	5 mL	25.0 mg of clay	60 min
AR57	5 mL	24.5 mg of CNT-COL	60 min
AR58	5 mL	10.7 mg of CNT-X-COL/clay 1:1	60 min
AR59	5 mL	26.0 mg of CNT-X-COL/clay 1:0.2	60 min

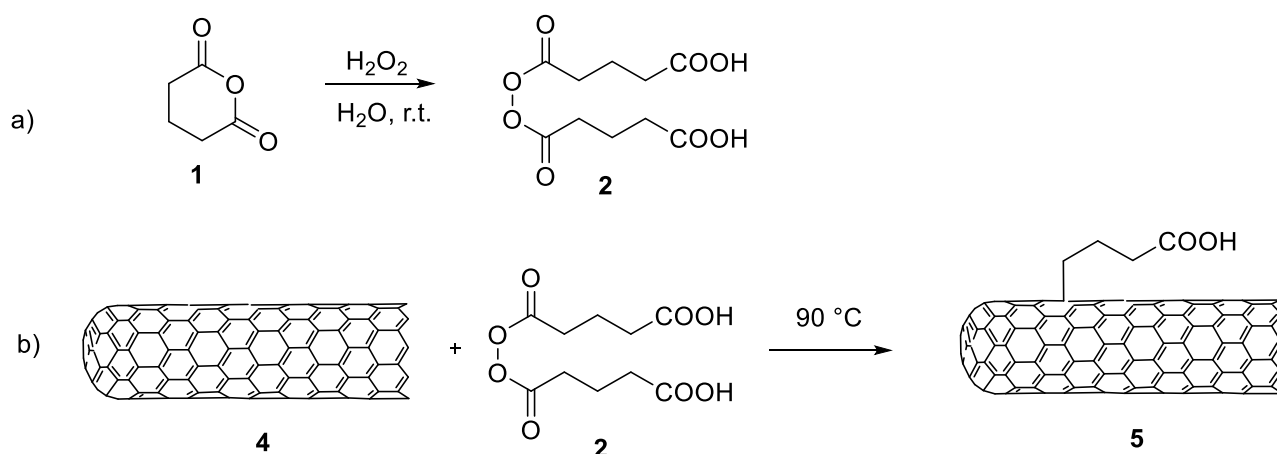
3 Results and Discussion

3.1. MWCNTs functionalization

3.1.1. MWCNTs functionalization with Glutaryl Peroxide

MWCNTs (CNTs) were modified following a literature procedure (134,135). First, by reaction of glutaric anhydride (**1**) with hydrogen peroxide, glutaryl peroxide (**2**) was prepared in good yield (scheme 3.1, a). The impurity is represented by glutaric acid (**3**).

Then, CNTs (CNT BASE, **4**) were modified by the free radical reaction performed at 90 °C in the presence of **2**, to obtain functionalized CNT-X-COOH **5** (scheme 3.1, b).



Scheme 3.1: Procedure for functionalization of CNTs to obtain CNT-X-COOH.

From the ^1H NMR analysis (Figure 3.1), it was deduced that the purity of the glutaryl peroxide is about 85% and the remaining 15% is glutaric acid (**3**).

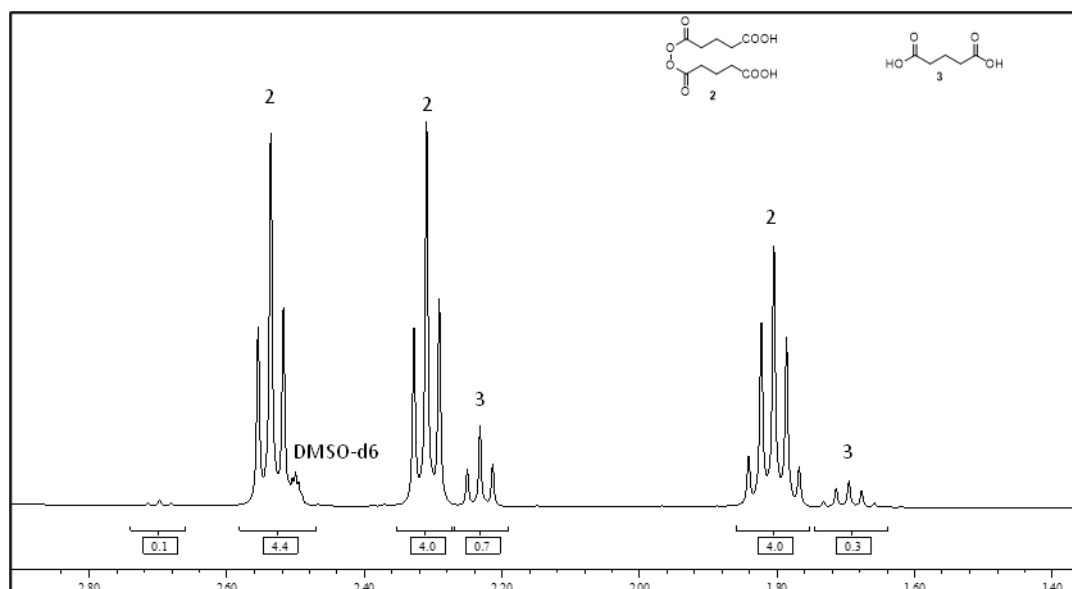


Figure 3.1: ^1H NMR analysis for glutaryl peroxide.

Thermogravimetric analysis (TGA) of CNT-X-COOH **5** obtained was performed (Figure 3.2). The red curve represents the percentage of weight loss as a function of temperature, whereas the blue curve represents the differential thermal analysis (DTA). The green one is the first derivative of the thermogravimetric red curve. The initial bend at 100 °C is due to moisture loss. The bend at 400 °C is due to the degradation of the -X-COOH chains attached to the CNT surface. Then, there is the complete combustion of the nanotube itself. The residue is represented by alumina and iron oxide. Therefore, from the analysis, it is deduced that 5% by weight of -X-COOH chains are grafted on the surface of the nanotube.

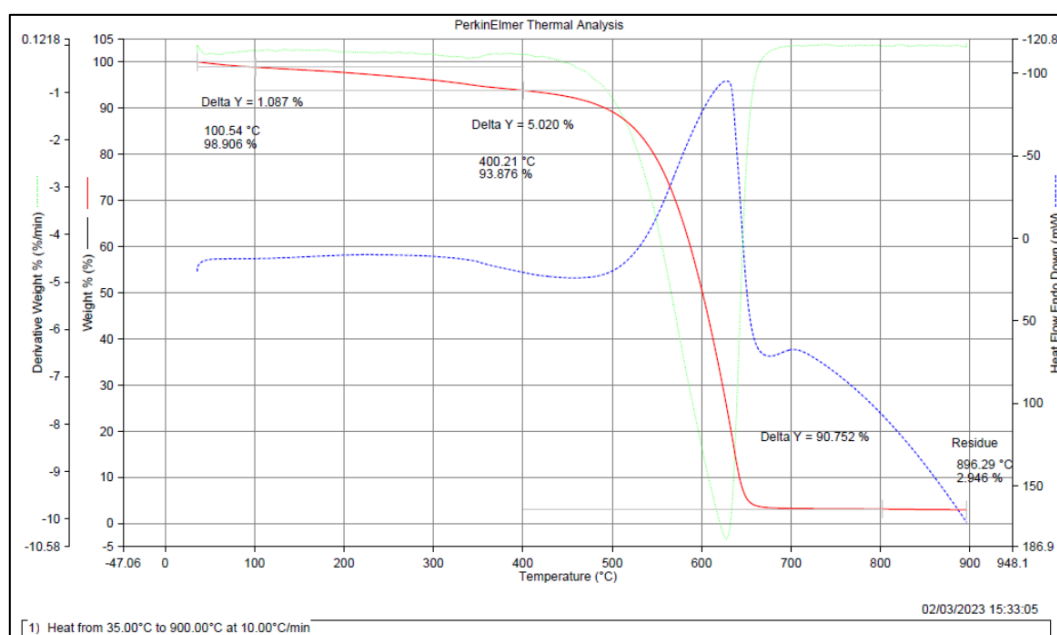
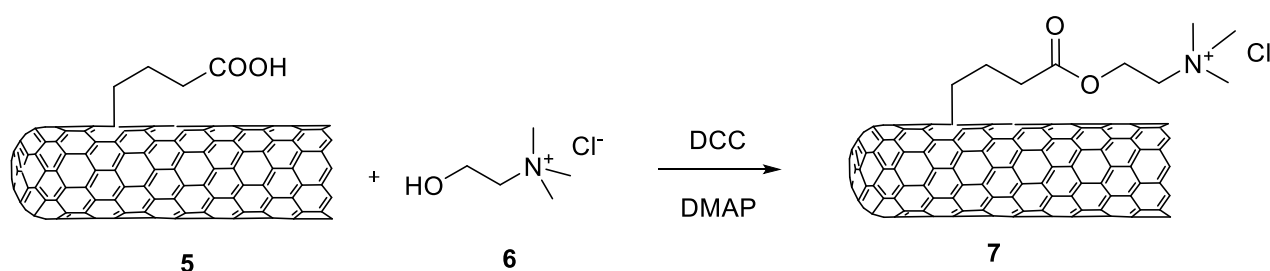


Figure 3.2: TGA of CNT-X-COOH.

CNT-X-COOH were then salified in the presence of NaOH obtaining CNT-X-COO⁻Na⁺ (CNT-X-COO⁻ 9).

3.1.2. Preparation of CNT-X-COL

Choline (6) was introduced on the chain -X-COOH by esterification of the carboxylic group in the presence of *N,N'*-dicyclohexylcarbodiimide (DCC) and 4-dimethylaminopyridine (DMAP) (Scheme 3.2). Modified nanotubes CNT-X-COL 7 were obtained. At the end of the reaction, together with the catalyst (DMAP), dicyclohexylurea (DCU) is present as co-product and both are not recovered.



Scheme 3.1: Procedure for functionalization of CNT-X-COOH to obtain CNT-X-COL.

The TGA analysis of 7 was performed (Figure 3.3). From the TGA (red curve), a significant weight loss (approximately 8%) is observed between 100 and 400 °C and it is due to the degradation of the substituents grafted on the CNT surface.

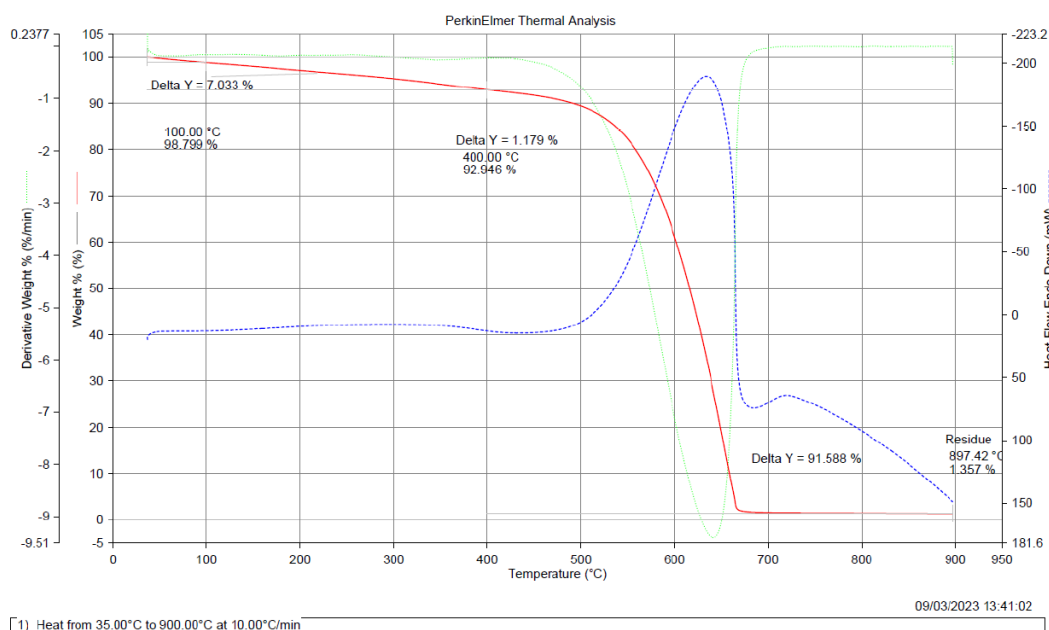


Figure 3.3: TGA of CNT-X-COL (7).

3.1.3. Preparation of CNTs/clay hybrid material

Although clays are natural porous material and widely used in the removal of inorganic pollutants from wastewater, they show insignificant applicability in treating numerous organic pollutants. Additionally, most clay materials exhibit a lower sedimentation capacity. Hence, the motivation to create a hybrid material that could adsorb both organic and inorganic pollutants (136). Since clay materials have exchangeable inorganic cations, these can be exchanged with organic cations: this mechanism allows the interaction between clay and the functional groups present on the surface of the nanotube.

The hybrid material was prepared by mixing clay (Montmorillonite-Nanofil 116) and CNT-X-COL. It was decided to carry out two different types of exchanges, one with a 1:1 ratio and the other with a 1:0.2 ratio.

3.2. Adsorption tests

Compared to traditional adsorbents like activated carbon and clay, carbon nanotubes (CNTs) are more attractive due to their favorable physicochemical stability, high selectivity, and unique structure. Many experiments have been conducted on the adsorption of inorganic contaminants on CNTs, and other studies have focused on the adsorption of organic pollutants. Therefore, CNTs could be ideal adsorbents for the removal of pollutants (137).

The adsorption efficiency of various functionalized CNTs including CNT-X-COOH, CNT-X-COL, CNT-X-COO⁻ (syntheses is discussed in Chapter 3, paragraph 1), CNT-COOH previously prepared in the laboratory and the pristine one (CNT BASE) (Figure 3.4) was investigated to understand how functionalization can enhance the adsorption of dyes and copper(II) in water. Among these nanotubes, two carboxylated CNTs were compared (5 and 8) to explore if the introduction of a short spacer (three carbon atoms) between the nanotube surface and the functional group could affect the adsorption efficiency. Then, CNT-X-COOH were modified to obtain two differently charged CNTs (7 and 9) to study a possible interaction with charged dyes.

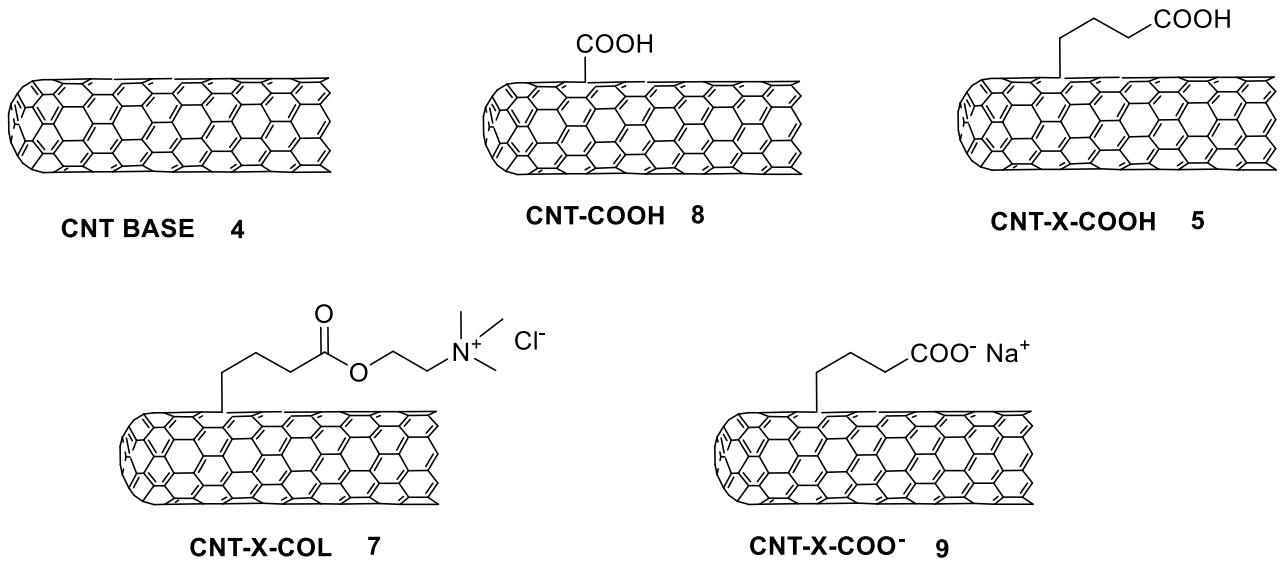


Figure 3.4: CNTs tested in this thesis.

It was decided to use dyes, in this case, Rhodamine B and Methyl orange, to simulate, in general, the adsorption of organic pollutants by functionalized nanotubes. At the same time copper (II) was used as model for the adsorption of metal cations.

Adsorption tests are performed by measuring the absorbance, using a UV-VIS spectrophotometer, of various solutions containing the four aforementioned pollutants.

The samples prepared for each pollutant were tested at room temperature (23-25°C) and prepared by varying either the quantity and type of adsorbent, or the contact time, or the pollutant concentration each time (Chapter 2, sections 5.1, 5.2, 5.3, and 5.4 for more details).

The adsorption efficiency of CNTs (Equation 3.1) was also compared, with that of a clay (Montmorillonite- Nanofil 116) and, with that of CNT/clay hybrid materials.

$$Efficiency (\%) = \frac{C_0 - C_e}{C_0} \times 100$$

Equation 3.1: Adsorption efficiency equation.

C_0 is the initial concentration of pollutant and C_e the final concentration of pollutant at the established contact time.

Generally, the concentration of pollutant has a significant effect on its removal. If the concentration is too high, the efficiency of removal cannot be correctly determined

because of to the saturation of adsorption sites on the surface of the adsorbent. For these reasons, the concentrations of the solutions were chosen in order to avoid the saturation of the adsorbent sites.

Moreover, adsorption capacity exhibits a rapid initial increase at the initial stage followed by a slower one and become constant after the equilibrium. This is because the available adsorption sites remain constant, and adsorption gradually reaches saturation at higher concentrations (138).

3.2.1. Calibration curves

The calibration curves are calculated for Cu(II) complexed by ammonia (maximum peak at 600 nm), Cu(II) nitrate trihydrate (maximum peak at 300 nm), Rhodamine B (maximum peak at 553 nm), and Methyl Orange (maximum peak at 465 nm) selected as references respectively for metal cation and dyes. These are obtained for each one through the readings of their respective absorbances at the peak.

wavelength corresponding to the above reported maximum peak. The results obtained are reported in Figure 3.5.

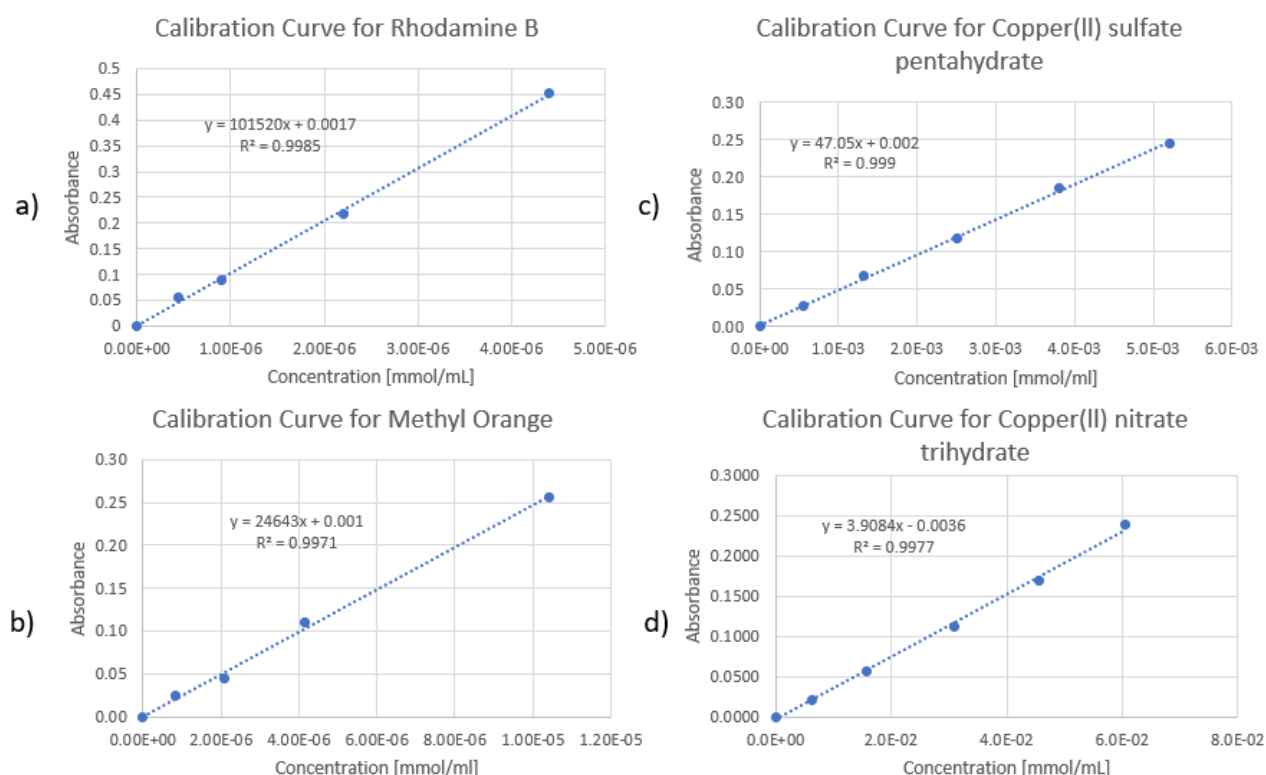


Figure 3.5: Calibration curves for Rhodamine B (a), Methyl Orange (b), Copper(II) sulfate pentahydrate (b) and Copper(II) nitrate trihydrate.

The four calibration lines show a high coefficient of determination R^2 , close to unity; therefore, a high predictive power of the linear model can be considered.

The residual pollutant concentrations, after the established contact time on the adsorbent, have been calculated from the absorbance value using the calibration curve equations.

3.3. Adsorption of Rhodamine B by CNTs

The solutions containing Rhodamine B (Chapter 2, paragraph 4.3) are at a neutral pH. This assumption is considered plausible because wastewater typically has a pH around neutrality. There are industrial activities that produce acidic or alkaline effluents due to specific treatments or processes. However, it is also true that before these effluents are discharged into the sewer or sent to treatment facilities, they are neutralized to bring the pH back to neutrality.

It is known that the adsorption of Rhodamine B depends on the pH, as it is a crucial parameter that affects the surface charge of the adsorbent, which can impact the dissociation of functional groups present on the potentially functionalized CNT, alter the structure of the dye molecule, and its degree of ionization.

It is reported that, neutral and basic pH are preferred for the adsorption of cationic dyes whereas a low pH is more suitable for the adsorption of anionic dyes (139).

In the case of carbon nanotubes functionalized with carboxylic groups, as those used in this study, (CNT-X-COOH and CNT-COOH), the functional group -COOH can undergo ionization, resulting in the formation of negative charge on the CNT surface.

Thus, the electrostatic attraction between negatively charged CNTs and the Rhodamine B would lead to an increase in adsorption capacity (140).

3.3.1. Comparison between the adsorbents used

The results regarding the experiments performed using CNTs in a solution of Rhodamine B (4.40×10^{-6} mmol/mL) (AR25, AR26, AR28, AR29, AR40, see paragraph 2.5.2 for details) after a contact time of 60 minutes are reported in Table 3.1 and plotted in Figure 3.6. An experiment using a clay (Montmorillonite-Nanofil 116) more than twofold in mass, in place of CNTs was also performed (AR14, paragraph 2.5.2). The samples are listed in descending order based on their adsorption efficiency (Table 3.1 and Figure 3.6).

Table 3.1: Adsorption efficiency obtained for Rhodamine B.

Sample name	Adsorbent	Adsorption efficiency
AR26	CNT-X-COOH	87%
AR29	CNT-X-COO-	84%
AR28	CNT BASE	73%
AR40	CNT-COOH	67%
AR25	CNT-X-COL	58%
AR14	Clay	28%

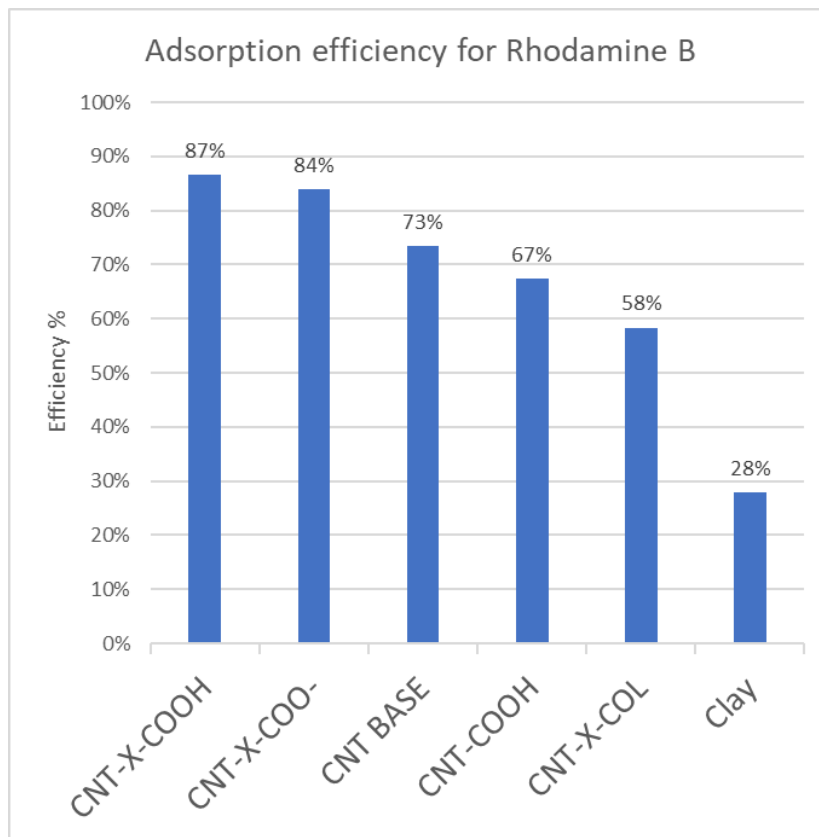


Figure 3.6: Efficiency for Rhodamine B.

As one might expect, clay proves to be not efficient as adsorbent for Rhodamine B (AR14) with respect to all the CNTs investigated. This is because of its chemical structure, that makes clay a good adsorbent primarily for inorganic substances such as metal ions.

As it can be seen from Figure 3.6, the adsorption efficiency depends on the substituents on CNTs surface. Taking as reference the pristine CNT (CNT BASE), CNT-COOH and CNT-X-COL are less efficient whereas CNT-X-COOH and CNT-X-COO⁻ have a higher efficiency.

The lower efficiency (58%) of nanotubes bearing the choline function (AR25) could be ascribed to the positive charge of choline itself, which results in little affinity with the cationic nature of the dye (Figure 3.7) due to the repulsion between positive charges.

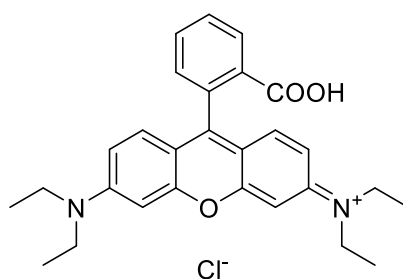


Figure 3.7: *Rhodamine B structure.*

Therefore, the positive charge of both the functional group of choline and Rhodamine B leads to limited interaction.

Interestingly, the two CNTs with the same functional group (COOH) gave different results: CNT-X-COOH (AR26) has an efficiency (87%) higher than CNT-COOH (AR40, 67%). The efficiency of anionic CNT-X-COO⁻ gave very similar results to that of CNT-X-COOH (AR29, 84%).

The study of the variation of efficiency as a function of contact time provides information on the adsorption mechanism and the various intermediate states leading to the formation of the final adsorbate-adsorbent complex and helps in developing appropriate mathematical models to describe the interactions between the components. Once the reaction rates are unequivocally known, they can be used to develop adsorbent materials for industrial applications and are valuable for understanding the intricate dynamics of the adsorption process (141).

The adsorption of Rhodamine B on CNT BASE and CNT-X-COOH (those with the highest adsorption efficiency) at constant initial concentrations was studied as a function of contact time (0, 15, 30, 45, 60 minutes) in order to determine the adsorption equilibrium time.

The tests were carried out at a temperature of 24 ± 2 °C, at a neutral pH. Specifically, 2.2 mg of CNT-X-COOH were dispersed in 25 mL of solution of Rhodamine B for the test with functionalized nanotubes, and similarly 2.2 mg of CNT BASE under the same conditions.

Contact times were set at 15, 30, 45, and 60 minutes. After the contact time elapsed, the solutions were filtered and analyzed using a UV-VIS spectrophotometer set at a wavelength of 553 nm.

Two curves were then drawn in which the contact time was plotted on the x-axis, and the percentage of pollutant absorbed by the nanotubes was plotted on the y-axis. It is evident that the adsorption of CNT-X-COOH is significantly higher than that of CNT BASE (Figure 3.8) also for times lower than the one reported in Table 3.1 (60 minutes).

The rapid initial adsorption can be attributed to the high availability of adsorbent sites on the surface of the nanotubes, particularly in the case of CNT-X-COOH, and to the concentration gradient of Rhodamine B in the solution compared to the still clean adsorbent (142).

At higher time values, the rate of dye adsorption decreases as it approaches the saturation of the surface of the CNTs.

Since a rather high efficiency, around 90%, was achieved for CNT-X-COOH with a contact time of 60 minutes, it can be assumed that the equilibrium is established shortly thereafter. This result is positive, as even for real applications, a contact time of 1 hour is a typical and not excessive value for adsorption treatments.

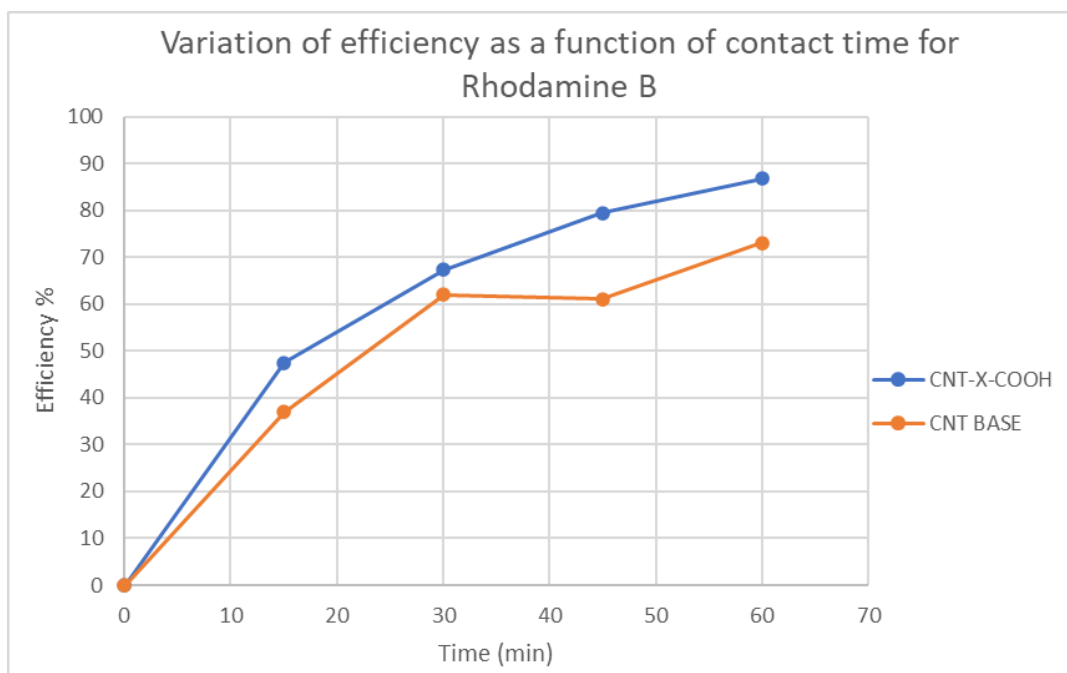


Figure 3.8: Variation of efficiency as function of time for Rhodamine B.

Moreover, two tests were conducted with a contact time of 24 hours to assess the adsorption efficiency over a longer period. Specifically, 2.2 mg of CNT-X-COOH were dispersed in 25 mL of Rhodamine B solution (AR46) for the test with functionalized nanotubes, and similarly, 2.2 mg of CNT BASE (AR45) under the same conditions. In both cases, the complete adsorption was observed.

3.3.2. Adsorption isotherm studies

As explained in the Chapter 1 Paragraph 1.4, adsorption isotherms provide qualitative information on the capacity of the adsorbent as well as the nature of the solute–surface interaction.

In this screening, as reported in literature, Langmuir and Temkin isotherm models were used for CNT-X-COOH to study the equilibrium characteristics of adsorption, since the adsorption tests showed that these nanotubes gave the best performances.

The tests were carried out at a temperature of 24 ± 2 °C, at a neutral pH.

Langmuir isotherm assumes that the single adsorbate binds to a single site on the adsorbent and that all surface sites on the adsorbents have the same affinity for the adsorbate (143). Thus, once a dye molecule occupies a site, no further adsorption can take place at that site.

The following linearized plot of the Langmuir equation was used in this study (Figure 3.9):

$$\frac{C_e}{q_e} = \frac{C_e}{q_{max}} + \frac{1}{q_{max}} b$$

Equation 3.2: *linearized Langmuir equation.*

C_e is the final concentration (mg/L), q_e represents equilibrium concentration (mg/g), b is the Langmuir constant (L/mg), which is related to the affinity of binding sites; and q_{max} is the theoretical saturation capacity of the monolayer (mg/g). The values of q_{max} and b derived from the intercept and slope of the linear plot of C_e/q_e versus C_e . (144)

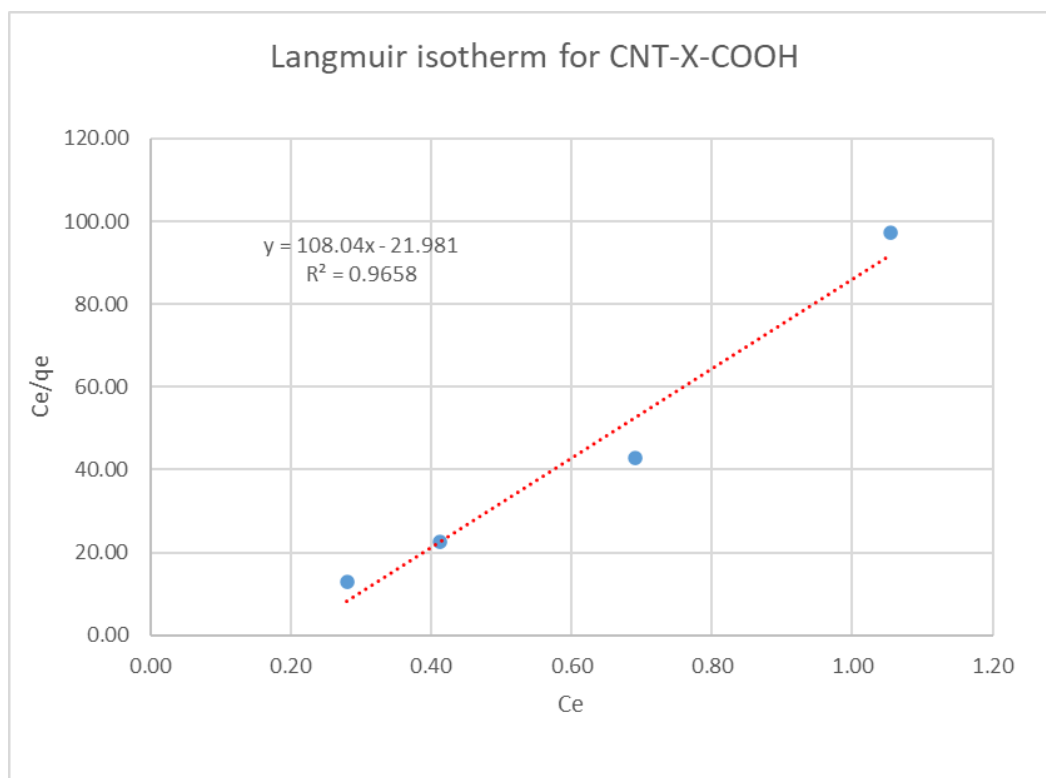


Figure 3.9: The result obtained for the adsorption of Rhodamine B by CNT-X-COOH. The b coefficient value is -0.204 (L/mg) and q_{max} is 9.256 (mg/g).

The Langmuir isotherm of Rhodamine B and CNT-X-COOH was found to be linear over the whole concentration range studied and the correlation coefficient is high ($R^2=0.9658$).

The Langmuir isotherm for CNT BASE was also studied, and the result obtained is shown in Figure 3.10.

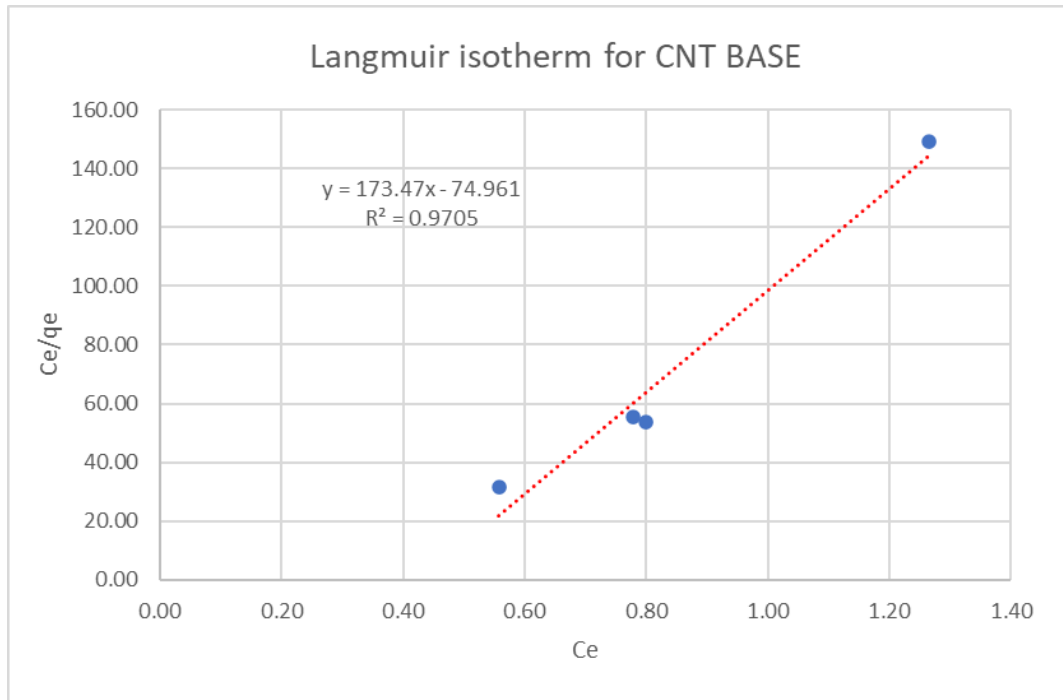


Figure 3.10: The result obtained for the adsorption of Rhodamine B by CNT BASE. The b coefficient value is -0.432 (L/mg) and q_{max} is 5.764 (mg/g).

The Langmuir isotherm was found to be linear over the entire concentration range studied in this case as well, and the R^2 value is high (0.9705).

The Temkin isotherm is used to describe the behavior of adsorption systems on a heterogeneous surface. It is built on the assumption that the decrease in heat of sorption is linear, rather than logarithmic. This model suggests that, due to interactions between the sorbate and the sorbent, the heat of sorption for all molecules in the adsorbed layer decreases linearly with coverage.

The equation is:

$$qe = \frac{RT}{b} (aC_e)$$

Equation 3.3: linearized Temkin equation.

where C_e is final conc. (mg/l), q_e represents equilibrium conc. (mg/g), b is the Temkin constant related to heat of sorption (KJ/mol), R is the gas constant [0.0083 KJ/(mol K)], a is the Temkin isotherm constant (L/g) and T the absolute temperature (K).

To determine the isotherm, a plot of q_e (the amount of adsorbate at equilibrium) versus $\ln(C_e)$ (the natural logarithm of the equilibrium concentration) is typically employed. (144)

Here is the result for CNT-X-COOH with Rhodamine B (Figure 3.11).

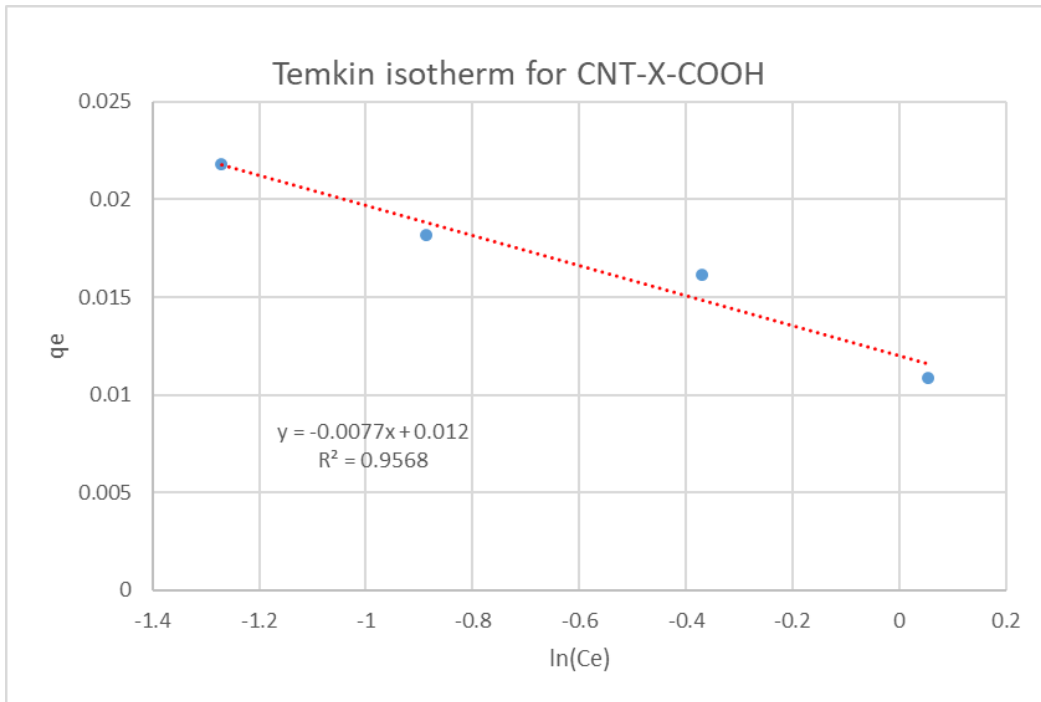


Figure 3.11: The result obtained for Temkin adsorption of Rhodamine B by CNT-X-COOH

The Temkin isotherm was found to be linear over the entire concentration range studied in this case as well, and the R^2 value is good (0.9568).

As before, the same procedure was carried out for CNT BASE to enable a comparison. The Temkin isotherm for CNT BASE is shown in Figure 3.12 and also exhibits a notable R^2 value, which is 0.9725.

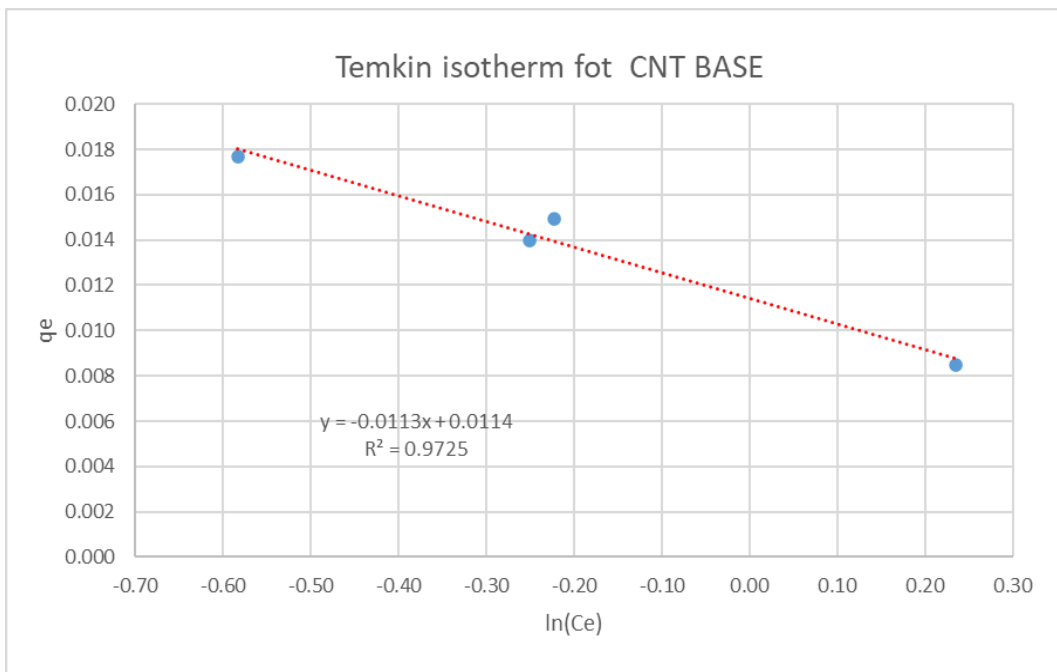


Figure 3.12: Temkin isotherm for CNT BASE.

3.4. Adsorption of Methyl Orange by CNTs

Methyl orange is a typical water-soluble anionic dye (Figure 3.13). It is one of the most widely used dyes in the textile industry (145), as well as in titrations and as a pH indicator; it is indeed an example of an acid-base indicator and changes color in response to variations in the pH of the environment in which it is present.

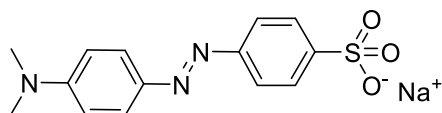


Figure 3.13: Methyl Orange structure.

Azo dyes and/or their metabolites in general are well-known carcinogenic organic substances (145). Like many other dyes of its class, Methyl Orange, when ingested and entering the body, is metabolized into aromatic amines by intestinal microorganisms. Reductive enzymes in the liver can catalyze the reductive cleavage of the azo bond to produce aromatic amines and may even lead to intestinal cancer; that's why the safe removal of such a dye allows for a thorough assessment of the removal efficiency of tested adsorbent materials for both the dye itself and other similar organic compounds. (146)

As in the case of Rhodamine B, the adsorption experiments with Methyl Orange (Chapter 2, paragraph 4.4) were performed at a neutral pH.

As mentioned before, this assumption is considered plausible because wastewater typically has a pH around neutrality; in any case, if the water is acidic or alkaline, it is neutralized before being sent to the treatment plant.

In previous studies (147) the effect of pH on Methyl Orange adsorption was investigated within a range of 2 to 10, and it was found that adsorption decreases with increasing pH. The higher adsorption of the anionic dye at low pH may be attributed to the neutralization of the negative charge, resulting from the presence of negative oxygen on the surface of the adsorbents, as previously explained in section 1.1 of Chapter 3. However, as pH increases, protonation decreases, resulting in an inhibition in the anion adsorption.

3.4.1. Comparison between the adsorbents used

As for the Rhodamine B, the residual pollutant concentration, after the contact time, is calculated using the calibration curve equations as described in Chapter 2, paragraph 4.4.

The results obtained for Methyl Orange (0.005210 mmol/mL) for a contact time of 60 minutes are listed in table 3.2. The experiments were performed using the two carboxylic functionalized CNTs (AR 34 and 38), the pristine ones (AR35) and the nanotubes bearing the choline moiety (AR33) (Chapter 2, paragraph 5.3).

In Table 3.2 and Figure 3.14, the samples are arranged in descending order based on their adsorption efficiency:

Table 3.2: Adsorption efficiency obtained for Methyl Orange.

Sample name	Adsorbent	Adsorption efficiency
AR34	CNT-X-COOH	92%
AR38	CNT-COOH	86%
AR35	CNT BASE	66%
AR33	CNT-X-COL	54%

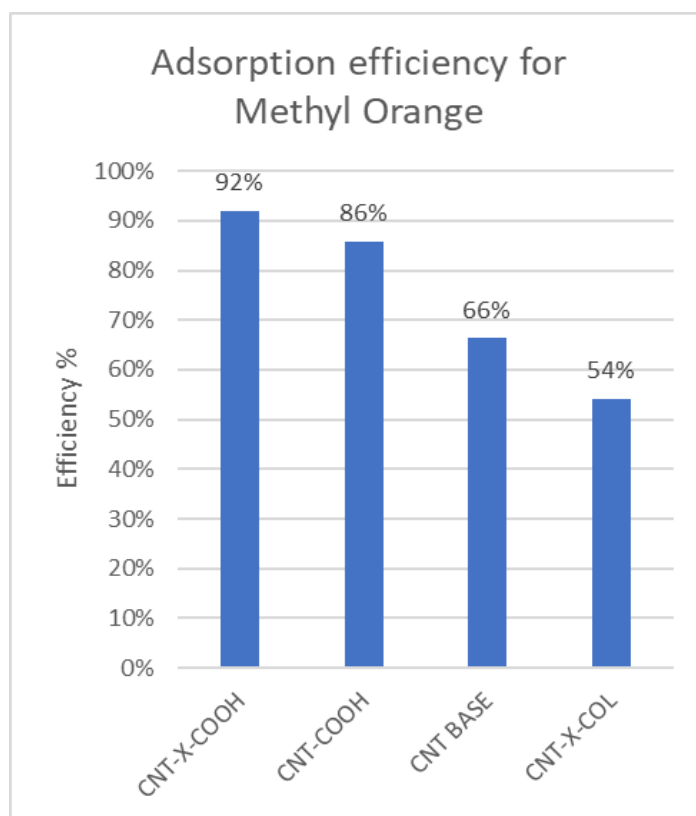


Figure 3.14: Adsorption efficiency for Methyl Orange in 60 minutes.

As in the case of Rhodamine B, also with Methyl Orange, carbon nanotubes functionalized with choline (CNT-X-COL) showed the lowest efficiency (54%) and, unlike the tests with Rhodamine B, the CNT-COOH (86%) revealed to be more efficient than CNT BASE (66%). Anyway, the CNT-X-COOH (92%) are the most efficient even in these tests.

3.4.2. Variation of efficiency as a function of contact time

The adsorption of Methyl Orange on CNT BASE and CNT-X-COOH (the CNTs with the higher efficiency) at constant initial concentrations was studied as a function of contact time to determine the adsorption equilibrium time.

The tests were carried out at a temperature of 24 ± 2 °C, at a neutral pH. Specifically, 2.2 mg of CNT-X-COOH were placed in 25 mL of 'Solution 1' of Methyl Orange (Chapter 2, paragraph 4.4) for the test with functionalized nanotubes, and 2.2 mg of CNT BASE in the same solution and under the same conditions.

Contact times were set at 15, 30, 45, and 60 minutes. After the contact time elapsed, the solutions were filtered and the absorbances were measured at a wavelength of 465 nm.

The two curves in which the contact time was plotted on the x-axis, and the percentage of pollutant absorbed by the nanotubes was plotted on the y-axis are reported in Figure 3.15. The adsorption of CNT-X-COOH is significantly higher than that of CNT BASE (Figure 3.15) also at times shorter than 60 minutes (Table 3.2).

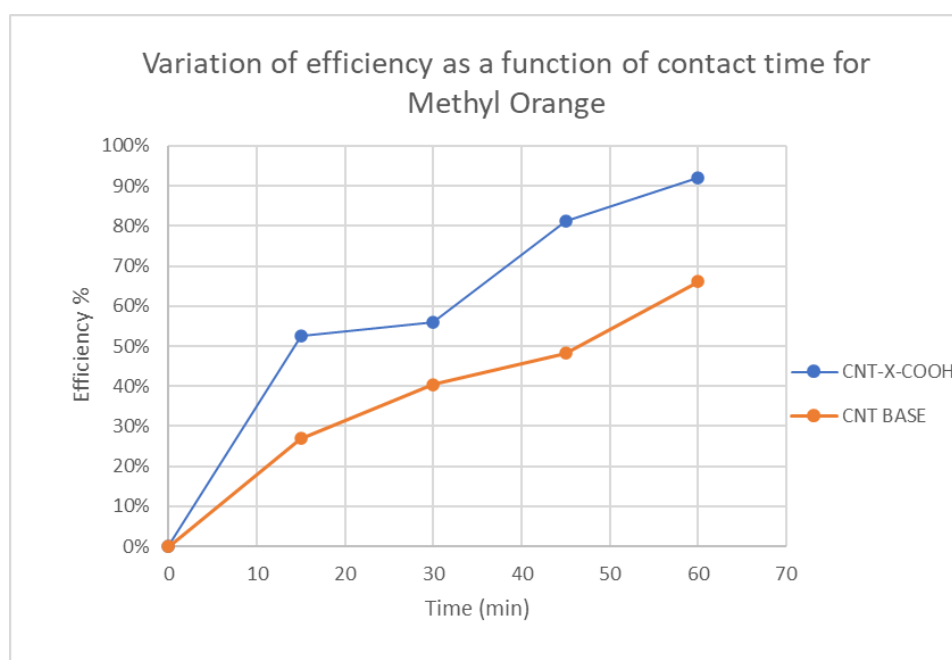


Figure 3.15: Variation of efficiency as function of time for Methyl Orange.

The rapid initial adsorption can be attributed to the high availability of adsorbent surface area of the nanotubes, particularly in the case of CNT-X-COOH, and the concentration gradient of Methyl Orange in the contaminated solution compared to the still clean adsorbent.

At longer times, the rate of Methyl Orange adsorption decreases as it approaches the saturation point of the CNT surface.

Having achieved a relatively high efficiency of approximately 90% for CNT-X-COOH within a 60-minute contact time, it can be reasonably assumed that equilibrium is established shortly after this period. This is a favorable result, as even in practical field applications, a contact time of 1 hour is a typical and reasonable duration for adsorption treatments.

Anyway, it was then decided to evaluate the adsorption over a 24-hour period to determine if the results remained consistent, aiming to confirm that CNT-X-COOH indeed had higher efficiency even over longer contact time. A comparison was made between CNT BASE (AR36) and CNT-X-COOH (AR47), and once again, the functionalized nanotubes were found to have higher efficiency in this case as well. The results obtained for the samples AR47 and AR36 (Chapter 2, paragraph 5.3) are shown in Table 3.3 and Figure 3.16.

Table 3.3: *Adsorption efficiency obtained for Methyl Orange for 24h.*

Sample name	Adsorbent	Adsorption efficiency
AR47	CNT-X-COOH	>99.0%
AR36	CNT BASE	91.6%

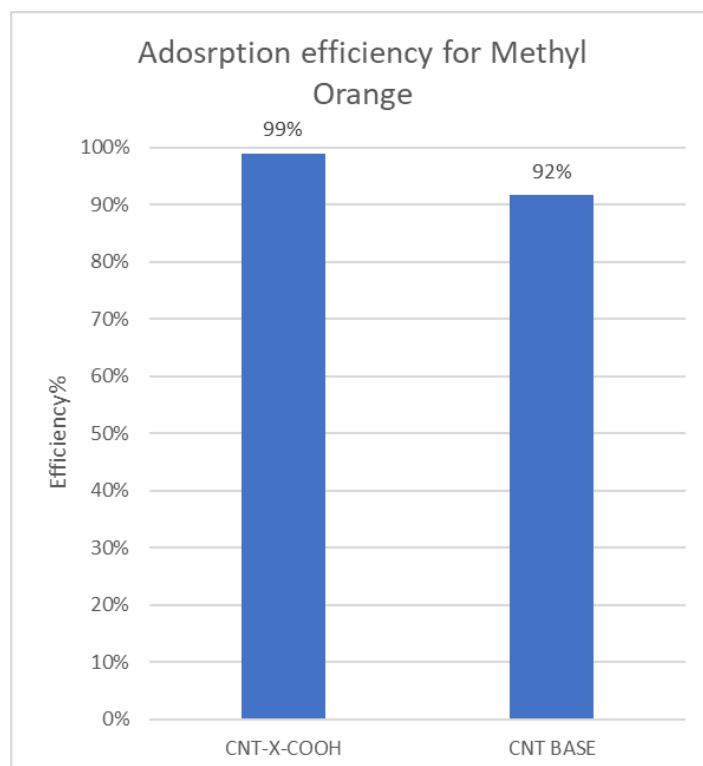


Figure 3.16: Efficiency for Methyl Orange in 24h.

Differently from Rhodamine B, the adsorption efficiency of CNT BASE toward Methyl Orange even at a very long time was not complete.

3.4.3. Adsorption isotherm studies

The isotherms analyzed for methyl Orange once again include Langmuir and Temkin curves for both CNT-X-COOH and CNT BASE.

The linear mathematical model of Langmuir used is the same discussed in Chapter 3, paragraph 1.5.

The Langmuir isotherm for CNT-X-COOH (Figure 3.17) has a low correlation coefficient (0.6491).

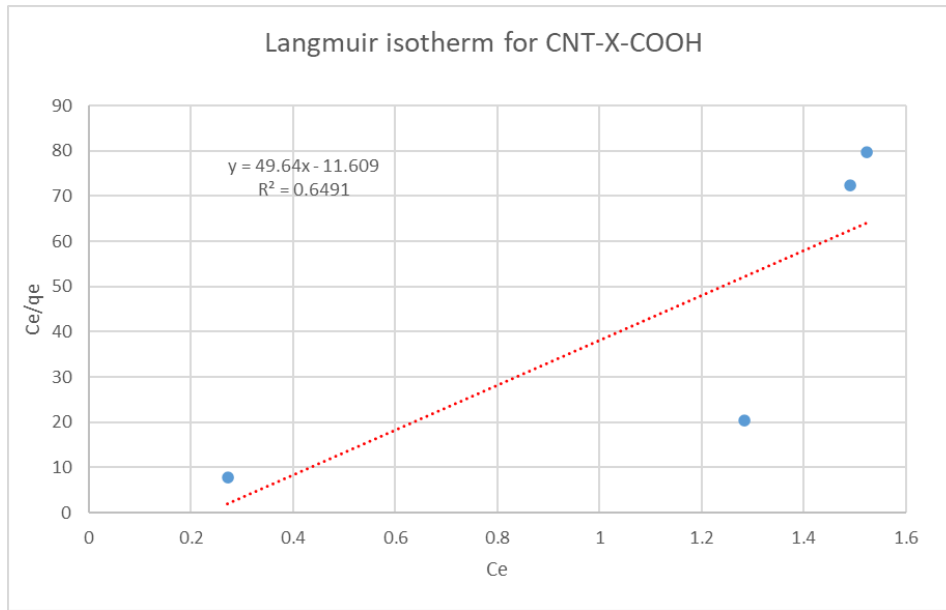


Figure 3.17: The result obtained for the adsorption of by CNT-X-COOH. The b coefficient value is -0.234 (L/mg) and q_{max} is 20.145 (mg/g).

The Langmuir isotherm for CNT BASE was also studied, and the result obtained is shown in Figure 3.18.

In this case, the correlation coefficient of the isotherm is higher than the previous case (0.8909) as previously emphasized.

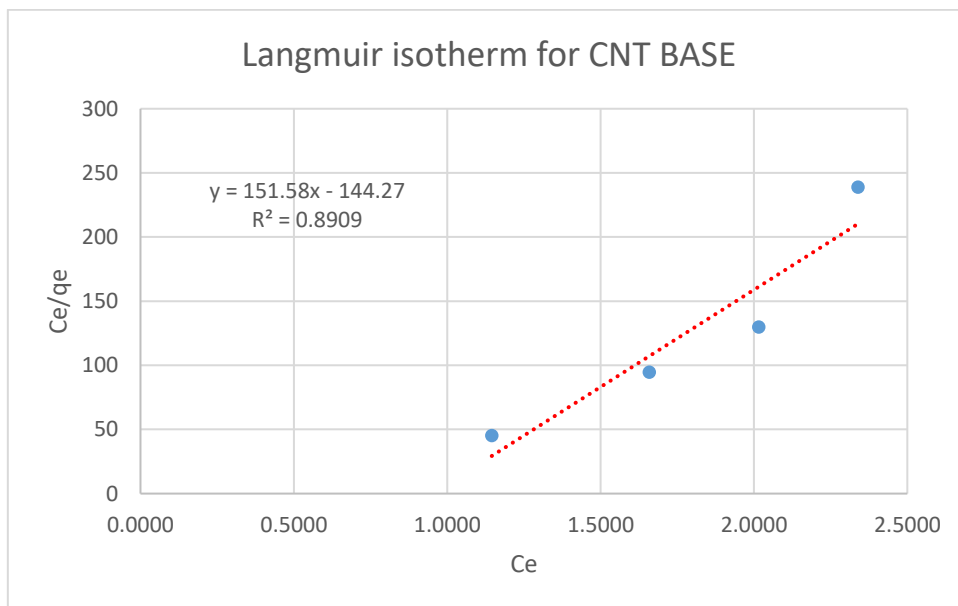


Figure 4.18: The result obtained for the adsorption of by CNT BASE. The b coefficient value is -0.952 (L/mg) and q_{max} is 6.597 (mg/g).

The Temkin isotherm, as discussed in paragraph 3.2 of Chapter 3, is an isotherm that describes adsorption on a heterogeneous surface.

To determine the isotherm, a plot of q_e (the amount of adsorbate at equilibrium) versus $\ln(C_e)$ (the natural logarithm of the equilibrium concentration) is typically employed. The result for CNT-X-COOH with Methyl Orange is shown in Figure 3.19.

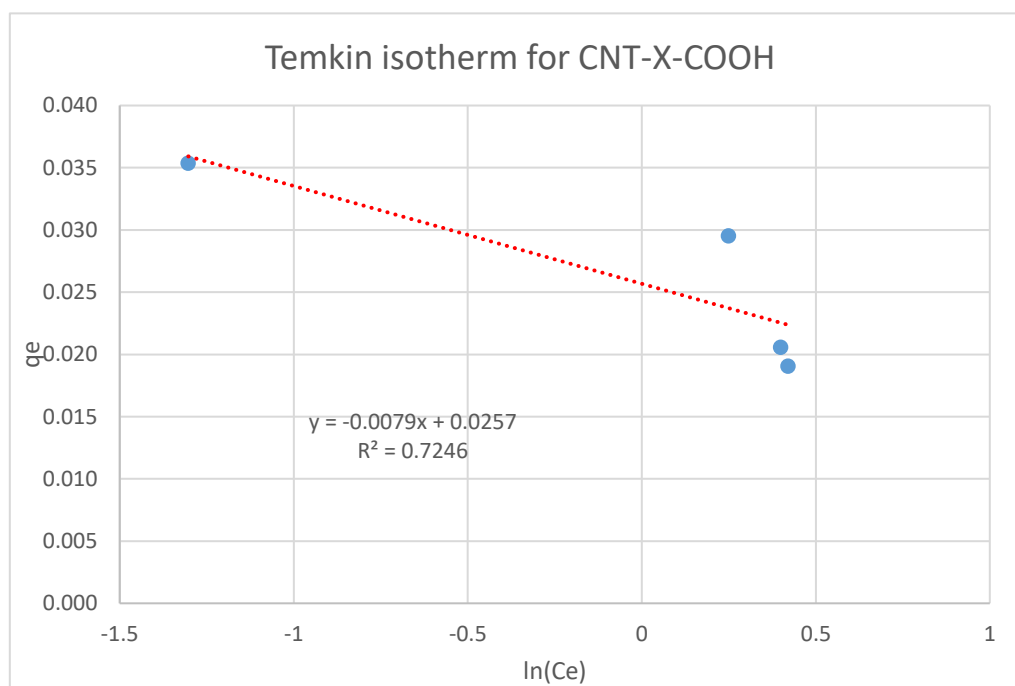


Figure 3.19: The result obtained for the adsorption of Methyl Orange by CNT-X-COOH.

In this case as well, the isotherm does not have a good R^2 (0.7246).

As before, the same procedure was carried out for CNT BASE to enable a comparison. The Temkin isotherm for CNT BASE is shown in Figure 3.20 and exhibits a modest R^2 value, which is 0.8971.

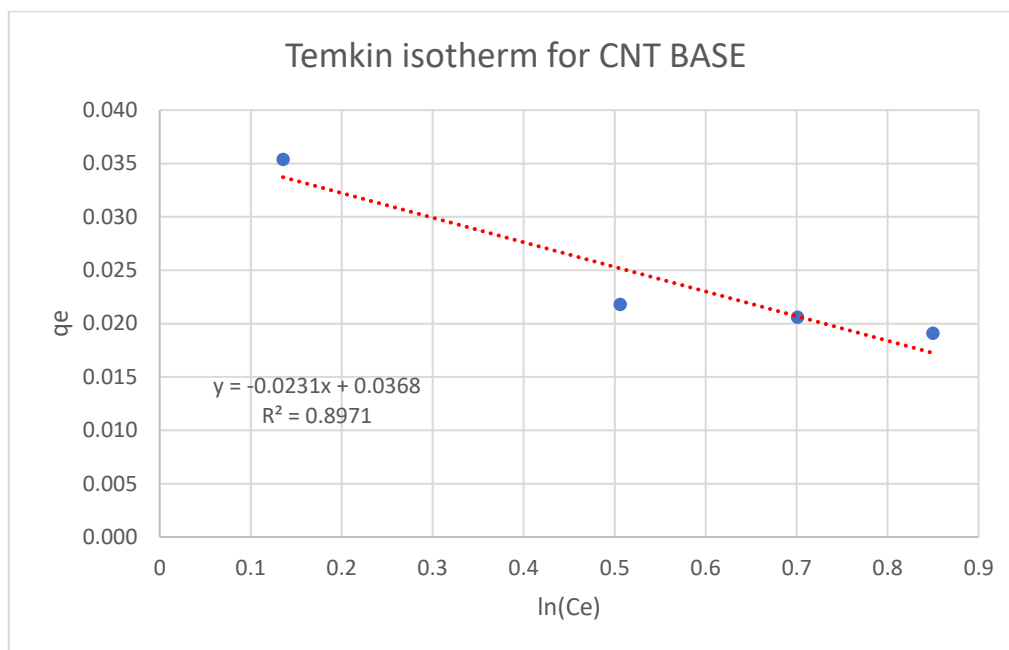


Figure 3.20: The result obtained for the adsorption of Methyl Orange by CNT BASE.

In conclusion, as the correlation coefficients of Langmuir and Temkin isotherms for CNT BASE are not so close to 1 but higher than the values obtained in the case of CNT-X-COOH, it is clear that further investigations are necessary to exclude that the models are not suitable for the describing the adsorption mechanism in these cases.

3.4.4. Efficiency in different conditions

Two new tests were then conducted to compare the efficiency of the CNT BASE and CNT-X-COOH, varying the doses of the pollutant and adsorbent. In particular, a ratio mg (Methyl Orange)/mg CNT = 0.085 instead that 0.039 (Chapter 2, paragraph 4.4) was used maintaining 60 minutes as contact time. In Figure 3.21 and Table 3.4, results regarding the samples AR53 and AR52 (Chapter 2, paragraph 5.3) are arranged in descending order based on their adsorption efficiency:

Table 3.4: Adsorption efficiency obtained for Methyl Orange for different conditions.

Sample name	Adsorbent	Adsorption efficiency
AR53	CNT-X-COOH	70%
AR52	CNT-BASE	61%

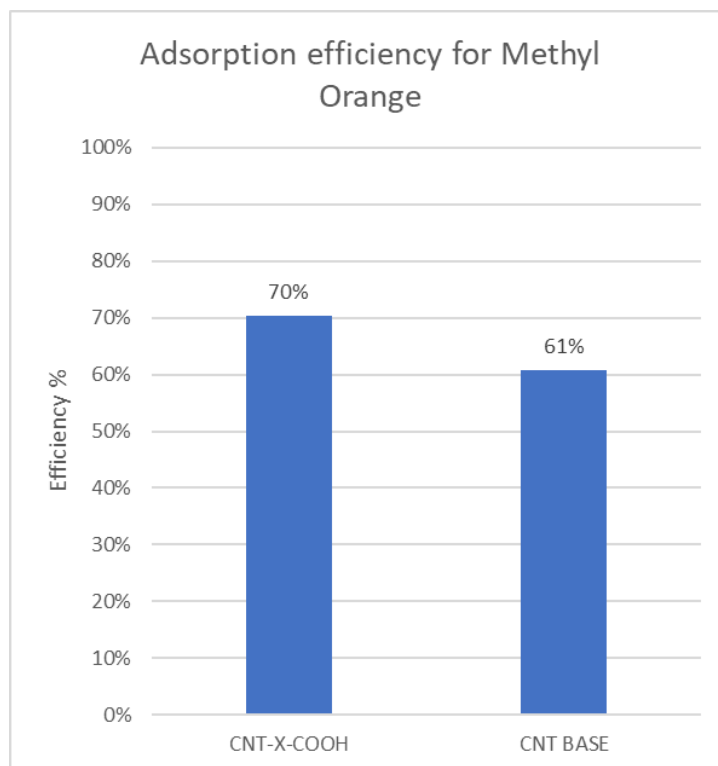


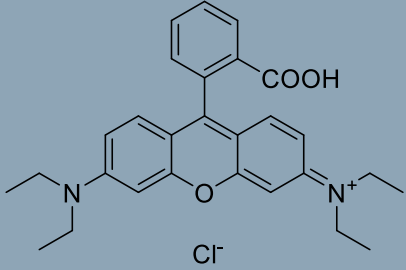
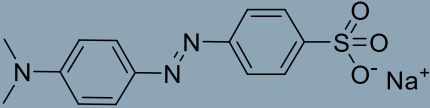
Figure 3.21: Efficiency for Methyl Orange with a ratio $\text{mg (Methyl Orange)}/\text{mg CNT} = 0.085$.

The result demonstrates that even using of a different ratio pollutant/CNTs, the functionalized nanotubes CNT-X-COOH still exhibit higher efficiency.

3.5. Discussion of the data for dyes

The percentage of dye removal reported Table 3.1 (paragraph 3.3.1) and 3.2 (paragraph 3.4.1) are summarized in Table 3.5.

Table 3.5: Summary of the results obtained for the dyes.

CNT	Rhodamine B  Cl ⁻	Methyl Orange 
CNT-X-COOH	87%	92%
CNT-X-COO ⁻	84%	not performed
CNT BASE	73%	66%
CNT-COOH	67%	86%
CNT-X-COL	58%	54%

Nanotubes bearing a carboxylic group bound to a three-carbon chain spacer (CNT-X-COOH) revealed to be the most efficient in the adsorption of both a cationic (Rhodamine B) and an anionic dye (Methyl Orange). The functionalization with this polar group increases hydrophilicity of the CNTs and at the same time, the small spacer may have the effect to promote the separation between the nanotubes, that in turn could show a higher surface.

As discussed in Chapter 1, paragraph 4.1, the adsorption by CNTs can be explained in terms of their interactions with the dyes. Electrostatic interactions, ion exchange, hydrogen bonding, hydrophilic interactions and π - π electron binding are the significant factors that can affect the efficiency.

Although it is not straightforward to compare different CNTs, some comments on the different efficiency can be tentatively proposed.

Regarding the study of the absorbance of Rhodamine B by CNTs, as proposed in paragraph 3.3.1, the lower efficiency of the positively charged CNT-X-COL compared to that of CNT-BASE could be ascribed to the non-favorable interactions between the two equally charged adsorbent and dye. However, as almost the same efficiency is observed in the case of CNT-X-COL with an anionic dye (MO), it seems that these interactions are not so important in the absorbance process. If this is true, the longer spacer in CNT-X-COL between the positive charged nitrogen atom and the nanotube

surface may play a role, perhaps because in this case the spacer is too long, having the effect to reduce the π - π interaction between the dye and the nanotube.

The adsorption efficiency, toward Rhodamine B, of nanotubes bearing carboxylic groups directly bound to the surface (CNT-COOH) or through the spacer (CNT-X-COOH) was compared with that of non-functionalized CNT BASE. In this case, only the efficiency of CNT-X-COOH was higher than that of CNT BASE, whereas for CNT-COOH the value was lower. This finding suggests that again, the interactions between the cationic dye and CNTs seems to be not the main responsible of the adsorption phenomena. The experiment performed with CNT-X-COO⁻ (in which the negative charge should be higher with respect to that of "neutral" CNT-X-COOH) gave a slight decrease of the efficiency with respect of CNT-X-COOH (AR26, 87%), and this support the hypothesis discussed above.

In the case of Methyl Orange (an anionic dye), CNT-COOH and CNT-X-COOH showed a higher removal efficiency compared to CNT BASE, and, at the same time, the difference was small (92% for CNT-X-COOH and 86% for CNT-COOH). Anyway, also in this case, CNT-X-COOH still gave the higher performances. Therefore, this spacer (C3) seems to be a structural moiety that enhances the effect of the interactions.

In conclusions, it seems that there is an optimal length of the substituent chain on the CNTs and this represents an interesting potential development of the study. Nevertheless, further investigations are necessary to verify the validity of this hypothesis quantitatively and through computational simulation. These studies, together with specific surfaces analysis (BET) are in progress.

In the case of Rhodamine B, the Langmuir and Temkin isotherms gave substantially the same good correlations for both for CNT BASE (as expected from literature) and for CNT-X-COOH. Differently, in the case of Methyl Orange, the isotherm showed very low correlation coefficients.

3.6. Adsorption of Cu(II) sulfate pentahydrate by CNT/clay hybrid materials

Heavy metals, known to have harmful effects on health and cause bioaccumulation, as mentioned in Chapter 1, can be treated in wastewater using various physico-chemical methods.

Copper(II), the ion chosen in this study, can be released into the environment from various sources. It is a highly toxic element for drinking water, second only to mercury in toxicity. While copper is important for animal metabolism, excessive intake of copper can lead to severe consequences, including increased blood pressure, impaired kidney and liver function, seizures, cramps, and even death.

The preferred removal method is adsorption because it exhibits high efficiency in removing heavy metals such as Cu(II). While there are numerous adsorbents used in adsorption methods, activated carbon is the most commonly used in wastewater treatment worldwide. However, its high cost limits its usage, leading to the preference for clays, which are versatile, cost-effective, and readily available adsorbents of various types.

As mentioned, carbon nanotubes represent a valuable asset in addressing the growing challenges of environmental remediation, particularly in the context of water. Enhancing their ability to remove hazardous pollutants like heavy metals from wastewater could have a significantly positive impact on human health. However, to efficiently adsorb metal ions, CNTs must be suitably functionalized for this purpose since they are inherently geared towards the removal of organic pollutants.

A hybrid material composed by a functionalized CNT and a clay could combine, in a single multifunctional material, the advantages of the high affinity of CNTs toward the organic pollutants and the efficiency of the clay in the removal of metal cations.

In order to allow an ion exchange with the clay, the positively charged CNT-X-COL, even if showed a lower efficiency with respect to the base one, were used (paragraph 3.1.3) to obtain two hybrid materials with a different ratio CNTs/clay. The hybrid materials were therefore tested for the removal of copper(II), and their adsorbance efficiency was compared to those obtained for the clay and CNTs separately.

The pH of "Solution 1" prepared by adding ammonia to a solution of copper(II) sulfate pentahydrate was measured and found to be 11.4, (Chapter 2, paragraph 4.1).

The adsorption of copper ions is strongly influenced by pH. From various studies (149), it has been demonstrated that the adsorption of Cu(II) increases as the pH shifts from neutral to alkaline, while it is less favorable under acidic pH conditions.

At low pH, few copper ions are removed, and this is attributed to the competition between hydrogen ions from water and copper ions (150).

3.6.1. Comparison between the adsorbents used

The adsorption efficiency was determined as discussed above (paragraph 3.2).

The results obtained for a contact time of 60 minutes are reported in Table 3.6 and Figure 3.22.

The samples AR05b, AR09, AR07, AR08, AR12, AR11 (refer to Chapter 2, paragraph 5.1) are arranged in descending order based on their adsorption efficiency.

Table 3.6: Results obtained for copper (II).

Sample	Adsorbent	Mass of adsorbent	Efficiency
AR05b	Clay	25 mg	67%
AR09	CNT-X-COL/clay 1:1	50 mg (25 mg/25 mg)	67%
AR12	CNT-X-COL/clay 1:0.2	30 mg (25 mg/5 mg)	28%
AR06b	Clay	5.1 mg	22%
AR11	CNT-X-COL	25 mg	9%

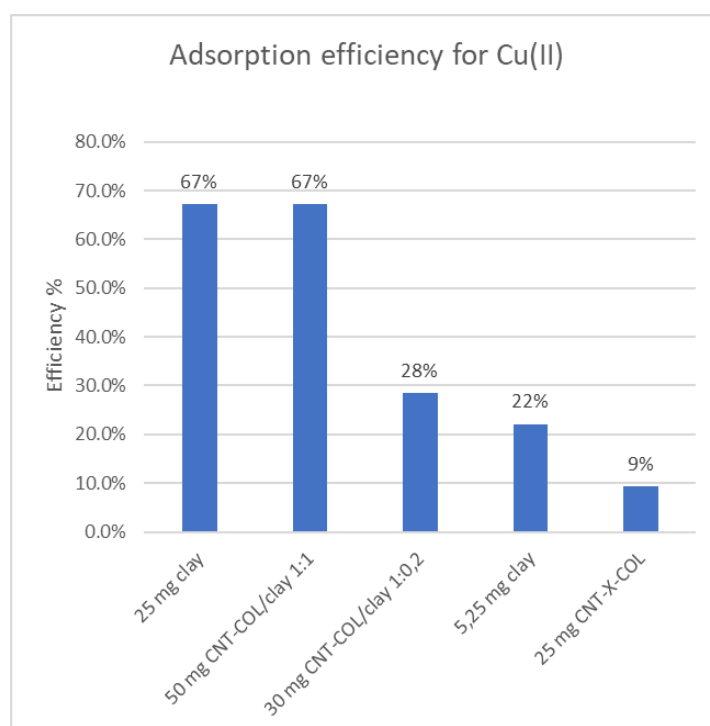


Figure 3.22: Adsorption efficiency for copper(II).

The lower efficiency was obtained, as expected, using the positively charged CNT-X-COL (AR11).

The sample containing only clay (AR05b) shows an efficiency of 67% as well as the sample the hybrid material (AR09) containing the same amount of clay (25 mg) as in the case of sample AR05b.

To the light of these results, the adsorption of copper (II) seems to be exclusively related the amount of clay and the presence of CNT-X-COL in the 1:1 hybrid material

did not enhance the efficiency of the material. Thus, Scanning Electron Microscopy (SEM) observations were performed to find a possible explanation. As it can be seen (figure 3.23), the CNTs are completely incorporated in the clay so that the surface of the nanotube cannot interact with any compounds present in the solution to be purified.

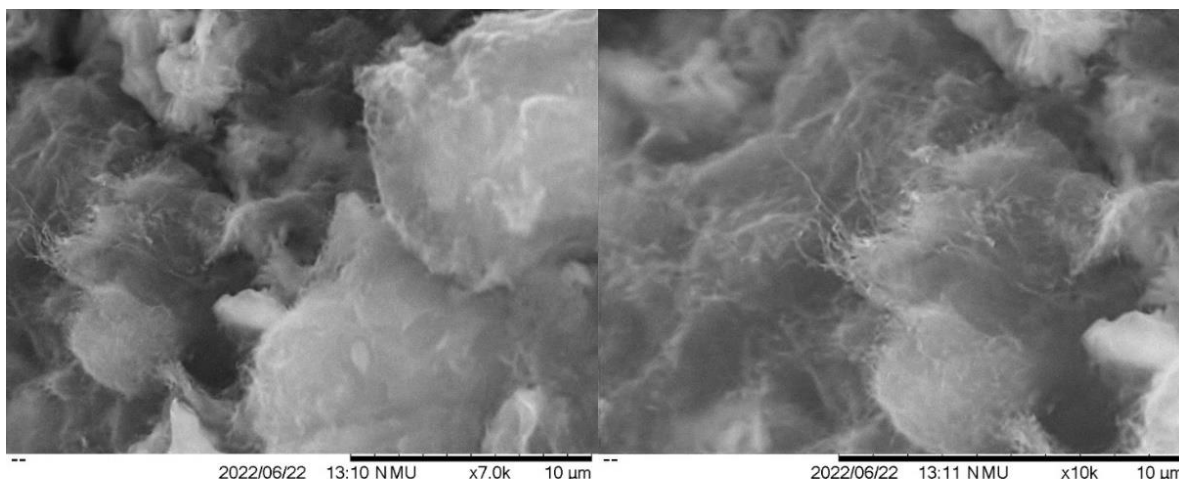


Figure 3.23: SEM of hybrid material CNT-X-COL/clay in a ratio of 1:1.

The amount of clay in the hybrid material was then reduced to 20% with respect to CNT-X-COL and the adsorbance efficiency was compared with that of an experiment containing only clay in the same amount (AR06b). Interestingly, in this case, despite the same amount of clay as in AR06b, the presence of CNT in the hybrid material seems to contribute to the adsorption.

The results obtained with the 1:0.2 CNT/clay hybrid material seem to be promising, nevertheless more experiments using this material using different conditions including different doses and clays will be performed to complete this study as well as their efficiency within the organic dyes solutions.

3.6.2. Variation of efficiency as a function of contact time

The effect of contact time on adsorption efficiency is highly significant. As 60 minutes was a time sufficient to have a high removal efficiency towards organic dyes, the same contact time was used also in the case of clays. This because in a real application, the contact time must be sufficient to remove all the pollutants. Anyway, experiments with lower contact times were performed.

Interestingly, the absorbance values of clay, obtained after 30 minutes values were substantially the same of those obtained after 60 minutes. This suggests that the saturation equilibrium has already been reached after 30 minutes, which is more than a reasonable timeframe for practical clay adsorption applications.

3.7. Adsorption of Cu(II) nitrate trihydrate by clay and its problem

A solution of Cu(II) nitrate was then prepared to test the efficiency at a neutral pH in order to simulate typical environmental conditions.

Unfortunately, in this case, after the contact time it was no possible to completely separate the solid from the solution even using prolonged centrifugation and filtration on cotton. In all the cases, nanoscale clay particles remained dispersed within the solution invalidating the adsorbance measures because of scattering phenomenon.

Even allowing the nanoparticle dispersed to settle for several days, but the adsorbance values were still not consistent.

Even visually, when observing the samples, a slight turbidity can be seen by naked eye. This feature was not observed in the ammoniacal solution of Cu(II).

To solve this problem, an alternative would be to perform a nanofiltration. However, this approach was not pursued because, from a field application perspective, such filtrations require very long times and a substantial energy cost that an industrial facility or plant would be unlikely to undertake.

4 Conclusion and future developments

The study was focused on the preparation and tests of new efficient adsorbents, based on modified carbon nanotubes (CNTs) and hybrid materials composed by CNTs and clay, to be used in the removal of Rhodamine B, Methyl Orange and Cu(II) cation chosen as reference pollutants. Their efficiencies were compared with non-functionalized nanotubes, to those bearing a carboxylic group directly bound to the surface (CNT-COOH) and with the pure clay.

Functionalized CNTs bearing carboxylic groups bound to the surface through a spacer made of three carbon atoms (CNT-X-COOH) and CNTs containing a choline moiety (CNT-X-COL) were prepared from non-functionalized nanotubes.

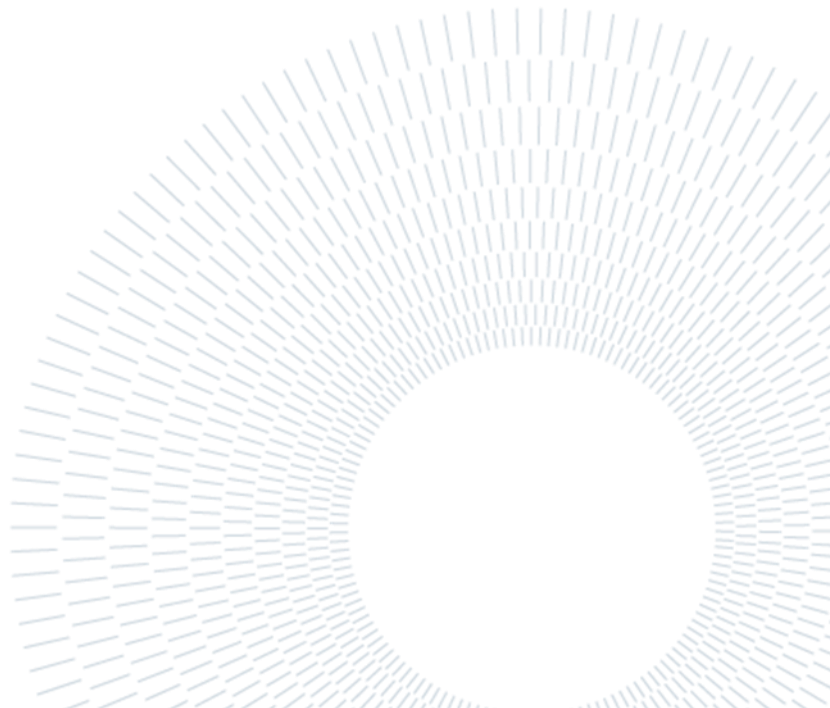
Several experiments were performed by varying parameters such as the amount of adsorbent, the amount of pollutant, contact time and the adsorption efficiency was determined by UV-VIS measurements.

For both organic dyes, CNT-X-COOH have shown the higher efficiency not only compared to the non-functionalized CNTs (used as reference) but also with respect to CNT-COOH. Therefore, the spacer (C3) seems to be a structural moiety that enhances the adsorption efficiency. The reasons why these nanotubes are the best need to be further explored by means of computational simulation and specific surfaces analysis (BET).

The positively charged CNT-X-COL, even if showed a lower efficiency with respect to the base one, were used to prepare hybrid adsorbents composed by the combination of CNT-X-COL with clay (Montmorillonite-Nanofil 116) in two different ratios, 1:1 and 1:0.2 (CNT-X-COL/clay 1:1, CNT-X-COL/clay 1:0.2) were also prepared with the aim to develop an adsorbent active toward both inorganic and organic pollutants. The results obtained with the 1:0.2 CNT/clay hybrid material seem to be the most promising in the removal of copper(II) because their adsorbance efficiency is higher than that of pure clay in the same amount as also CNT seems to contribute. Conversely, the 1:1 hybrid material showed the same results obtained with pure clay. Anyway, more experiments using these materials under different conditions need to be performed.

In conclusion, this study has shown that the spacer in CNT-X-COOH makes them more efficient adsorbents towards organic dyes with respect to the well-known CNT-COOH. Therefore, it is clear that appropriate functionalization significantly enhances the efficiency of non-functionalized nanotubes which have been gaining increasing

interest in the scientific community in recent years due to their exceptional properties. A thorough understanding of their behavior and potential in the field of wastewater treatment could bring exceptional benefits, especially in a context where wastewater reuse is becoming increasingly important in light of climate change and water resource scarcity.



Bibliography

- [1] European Investment Bank. Wastewater as Resource, May 2022.
- [2] Naidoo S., Olaniran A.O. Treated Wastewater Effluent as a Source of Microbial Pollution of Surface Water Resources. *International Journal of Environmental Research and Public Health* 11(1): 249-270, 2014.
- [3] Unep. Sick water? the central role of wastewater management in sustainable development - A Rapid Response Assessment, 2010.
- [4] Wada Y., van Beek L. P. H., Bierkens M. F. P. Modelling global water stress of the recent past: on the relative importance of trends in water demand and climate variability. *Hydrol. Earth Syst. Sci.*, 15: 3785–3808, 2011.
- [5] FAO. Coping with water scarcity, 2007.
- [6] Damkjaer S., Taylor R. The measurement of water scarcity: Defining a meaningful indicator. *Ambio* 46: 513–531, 2017.
- [7] Masson-Delmotte V., Zhai P., Pörtner H.O., Roberts D., Skea J., Shukla P.R., Pirani A., Moufouma-Okia W., C. Péan, Pidcock R., Connors S., Matthews J.B.R., Chen Y., Zhou X., Gomis M.I., Lonnoy E., Maycock T., Tignor M., Waterfield T. IPCC, 2018: Global Warming of 1.5°C. An IPCC Special Report on the impacts of global warming of 1.5°C above pre-industrial levels and related global greenhouse gas emission pathways, in the context of strengthening the global response to the threat of climate change, sustainable development, and efforts to eradicate poverty. *Current Urban Studies* 9, 2021.
- [8] Morote Á.F., Olcina J., Hernández M. The Use of Non-Conventional Water Resources as a Means of Adaptation to Drought and Climate Change in Semi-Arid Regions: South-Eastern Spain. *Water* 11: 93, 2019.
- [9] Hanasaki N., Fujimori S., Yamamoto T., Yoshikawa S., Masaki Y., Hijioka Y., Kainuma M., Kanamori Y., Masui T., Takahashi K., Kanae S. A global water scarcity assessment under Shared Socio-economic Pathways – Part 1: Water use, *Hydrol. Earth Syst. Sci.* 17: 2375–2391, 2013.
- [10] Unep. Sick Water? The Central Role of Wastewater Management in Sustainable Development - A Rapid Response Assessment, 2010.
- [11] European Investment Bank-Wastewater as Resource, May 2022, pages 3-5.
- [12] European Investment Bank-Wastewater as Resource, May 2022, page 6.

- [13] Batstone D.J., Hülsen T., Mehta C.M., Keller J. Platforms for energy and nutrient recovery from domestic wastewater: A review. *Chemosphere* 140: 2-11, 2015.
- [14] ATSE- The Australian Academy of Technological Sciences and Engineering. Wastewater –an untapped resource?. 2015.
- [15] Tyagi V.K., Lo S.L. Sludge: A waste or renewable source for energy and resources recovery?. *Renewable and Sustainable Energy Reviews*, Elsevier 25(C): 708-728, 2013.
- [16] UN-Water Analytical Brief Unconventional Water Resources, 05 June 2020.
- [17] Vinod K.G., Imran A., Tawfik A. Saleh, Arunima N., Shilpi A. Chemical treatment technologies for waste-water recycling, an overview, 2, 6380-6388, 2012.
- [18] Pérez H., García O.J.G., Amezcua-Allieri M.A., Vázquez R.R. Nanotechnology as an efficient and effective alternative for wastewater treatment: an overview, *Water Sci Technol* 87 (12): 2971–3001, 2023.
- [19] Wei D., Li B., Huang H., Luo L., Zhang J., Yang Y., Guo J., Tang L., Zeng G., Zhou Y. Biochar-based functional materials in the purification of agricultural wastewater: Fabrication, application and future research needs. *Chemosphere*, 197:165-180, 2018.
- [20] Mahur J.S, Dixit S., Shrivastava R., Goswami C.S. Effect of activation parameters on the surface and mechanical properties of activated carbon spheres. *International Journal Metallurgical & Materials* 3: 75-84, 2023.
- [21] Shatanawi M., Hamdy A., Smadi H. Urban wastewater: problems, risks and its potential use for irrigation. *Options Méditerranéennes, Séries A n. 66*, 2005.
- [22] De Feo G., De Gisi S., Galasso M. *Acque reflue - Progettazione e gestione di impianti per il trattamento e lo smaltimento*, 2020.
- [23] Piccini S. *Convegno Nazionale sulla Bioenergia Roma*, 12 maggio 2004.
- [24] Bartram J. *Routledge Handbook of water and health*, 1st Edition, Published January 24, 2018, by Routledge.
- [25] Vaccaro M. *Trattamento biologico di rimozione del fosforo dalle acque reflue in un impianto pilota a basso tempo di residenza cellulare*. Politecnico di Torino, 2018-2019.
- [26] Naidoo S., Olaniran AO. Treated wastewater effluent as a source of microbial pollution of surface water resources. *Int J Environ Res Public Health* 11(1):249-70, 2014.
- [27] Environmental Protection Agency. *Wastewater Treatment Manuals—Primary, Secondary and Tertiary Treatment*; Environmental Protection Agency: Ireland, 1997.

- [28] Hreiz R., Latifi M.A., Roche N. Optimal design and operation of activated sludge processes: State-of-the-art. *Chemical Engineering Journal* 281: 900-920, 2015.
- [29] Dawi MA, Sanchez-Vila X. Simulating degradation of organic compounds accounting for the growth of microorganisms (Monod kinetics) in a fully Lagrangian framework. *J Contam Hydrol.* 2022 Dec; 251:104074. doi: 10.1016/j.jconhyd.2022.104074. Epub 2022 Sep 11. PMID: 36126368.
- [30] Chachuat, Benoit & Roche, Nicolas & Latifi, Abderrazak. Dynamic optimisation of small size wastewater treatment plants including nitrification and denitrification processes. *Computers & Chemical Engineering* 25: 585-593, 2001.
- [31] Xi H., Zhou X., Arslan M., Luo Z., Wei J., Wu Z., Gamal El-Din M. Heterotrophic nitrification and aerobic denitrification process: Promising but a long way to go in the wastewater treatment. *Sci Total Environment* 805, 2022.
- [32] Microbiological reviews, p. 43-70, Denitrification ROGER KNOWLES Department of Microbiology, Macdonald Campus of McGill University, Ste. Anne de Bellevue, Quebec H9X JCO, Canada, 1982.
- [33] Nota Tecnica allegata alla Linea Guida LG023 "Standard e requisiti minimi Ingegneria Sanitaria e Ambientale" – Criteri di dimensionamento", Acea Elabiori Spa.
- [34] Lou L., Luo H., Fang J., Liu G. The advance of heterotrophic nitrification aerobic denitrification microorganisms in wastewater treatment. *Bioresource Technology Reports* 22, 2023.
- [35] Madan S., Madan R., Hussain, A. Advancement in biological wastewater treatment using hybrid moving bed biofilm reactor (MBBR): a review. *Appl Water Sci* 12: 141, 2022.
- [36] Radjenović J., Matošić M., Mijatović I., Petrović M., Barceló M., Springer-Verlag Berlin Heidelberg Membrane Bioreactor (MBR) as an Advanced Wastewater Treatment Technolog. *Hdb Env Chem* 5, Part S/2: 37–101, 2007
- [37] Iorhemen O.T., Hamza R.A., Tay J.H. Membrane Bioreactor (MBR) Technology for Wastewater Treatment and Reclamation: Membrane Fouling. *Membranes (Basel)* 6(2):33, 2016.
- [38] Kimura K., Yamato N., Yamamura H., Watanabe Y. Membrane fouling in pilot-scale membrane bioreactors (MBRs) treating municipal wastewater. *Environ Sci Technol* 39(16):6293-9, 2015.
- [39] Iorhemen O.T.; Hamza R.A.; Tay J.H. Membrane Bioreactor (MBR) Technology for Wastewater Treatment and Reclamation: Membrane Fouling. *Membranes* 6: 33, 2016.

- [40] Kootenaeei, Golbabaei F., Aminirad H. "Membrane Biological Reactors (MBR) and Their Applications for Water Reuse." *International journal of Advanced Biological and Biomedical Research* 2: 1951-1962, 2014.
- [41] Longhi L., Basilico D., Meloni A., Canziani R. Ottimizzazione di un processo sbr per la rimozione biologica di azoto da acque reflue concentrate via nitrato. Politecnico di Milano, 2009.
- [42] Jafarinejad S. Recent developments in the application of sequencing batch reactor (SBR) technology for the petroleum industry wastewater treatment. *Chemistry International* 3, 2017.
- [43] Mahvi A. H. Sequencing batch reactor: a promising technology in wastewater treatment. 79-90, 2008.
- [44] Collivignarelli M.C., Abbà A., Miino, M.C., Caccamo F.M., Torretta V., Rada E.C., Sorlini S. Disinfection of Wastewater by UV-Based Treatment for Reuse in a Circular Economy Perspective. Where Are We at? *Int. J. Environ. Res. Public Health* 18: 77, 2021.
- [45] Bianchi G.F., Antonelli M. Modellazione e validazione a scala pilota della disinfezione di acque reflue con acido peracetico. Politecnico di Milano, 2018-2019.
- [46] Morrison C.M., Hogard S., Pearce R., Gerrity D., von Gunten U., Wert E.C. Ozone disinfection of waterborne pathogens and their surrogates: A critical review. *Water Res.* 2022.
- [47] Collivignarelli M.C., Abbà A., Miino, M.C., Caccamo F.M., Torretta V., Rada E.C., Sorlini S. Disinfection of Wastewater by UV-Based Treatment for Reuse in a Circular Economy Perspective. Where Are We at? *Int. J. Environ. Res. Public Health* 18: 77, 2021.
- [48] Mehta I., Hsueh H.Y., Taghipour S., Li W., Saeedi S. UV Disinfection Robots: A Review. *Rob Auton Syst*, 2023.
- [49] Disinfecting wastewater. The University of Waikato Te Whare Wānanga o Waikato, Science Learning Hub – Pokapū Akoranga Pūtaiao, 2008.
- [50] Rashid R., Shafiq I., Akhter P., Iqbal M.J., Hussain M. A state-of-the-art review on wastewater treatment techniques: the effectiveness of adsorption method. *Environ Sci Pollut Res Int* 28(8): 9050-9066, 2021.
- [51] Roque-Malherbe R. Applications of natural zeolites in pollution abatement ad industry. *Handbook of Surfaces and Interfaces of Materials*; Elsevier: Amsterdam, The Netherlands: 495-522, 2001.
- [52] Zhang T, Wang W., Zhao Y., Bai H., Wen T., Kang S., Song G., Song S., Komarneni S. Removal of heavy metals and dyes by clay-based adsorbents: From natural clays to 1D and 2D nano-composites. *Chemical Engineering Journal* 420: 127574, 2021.

- [53] USEPA. Primer for Municipal Wastewater Treatment Systems. Office of Water and Wastewater Management, 2004. Available online: <http://www.epa.gov.owm>.
- [54] El Gamal M., Mousa H. A., El-Naas M. H., Zacharia R., Judd S. Bio-regeneration of activated carbon: A comprehensive review. *Separation and Purification Technology* 197, 345-359, 2018.
- [55] Klaine S.J., Alvarez P.J., Batley G.E., Fernandes T.F., Handy R.D., Lyon D.Y., Mahendra S., McLaughlin M.J., Lead J.R. Nanomaterials in the environment: behavior, fate, bioavailability, and effects. *Environ Toxicol Chem* 27(9):1825-51, 2008.
- [56] Loevestam G., Rauscher H., Roebben G., Sokull-Kluettgen B., Gibson P., Putaud J., Stamm H. Considerations on a Definition of Nanomaterial for Regulatory Purposes. Luxembourg (Luxembourg): Publications Office of the European Union, 2010.
- [57] Mazari S., Ali E., Abro R., Khan F., Ahmed I., Ahmad M., Sabzoi N., Siddiqui M.T.H., Hossain N., Mujawar M., Shah A. Nanomaterials: Applications, waste-handling, environmental toxicities, and future challenges - A Review. *Journal of Environmental Chemical Engineering* 9, 2021.
- [58] Elkhwaga A., Zidan A., Abd El Mageed A. Preparation methods of different nanomaterials for various potential applications: A review. *Journal of Molecular Structure* 1281, 2023.
- [59] Rajput N. Methods of Preparation of Nanoparticles—A Review. *International Journal of Advances in Engineering and Technology*, 7: 1806-1811, 2015.
- [60] Niculescu A.G., Chircov C., Bîrcă A.C., Grumezescu A.M. Nanomaterials Synthesis through Microfluidic Methods: An Updated Overview. *Nanomaterials (Basel)* 11(4):864, 2021.
- [61] Titirici M., White R., Brun N., Budarin V., & Su D., Monte F., Clark J., MacLachlan M. Sustainable carbon materials. *Chemical Society reviews* 44, 2014.
- [62] Solmi M.V. Sintesi e caratterizzazione di carboni per applicazioni in catalisi. Alma Mater Studiorum - Università di Bologna, 2015.
- [63] Meagan S. Mauter and Menachem Elimelech. *Environmental Science & Technology* 42(16): 5843-5859, 2008.
- [64] Gatti T., Vicentini N., Menna E., Maggini M. Funzionalizzazione organica di nanostrutture di carbonio per lo sviluppo di materiali intelligenti a base polimerica, Dipartimento di Scienze Chimiche - disc Università di Padova. *La chimica e l'Industria online*, anno I, N°3, 2017.
- [65] Kharlamova M.V., Kramberger C., Chernov A.I. Advanced Carbon Nanostructures: Synthesis, Properties, and Applications. *Nanomaterials* 13: 1268, 2023.

- [66] Zhang B.T., Zheng X., Li H.F., Lin J.M. Application of carbon-based nanomaterials in sample preparation: a review. *Anal Chim Acta.* 784:1-17, 2023.
- [67] Hari Krishna R., Chandrababha M.N., Samrat K., Krishna Murthy T.P., Manjunatha C., Girish Kumar S. Carbon nanotubes and graphene-based materials for adsorptive removal of metal ions – A review on surface functionalization and related adsorption mechanism. *Applied Surface Science Advances* 16, 2023.
- [68] Ijaz H., Mahmood A., Abdel-Daim M.M., Sarfraz R.M., Zaman M., Zafar N., Alshehry S., Salem-Bekhit M. M., Ali M.A., Lienda Bashier Eltayeb, Benguerba Y. Review on carbon nanotubes (CNTs) and their chemical and physical characteristics, with particular emphasis on potential applications in biomedicine, *Inorganic Chemistry Communications* 155, 2023.
- [69] Rathinavel S., Priyadharshini K., Panda D. A review on carbon nanotube: An overview of synthesis, properties, functionalization, characterization, and the application. *Materials Science and Engineering: B.* 268, 2021.
- [70] Saifuddin N.M., Raziah A.Z., Junizah AR. Carbon Nanotubes: A Review on Structure and Their Interaction with Proteins. *Journal of Chemistry*, 2013.
- [71] Suzuki S. Physical and Chemical Properties of Carbon Nanotubes. *InTech*, 2013.
- [72] Kim H.I., Wang M., Lee S.K., Kang J., Nam J.D., Ci L., Suhr J. Tensile properties of millimeter-long multi-walled carbon nanotubes. *Sci Rep* 7(1):9512, 2017.
- [73] Kumar S., Nehra M., Deepak K., Dilbaghi N., Tankeshwar K., Ki-Hyun K. Carbon nanotubes: A potential material for energy conversion and storage. *Progress in Energy and Combustion Science*, 2017.
- [74] Baig N., Kammakam I., Falath W. Nanomaterials: A review of synthesis, properties, recent progress, and challenges. *Materials Advances* 2, 2021.
- [75] Kolahdouz M., Xu B., Nasiri A.F., Fathollahzadeh M., Manian M., Aghababa H., Wu Y., Radamson H.H. Carbon-Related Materials: Graphene and Carbon Nanotubes in Semiconductor Applications and Design. *Micromachines (Basel)* 13(8):1257, 2022.
- [76] Saeed K., Khan I. Carbon nanotubes–properties and applications: a review. *Carbon letters* 14: 131-144, 2013.
- [77] Hari Krishna R., Chandrababha M.N., Samrat K., Krishna Murthy T.P., Manjunatha C., Girish Kumar S. Carbon nanotubes and graphene-based materials for adsorptive removal of metal ions – A review on surface functionalization and related adsorption mechanism. *Applied Surface Science Advances* 16, 2023.
- [78] Al-Jammal N. Abdullah T., Yuzakova T., Zsirka B., Cretescu I., Vagvolgyi V., Sebestyén V., Le Phuoc C., Rasheed R., Domokos E. (2019). Functionalized Carbon

- Nanotubes for Hydrocarbon Removal from Water. *Journal of Environmental Chemical Engineering* 8, 2019.
- [79] Rathinavel S., Priyadharshini K., Panda D. A review on carbon nanotube: An overview of synthesis, properties, functionalization, characterization, and the application. *Materials Science and Engineering: B*. 268, 2021.
- [80] Ijaz H., Mahmood A., Abdel-Daim M.M., Sarfraz R.M., Zaman M., Zafar N., Alshehery S., Salem-Bekhit M. M., Ali M.A., Lienda Bashier Eltayeb, Benguerba Y. Review on carbon nanotubes (CNTs) and their chemical and physical characteristics, with particular emphasis on potential applications in biomedicine, *Inorganic Chemistry Communications* 155, 2023.
- [81] De Volder M.F., Tawfick S.H., Baughman R.H., Hart A.J. Carbon nanotubes: present and future commercial applications. *Science* 339(6119):535-9, 2013.
- [82] Colvin V.L. The potential environmental impact of engineered nanomaterials. *Nat Biotechnol* 21(10):1166-1170, 2003.
- [83] Kuhn R., Bryant I.M., Jensch R., Böllmann J. Applications of Environmental Nanotechnologies in Remediation, Wastewater Treatment, Drinking Water Treatment, and Agriculture. *Appl. Nano* 3: 54-90, 2022.
- [84] Mobasser S., Firoozi A. A. Review of nanotechnology applications in science and engineering. *J Civil Eng Urban* 6(4): 84-93, 2016.
- [85] A.K. Haritash, C.P. Kaushik, Biodegradation aspects of Polycyclic Aromatic Hydrocarbons (PAHs): A review, *Journal of Hazardous Materials* 169: 1-15, 2009.
- [86] Ramírez Carnero A., Lestido-Cardama A., Vazquez Loureiro P., Barbosa-Pereira L., Rodríguez Bernaldo de Quirós A., Sendón R. Presence of Perfluoroalkyl and Polyfluoroalkyl Substances (PFAS) in Food Contact Materials (FCM) and Its Migration to Food. *Foods* 10(7):1443, 2021.
- [87] Jain K., Patel A.S., Pardhi V.P., Flora S.J.S. Nanotechnology in Wastewater Management: A New Paradigm Towards Wastewater Treatment. *Molecules* 26(6):1797, 2021.
- [88] Kuhn R., Bryant I.M., Jensch R., Böllmann J. Applications of Environmental Nanotechnologies in Remediation, Wastewater Treatment, Drinking Water Treatment, and Agriculture. *Appl. Nano* 3: 54-90, 2022.
- [89] Mauter M.S., Elimelech M. Environmental applications of carbon-based nanomaterials. *Environ Sci Technol*. 42(16):5843-59, 2008.
- [90] Dąbrowski A. Adsorption-from Theory to Practice. *Advances in colloid and interface science* 93: 135-224, 2001.
- [91] Gusain R., Kumar N., Sinha Ray S. (2019). Recent advances in carbon nanomaterial-based adsorbents for water purification. *Coordination Chemistry Reviews* 405, 2019.

- [92] Crini G., Lichtfouse E., Wilson L.D., Morin-Crini N. Conventional and nonconventional adsorbents for wastewater treatment, *Environ. Chem. Lett.* 1–19, 2018.
- [93] Gusain R., Kumar N., Sinha Ray S. (2019). Recent advances in carbon nanomaterial-based adsorbents for water purification. *Coordination Chemistry Reviews* 405, 2019.
- [94] Faust S.D., Aly O.M. *Adsorption Processes for Water Treatment*, Butterworth-Heinemann, 1987.
- [95] Kaykhaii M., Sasani M., Marghzari S. Removal of Dyes from the Environment by Adsorption Process. *Chemical and Materials Engineering* 6: 31-35, 2018.
- [96] Foo K.Y., Hameed B.H. Insights into the modeling of adsorption isotherm systems, *Chemical Engineering Journal* 156: 2-10, 2010.
- [97] Al-Ghouti M.A., Da'ana D.A. Guidelines for the use and interpretation of adsorption isotherm models: A review, *Journal of Hazardous Materials*, Volume 393, 2020.
- [98] Buttolo G. *Il controllo microclimatico passivo: caratterizzazione sperimentale delle isoterme di adsorbimento dei materiali essiccanti e applicazione numerica in ambito museale*. Politecnico di Milano, 2016.
- [99] Almeida-Naranjo C.E.; Guerrero V.H.; Villamar-Ayala C.A. Emerging Contaminants and Their Removal from Aqueous Media Using Conventional/Non-Conventional Adsorbents: A Glance at the Relationship between Materials, Processes, and Technologies. *Water* 15: 1626, 2023.
- [100] Yang K., Xing B. Adsorption of organic compounds by carbon nanomaterials in aqueous phase: Polanyi theory and its application, *Chem. Rev.* 110, 2010.
- [101] Pérez H., Quintero García O.J., Amezcua-Allieri M.A., Rodríguez Vázquez R. Nanotechnology as an efficient and effective alternative for wastewater treatment: an overview. *Water Sci Technol.* 87(12): 2971-3001, 2023.
- [102] Shatkin J.A. *Nanotechnology: Health and Environmental Risks*, Second Edition, 2012.
- [103] Maynard A.D. Nanotechnology: assessing the risks, *Nano Today*, Volume 1: 22-33, 2006.
- [104] Arora B., Attri P. Carbon Nanotubes (CNTs): A Potential Nanomaterial for Water Purification. *J. Compos. Sci.* 4: 135, 2020.
- [105] Qu X., Alvarez P.J., Li Q. Applications of nanotechnology in water and wastewater treatment. *Water Res.* 47(12): 3931-46, 2013.
- [106] Gusain R., Kumar N., Ray S.S. Recent advances in carbon nanomaterial-based adsorbents for water purification. *Coordination Chemistry Reviews.* 405, 2019.

- [107] Pérez H., Quintero García O.J., Amezcua-Allieri M.A., Rodríguez Vázquez R. Nanotechnology as an efficient and effective alternative for wastewater treatment: an overview. *Water Sci Technol.* 87(12):2971-3001, 2023.
- [108] Stafiej A., Pyrzynska K. Adsorption of heavy metal ions with carbon nanotubes. *Separation and purification technology* 58.1: 49-52, 2007.
- [109] Rao G.P., Lu C., Su F. Sorption of divalent metal ions from aqueous solution by carbon nanotubes: A review. *Separation and Purification Technology* 58, 2007.
- [110] Xu J., Cao Z., Zhang Y., Yuan Z., Lou Z., Xu X., Wang X. A review of functionalized carbon nanotubes and graphene for heavy metal adsorption from water: Preparation, application, and mechanism. *Chemosphere* 195: 351-364, 2018.
- [111] Pyrzynska K., Stafiej A. Sorption behavior of Cu (II), Pb (II), and Zn (II) onto carbon nanotubes. *Solvent Extraction and Ion Exchange* 30.1: 41-53, 2012.
- [112] Gao Z., Bandosz T., Zhao Z., Han M., Qiu, J. Investigation of factors affecting adsorption of transition metals on oxidized carbon nanotubes. *Journal of hazardous materials* 167: 357-65, 2009.
- [113] Anitha K., Namsani S., Singh J.K. Removal of Heavy Metal Ions Using a Functionalized Single-Walled Carbon Nanotube: A Molecular Dynamics Study. *J Phys Chem A.* 119(30): 8349-58, 2015.
- [114] Lu C., Chiu H., Liu, C.T. Removal of Zinc(II) from Aqueous Solution by Purified Carbon Nanotubes: Kinetics and Equilibrium Studies. *Industrial & Engineering Chemistry Research* 45: 2850-2855, 2006.
- [115] Lu C., Chiu H., Liu, C.T. Removal of Zinc(II) from Aqueous Solution by Purified Carbon Nanotubes: Kinetics and Equilibrium Studies. *Industrial & Engineering Chemistry Research* 45: 2850-2855, 2006.
- [116] Li Y.H., Wang S., Wei J., Zhang X., Xu C., Luan Z., Wu A., Wei B. Lead Adsorption on Carbon Nanotubes. *Chemical Physics Letters* 357: 263-266, 2002.
- [117] Song B., Xu P., Zeng G., Gong J., Zhang P., Feng H., Liu Y., Ren X. Carbon nanotube-based environmental technologies: the adopted properties, primary mechanisms, and challenges. *Reviews in Environmental Science and Bio/Technology* 17, 2018.
- [118] Pan B., Xing B. Adsorption mechanisms of organic chemicals on carbon nanotubes. *Environ Sci Technol.* 42(24): 9005-13, 2008.
- [119] Kurwadkar S., Hoang T.V, Malwade K., Kanel S., Harper W., Struckhoff G.C. Application of carbon nanotubes for removal of emerging contaminants of concern in engineered water and wastewater treatment systems. *Nanotechnology for Environmental Engineering* 4: 1-16, 2019.
- [120] Ghaedi M., Haghdoust S., Kokhdan S., Mihandoust A., Sahraei R., Daneshfar A. Comparison of Activated Carbon, Multiwalled Carbon Nanotubes, and Cadmium Hydroxide Nanowire Loaded on Activated Carbon as Adsorbents for

- Kinetic and Equilibrium Study of Removal of Safranin O. *Spectroscopy Letters* 45: 500-510, 2012.
- [121] Yu J.G., Zhao X.H., Yang H., Chen X.H., Yang Q., Yu L.Y., Jiang J.H., Chen X.Q. Aqueous adsorption and removal of organic contaminants by carbon nanotubes. *Sci Total Environ* 482-483: 241-51, 2014.
- [122] Yang K., Wu W., Jing Q., Zhu L. Aqueous adsorption of aniline, phenol, and their substitutes by multi-walled carbon nanotubes. *Environ Sci Technol* 42(21):7931-6, 2008.
- [123] Ministero della Salute, Direzione generale della prevenzione sanitaria- Tetracoloroetilene e Tricloroetilene, 2016.
- [124] Naghizadeh A., Nasser S., Nazmara S. Removal of Trichloroethylene from water by adsorption on to Multiwall Carbon Nanotubes. *Iranian Journal of Environmental Health Science & Engineering* 8: 317-324, 2011.
- [125] Shao D., Hu J., Jiang Z., Wang X. Removal of 4,4'-dichlorinated biphenyl from aqueous solution using methyl methacrylate grafted multiwalled carbon nanotubes. *Chemosphere* 82 5: 751-8, 2011.
- [126] Ma X., Tsige M., Uddin S., Talapatra S. Application of Carbon Nanotubes for Removing Organic Contaminants from Water. *Materials Express* 1, 2011.
- [127] Glüge J., Scheringer M., Cousins I.T., DeWitt J.C., Goldenman G., Herzke D., Lohmann R., Ng C.A., Trier X., Wang Z. An overview of the uses of per- and polyfluoroalkyl substances (PFAS). *Environ Sci Process Impacts* 22(12): 2345-2373, 2020.
- [128] <https://www.legambienteveneto.it/pfas-cosa-sono-e-come-incidono-sulla-salute-delluomo/>
- [129] Lu D., Sha S., Luo J., Huang Z., Jackie X.Z. Treatment train approaches for the remediation of per- and polyfluoroalkyl substances (PFAS): A critical review. *Journal of Hazardous Materials* 386, 2020.
- [130] Yamada T., Taylor P.H., Buck R.C., Kaiser M.A., Giraud R.J. Thermal degradation of fluorotelomer treated articles and related materials. *Chemosphere* 61(7): 974-84, 2005.
- [131] Birch Q., Birch M., Nadagouda M., Dionysiou D. Nano-enhanced treatment of per-fluorinated and poly-fluorinated alkyl substances (PFAS). *Current Opinion in Chemical Engineering* 35, 2022.
- [132] Zhang D.Q., Zhang W.L., Liang Y.N. Adsorption of perfluoroalkyl and polyfluoroalkyl substances (PFASs) from aqueous solution - A review. *Sci Total Environ.*, 2019.
- [133] Apul O.G., Karanfil T. Adsorption of synthetic organic contaminants by carbon nanotubes: a critical review. *Water Res.* 68: 34-55, 2015.

- [134] Boudalis A.K., Xavier Policand, Sournia-Saquet A., Donnadiou B., Tuchagues J-P. *Chim. Acta* 361: 1681–1688, 2008.
- [135] Peng H., Alemany L.B, Margrave J.L, Khabashesku J V.N. *Am. Chem. Soc.* 125: 15174-15182, 2003.
- [136] Thanhmingliana, Diwakar Tiwari. Efficient use of hybrid materials in the remediation of aquatic environment contaminated with micro-pollutant diclofenac sodium. *Chemical Engineering Journal* 263: 364-373, 2015.
- [137] Yao Y., Bing H., Feifei X., Xiaofeng C. Equilibrium and kinetic studies of methyl orange adsorption on multiwalled carbon nanotubes. *Chemical Engineering Journal* 170: 82-89, 2011.
- [138] Shirmardi M., Mesdaghinia A., Mahvi A.H., Nasser S., Nabizadeh R. Kinetics and Equilibrium Studies on Adsorption of Acid Red 18 (Azo-Dye) Using Multiwall Carbon Nanotubes (MWCNTs) from Aqueous Solution. *E-Journal of Chemistry* 9(4): 2371-2383, 2012.
- [139] Rajabi M., Mahanpoor K., Moradi O. Removal of dye molecules from aqueous solution by carbon nanotubes and carbon nanotube functional groups: critical review. *RSC Adv.* 7: 47083-47090, 2017.
- [140] Kumar S., Bhanjana G., Jangra K., Dilbaghi N., Umar A. Utilization of Carbon Nanotubes for the Removal of Rhodamine B Dye from Aqueous Solutions. *Journal of nanoscience and nanotechnology* 14: 4331-6, 2014.
- [141] Sen Gupta S., Bhattacharyya K.G. Kinetics of adsorption of metal ions on inorganic materials: A review. *Advances in Colloid and Interface Science* 162: 39-58, 2011.
- [142] Ghaedi M., Shokrollahi A., Tavallali H., Shojaiepoor F., Keshavarz B., Hossainian H., Soylak M., Purkait M.K. Activated carbon and multiwalled carbon nanotubes as efficient adsorbents for removal of arsenazo(III) and methyl red from waste water. *Toxicological & Environmental Chemistry* 93(3): 438-449, 2011.
- [143] Mishra A.K., Arockiadoss T., Ramaprabhu S. Study of removal of azo dye by functionalized multi walled carbon nanotubes. *Chemical Engineering Journal* 162: 1026–1034, 2010.
- [144] Kumar S., Bhanjana G., Jangra K., Dilbaghi N., Umar A. Utilization of Carbon Nanotubes for the Removal of Rhodamine B Dye from Aqueous Solutions. *Journal of nanoscience and nanotechnology* 14: 4331-6, 2014.
- [145] Haque E., Jun J.W., Jhung S.H. Adsorptive removal of methyl orange and methylene blue from aqueous solution with a metal-organic framework material, iron terephthalate (MOF-235). *Journal of Hazardous Materials* 85: 507-511, 2011.

- [146] Hanafi M.F., Sapawe N. A review on the water problem associate with organic pollutants derived from phenol, methyl orange, and remazol brilliant blue dyes. *Materials Today: Proceedings* 31: A141-A150, 2020.
- [147] Robati D., Bagheriyan S., Rajabi M., Moradi O., Ahmadi Peyghan A. Effect of electrostatic interaction on the methylene blue and methyl orange adsorption by the pristine and functionalized carbon nanotubes. *Physica E: Low-dimensional Systems and Nanostructures* 83: 1-6, 2016.
- [148] Mittal A., Malviya A., Kaur D., Mittal J., Kurup L. Studies on the adsorption kinetics and isotherms for the removal and recovery of Methyl Orange from wastewaters using waste materials. *Journal of Hazardous Materials* 148: 229-240, 2007.
- [149] Veli S., Alyüz B. Adsorption of copper and zinc from aqueous solutions by using natural clay. *Journal of Hazardous Materials* 149: 226-233, 2007.
- [150] Zhang J., Huang Z.H., Lv R., Yang Q., Feiyu Kang F. Effect of Growing CNTs onto Bamboo Charcoals on Adsorption of Copper Ions in Aqueous Solution. *Langmuir* 25 (1): 269-274, 2009.

List of Figures

Figure 1.1: Estimated net sectoral and total water demand from 1960 to 2001 in km ³ yr ⁻¹ ,(4).....	1
Figure 1.2: (10).....	3
Figure 1.3: Global water reuse after tertiary treatment: market share by application, (12)..	4
Figure 1.4: Value in dollars per ton of substance, material, or product recovered from wastewater treatment, (14).....	4
Figure 1.5: General scheme for treatment of wastewater, (25). Errore. Il segnalibro non è definito.	
Figure 1.6: Cross-section and frontal section of a grid, (Source: Politecnico di Milano, Trattamento delle acque reflue). .	8
Figure 1.7: Aerated sand trap and oil separator, (Source: Politecnico di Milano, Trattamento delle acque reflue)..	8
Figure 1.8: Lamellar settler, (Source: Politecnico di Milano, Trattamento delle acque reflue)..	9
Figure 1.9: Pre-denitrification, (33) . .	13
Figure 1.10: MBBR schematic process. .	14
Figure 1.11: Membrane fouling, (39) ..	15
Figure 1.12: (a)Submerged MBR configuration (b) External MBR configuration, (40)..	15
Figure 1.13: SBR configuration, (43). .	16
Figure 1.14: UV configuration consisting of a channel through which the polluted fluid flows, passing through UV lamps, (49). .	18
Figure 1.15: Application of nanomaterials, (57)..	20
Figure 1.16: Graphitic nanostructures, (62). .	21
Figure 1.17: Single-wall and multiwall carbon nanotubes, (69). .	22
Figure 1.18: Surface functionalization, (80). .	24
Figure 1.19: PCBs. .	25

Figure 1.20: PAHs, (85)	26
Figure 1.21: Chemical structure of some PFAS, (86)..	26
Figure 1.22: The adsorption mechanisms, (93).	28
Figure 1.23: IUPAC classification, (98)..	29
Figure 1.24: Schematic illustration of the adsorption process for CNTs, (107).	31
Figure 1.25: PCE and TCE structures..	34
Figure 2.1: TEM images of MWCNTs.	36
Figure 2.2: ¹ H NMR analysis of glutaryl peroxide in DMSO-d ₆	38
Figure 2.3: Glutaric acid.....	38
Figure 2.4: TGA of CNT-X-COOH.....	39
Figure 2.5: DMAP structure	40
Figure 2.6: DCC structure	40
Figure 2.7: TGA of CNT-X-COL.....	41
Figure 2.8: Copper(II) sulfate pentahydrate.	42
Figure 2.9: Calibration curve for Copper(II) sulfate pentahydrate.	44
Figure 2.10: Copper(II) nitrate trihydrate structure.	45
Figure 2.11: Calibration curve for Copper(II) nitrate trihydrate.	46
Figure 2.12: Rhodamine B structure..	46
Figure 2.13: Calibration curve for Rhodamine B.	47
Figure 2.14: Methyl Orange structure..	48
Figure 2.15: Calibration curve for Methyl Orange..	49
Figure 2.16: CNTs tested in the thesis.	50
Figure 3.1: NMR analysis for glutaryl peroxide..5 Errore. Il segnalibro non è definito.	
Figure 3.2: TGA of CNT-X-COOH.....5 Errore. Il segnalibro non è definito.	
Figure 3.3: TGA of CNT-X-COL.	58
Figure 3.4: CNTs tested in this thesis.	60
Figure 3.5: Calibration curves for Rhodamine B (a), Methyl Orange (b), Copper(II) sulfate pentahydrate (b) and Copper(II) nitrate trihydrate.....	61
Figure 3.6: Efficiency for Rhodamine B.	63
Figure 3.7: Rhodamine B structure.	64

Figure 3.8: Variation of efficiency as function of time for Rhodamine B..	65
Figure 3.9: The result obtained for the adsorption of Rhodamine B by CNT-X-COOH..	Errore. Il segnalibro non è definito.
Figure 3.10: The result obtained for the adsorption of Rhodamine B by CNT BASE. .	68
Figure 3.11: The result obtained for Temkin adsorption of Rhodamine B by CNT-X-COOH .	69
Figure 3.12: Temkin isotherm for CNT BASE. .	69
Figure 3.13: Methyl Orange structure. .	70
Figure 3.14: Efficiency for Methyl Orange in 60 minutes..	Errore. Il segnalibro non è definito.2
Figure 3.15: Variation of efficiency as function of time for Methyl Orange..	Errore. Il segnalibro non è definito.3
Figure 3.16: Efficiency for Methyl Orange in 24h..	Errore. Il segnalibro non è definito.4
Figure 3.17: The result obtained for the adsorption of by CNT-X-COOH..	Errore. Il segnalibro non è definito.5
Figure 3.18: The result obtained for the adsorption of by CNT BASE. .	Errore. Il segnalibro non è definito.6
Figure 3.19: The result obtained for the adsorption of Methyl Orange by CNT-X-COOH. .	Errore. Il segnalibro non è definito.6
Figure 3.20: The result obtained for the adsorption of Methyl Orange by CNT BASE..	Errore. Il segnalibro non è definito.7
Figure 3.21: Efficiency for Methyl Orange with a ratio mg (Methyl Orange)/mg CNT = 0.085.....	Errore. Il segnalibro non è definito.8
Figure 3.22: Efficiency for copper(II).....	83
Figure 3.23: SEM of hybrid material CNT-X-COL/clay in a ratio of 1:1.....	84

List of Tables

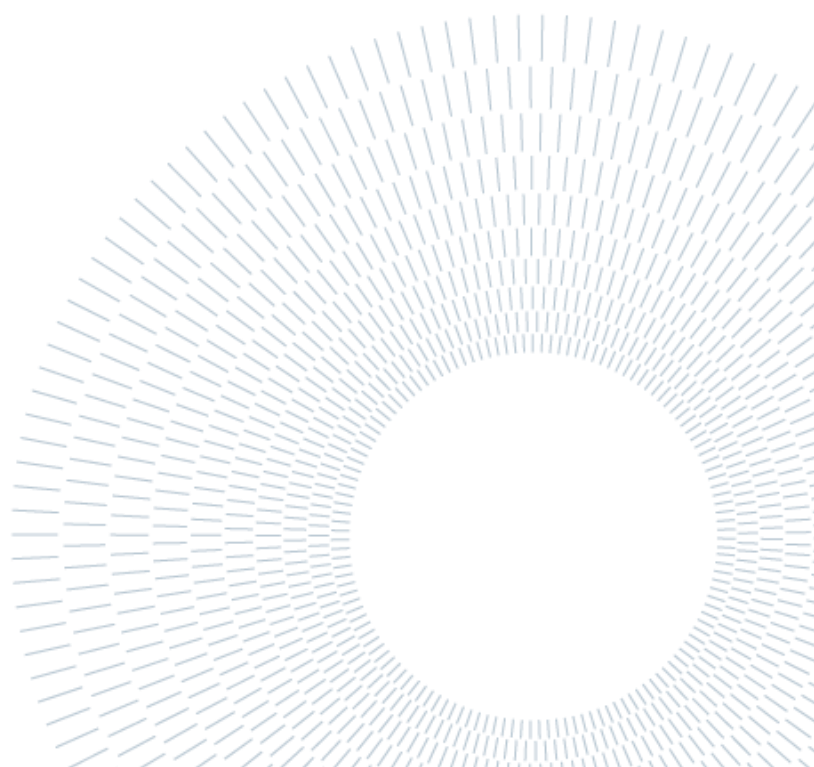
Non è stata trovata alcuna voce dell'indice delle figure.	
Table 2.4: Weight, concentration and absorbance for $\text{Cu}(\text{NO}_3)_2$	45
Table 2.5: Weight, concentration and absorbance for Rhodamine B.	47
Table 2.6: Weight, concentration and absorbance for Methyl Orange..	4Errore. Il segnalibro non è definito.
Table 2.7: Tests for CuSO_4	51
Table 2.8: Tests for Rhodamine B.....	52
Table 2.9a: Experimental parameters for "Solution 1".	54
Table 2.9b: Experimental parameters for standard solution.....	54
Table 2.10: Tests for $\text{Cu}(\text{NO}_3)_2$	55
Table 3.1: Adsorption efficiency obtained for Rhodamine B.	63
Table 3.2: Adsorption efficiency obtained for Methyl Orange..	71
Table 3.3: Adsorption efficiency obtained for Methyl Orange for 24h.....	74
Table 3.4: Adsorption efficiency obtained for Methyl Orange for different conditions..	7Errore. Il segnalibro non è definito.
Table 3.5: Summary of the results obtained for the dyes..	79
Table 3.6: Results obtained for copper (II)..	Errore. Il segnalibro non è definito.2

List of Schemes

Non è stata trovata alcuna voce dell'indice delle figure.

Acknowledgments

We are grateful to Prof. Nadka Dintcheva and Marina Amodeo (Università degli Studi di Palermo) to have furnished the clay (Montmorillonite-Nanofil 116) and for the SEM observations of the CNT-X-COL/clay 1:1.



Il ringraziamento più sincero e profondo lo devo ai miei genitori.

Non solo hanno reso possibile nel concreto questo traguardo dandomi la possibilità, per nulla scontata, di intraprendere questo duro percorso, ma anche perché hanno saputo sostenermi dal primo giorno all'ultimo, spesso sopportando e incassando i miei colpi di testa con estrema dolcezza.

So di non essere una persona semplice, forse più simile ad un treno in corsa, ma io e la mia grande complessità vi dobbiamo tutto.

Ringrazio mia sorella, che ha sempre trovato una parola di conforto e di amore per me, quando le cose non andavano bene. Ti sono grata per averci sempre creduto. Per me sei una grande fonte di ispirazione per la dedizione e la disciplina.

Ringrazio Alice e Jacopo, gli amici che ognuno di noi dovrebbe avere, per me come fratelli. Siete la mia leggerezza, il mio punto fermo se ho bisogno di aiuto, una mano tesa quando pensavo di non farcela.

Grazie per avermi sempre detto la verità anche quando facevo fatica ad accettarla. La mia gratitudine per voi è immensa.

Ringrazio il mio relatore, il Prof. Cristian Gambarotti e la mia correlatrice Ada Truscello. La mia stima nei vostri confronti va oltre l'ambito accademico. Non siete stati solo una guida in questo progetto, ma siete per me due persone di cui potermi fidare, che mi hanno accolto in modo sincero. Ricorderò sempre i miei giorni in laboratorio come un periodo bellissimo. Mi avete dato tanto, spero di avervi lasciato anche io qualcosa.

Un grazie speciale agli amici di una vita. A tutti quei momenti e quelle giornate in cui riesco ad evadere dai problemi grazie alla vostra compagnia, alle vostre risate e alla vostra gentilezza. Ogni serata per me è sempre stata una bella avventura.

Infine, ringrazio infinitamente anche chi oggi non è qua, a chi che nonostante abbia visto i miei mille volti, quelli felici e soprattutto quelli impetuosi, non mi hai mai lasciata sola. Il sostegno e la pazienza sono stati la mia forza.

“Il futuro è in mano ai deboli che si sono fatti coraggio,
e io me lo sono fatto.

Ma per farsi coraggio bisogna sapersi guardare dentro.

L'autocritica pretende consapevolezza.

Auguro a tutti voi che la vostra umiltà non si trasformi in insicurezza
e che la vostra sicurezza non si trasformi in arroganza.”

